

**Establishing an RNA-sequencing approach to analyse the
migration of B cells in the chicken embryo**

Catarina Luz Correia Tavares Cavaleiro

Thesis to obtain the Master of Science Degree in

Biotechnology

Supervisor: Prof. Dr. Benjamin Schusser

Co-supervisor: Dr. Nuno Filipe Santos Bernardes

Examination Committee

Chairperson: Prof. Dr. Leonilde de Fátima Morais Moreira

Supervisor: Prof. Dr. Benjamin Schusser

Member of the Committee: Dr. Tom Berghof

November 2022

Preface

The work presented in this thesis was performed at the Department of Reproductive Biotechnology of the Technical University of Munich (Munich, DE), during the period February-August 2022, under the supervision of Prof. Dr. Benjamin Schusser and Milena Brunner, and within the frame of the Erasmus+ programme. The thesis was co-supervised at Instituto Superior Técnico by Dr. Nuno Bernardes.

Declaration

I declare that this document is an original work of my own authorship and that it fulfils all the requirements of the Code of Conduct and Good Practices of the University of Lisbon.

Acknowledgements

In the past year, I counted on the counselling and support of several people who made this work possible and enabled me to have a fantastic experience abroad.

I sincerely thank my supervisor, Professor Dr. Benjamin Schusser, for all the counselling through this project and for granting me an amazing opportunity abroad at TUM. I would also like to thank Professor Dr. Nuno Bernardes for his help and preoccupation during the development of this thesis. Additionally, I would like to acknowledge the Erasmus+ program for enabling me to live a unique experience.

A special thanks go to Milena Brunner for all the help, patience, care and companionship during my six months in Germany. None of this could have been done without you, and I am really grateful for having met you through this project. Not even one hundred *thank yous* will be enough. I would also like to thank Dr. Tom Berghof for being an outstanding example to follow and for all the great ideas and counselling in this work.

I would also like to thank everyone from the Reproductive Biotechnology and the Livestock Biotechnology groups for welcoming me so well and making me feel at home.

To my family, in particular my parents and my brother, who have always supported and rooted for me. For all the care and for being there for me in moments of excellence, but also in the not-so-positive times.

To all my friends accompanying me in this journey, for all the shared thoughts and fears that made us to feel at ease.

Finally, to Daniel, for all the care and love during this year.

Tausend Dank

Abstract

B lymphocytes have unquestionable importance in the immune system. In chickens, the B cell precursors initiate their development in the spleen and later migrate into the bursa of Fabricius via the blood, to become fully mature and diversified. However, the mechanisms and signals regulating such migration remain mostly unknown, as the methodology to isolate B cells in such early stages is challenging. In this work, a FACS-based methodology and RNA-sequencing analysis was established to isolate B cells from the crucial time points and locations of their development, starting at embryonic day 12 and the spleen, bursa and blood. Previous studies identified the CXCR4/CXCL12 mechanism as involved in B cell migration into the bursa, yet it was not necessary. RNA-sequencing analysis performed here revealed seven mechanisms possibly involved in B cell migration. Two of these are implicated in negative regulation, and five in positive regulation of cell migration. Overall, the CXCR5 receptor and its ligand CXCL13 are proposed here as necessary and sufficient mechanism for B cell migration, with their genes being highly expressed in the ED14 and ED16 bursal B cells. Further pathway enrichment analysis disclosed that the most prevalent pathways involved in B cell migration into the bursa were the cytokine-cytokine receptor interaction, MAPK and axon guidance. Overall, in this work a protocol for B cell isolation and a pipeline for obtaining good results with the further RNA-sequencing analysis were established.

Keywords: B lymphocytes, CXCR5/CXCL13, CXCR4/CXCL12, Chicken, Bursa, Migration, Spleen, Chemokines, RNA-sequencing, Transcriptomics

Resumo

Os linfócitos B têm uma importância inquestionável no sistema imune. Em galinhas, os precursores das células B iniciam o seu desenvolvimento no baço e depois migram para a bursa de Fabricius, através do sangue, para se maturarem e diversificarem. No entanto, os mecanismos e sinais que regulam esta migração permanecem, em grande parte desconhecidos, pois a metodologia para isolar estes linfócitos em períodos tão iniciais é desafiadora. Neste trabalho, uma metodologia baseada em FACS e sequenciação de RNA foi estabelecida com vista a isolar as células B nos períodos e locais cruciais do seu desenvolvimento, iniciando-se no dia embrionário (ED) 12 e do baço, bursa e sangue. Estudo anteriores identificaram o mecanismo CXCR4/CXCL12 como envolvido, mas não crítico na migração dos linfócitos B para a bursa. A análise dos dados de sequenciação de RNA realizada neste trabalho revelou sete mecanismos possivelmente envolvidos na migração de células B. Dois estão provavelmente implicados na regulação negativa, e os outros cinco na regulação positiva da migração celular. O recetor CXCR5 e seu ligando CXCL13 são propostos como um mecanismo necessário e suficiente para a migração de células B, com a sua expressão bastante acentuada no ED14 e 16 na bursa. Análises de enriquecimento de vias de sinalização revelaram que os sinais mais prevalentes envolvidos na migração de células B foram as interações citocina-recetor de citocina, MAPK e orientação de axónios. Em suma, neste trabalho foi estabelecido um protocolo para isolar linfócitos B e para realizar uma análise da sequenciação do RNA com êxito.

Palavras-chave: Linfócitos B, CXCR5/CXCL13, CXCR4/CXCL12, Galinha, Bursa, Migração, Baço, Quimiocinas, Sequenciação de RNA, Transcriptómica

Table of Contents

1. Introduction.....	1
1.1. Poultry Industry	1
1.2. Structure of the Avian Immune System	1
1.2.1. Bursa of Fabricius	2
1.2.1.1. Medulla and Cortex	4
1.2.2. The Spleen	4
1.2.2.1. Red pulp	5
1.2.2.2. White pulp.....	5
1.2.2.3. Germinal centre	5
1.3. Generation of the antibody repertoire	6
1.3.1. Avian Immunoglobulins	6
1.3.2. V(D)J recombination	7
1.3.3. Gene conversion	9
1.3.4. Immunoglobulin diversification	11
1.3.4.1. Immunoglobulin Isotype Switch	11
1.3.4.2. Somatic hypermutation	11
1.4. Development of B cells	12
1.4.1. Pre-bursal.....	12
1.4.2. Bursal	13
1.4.3. Post-bursal	17
1.4.4. Factors involved in B cell development.....	17
2. Objectives and Motivation	22
3. Materials and Methods.....	24
3.1. Buffers and media.....	24
3.2. Animals	24
3.3. Isolation of embryonic spleens and bursae	24
3.4. <i>In ovo</i> Blood Collection	24
3.5. Mononuclear Leucocytes Isolation	25
3.6. Cell Counting	25
3.7. MACS-based cell sorting	26

3.8. FACS-based cell sorting	27
3.9. Invitrogen Attune NxT Flow Cytometer and CytoFLEX SRT Cell Sorter	28
3.10. RNA Extraction	28
3.11. Bioanalyzer	29
3.12. cDNA Synthesis	30
3.13. Library Preparation and Illumina Next-Generation Sequencing	30
3.14. RNA-Sequencing Analysis.....	31
4. Results and Discussion	33
4.1. Methodology optimisation	33
4.1.1. Magnetic-activated cell sorting.....	33
4.1.1.1. MACS enriched B cells in the ED12 spleen but failed in the bursa.....	37
4.1.2. Fluorescence-activated cell sorting.....	38
4.1.2.1 FACS successfully isolated B cells in the spleen and bursa	41
4.2. The migration of B lymphocytes into the bursa might occur at later time points	42
4.2.1. Bu-1 ⁺ cell percentage in the ED12 bursa was higher than in the ED12 spleen.....	42
4.2.2. Bu-1 ⁺ cell percentage in the spleen and bursa increased in ED14.....	43
4.2.3. Bu-1 ⁺ cell percentage increased in the ED16 bursa and decreased in the ED16 spleen....	43
4.3. Gene expression analysis of B cells in the early stages of development.....	45
4.3.1. Similarity of the replicates was approved by Pearson correlation	47
4.3.2. Analysis of the differentially expressed genes between samples	48
4.3.3. Pathway Analysis	58
4.3.3.1. Cytokine-cytokine receptor interaction	58
4.3.3.2. The CXCR5/CXCL13 mechanism may be necessary and sufficient for B cell migration to the bursa.....	63
4.3.3.2. MAPK signalling Pathway.....	64
4.3.3.3. Axon guidance.....	65
5. Conclusions and Future Perspectives	68
6. References	69
7. Annexes.....	81

List of figures

- Figure 1. Schematic representation of a bursal follicle.** Each follicle is constituted by a cortical and a medullary region, in the upper part is the follicular associated epithelium (FAE), the interfollicular epithelium (IFE) and the bursal lumen. Inside the medulla are the B cells and the bursal secretory dendritic cell (BSDC). Separating the medulla and the cortex is the basement membrane, and interfollicular tissue exists between each follicle. This figure was retrieved from Madej J. *et al.* ¹⁵². 3
- Figure 2. The mechanism involved in the Immunoglobulin gene rearrangement.** On the left is illustrated the heavy chain rearrangement. The first step consists of rearranging the D_H and the J_H , and the second step is the junction of the V_H with the D_H . On the right is the Ig gene rearrangement of the light chain. The mechanism is alike, except that there is no D locus. This process involves the enzymes RAG-1 and RAG-2. The diversity generated is reduced, when combined the processes of the two chains there are around 1500 distinct Immunoglobulins. This figure was adapted from Avian Immunology (Third Edition) ⁴². 8
- Figure 3. Gene conversion event in the heavy and light chain of an immunoglobulin.** On the left is the gene conversion mechanism for the heavy chain. The arrows indicate the transfer of information from the pseudogenes to the V segment of the VDJ_H previously assembled. On the right is presented the same mechanism for the V segment of the light chain. The combinatorial diversity of three gene conversion events is much larger than the Ig gene rearrangement, it creates around 3,000,000,000 distinct combinations. The process of gene conversion is started by the AID enzyme stated. This scheme was adapted from Avian Immunology (Third Edition) ⁴². 9
- Figure 4. Schematic representation of the distinct stages of B cell development.** **A.** Migration of granulocytes and B cells to the bursal mesenchyme. **B.** Dendritic cells enter first in the epithelial buds. **C.** The follicles are colonised by B cells. **D.** Rapid proliferation and gene conversion events occur in the follicle until the hatch. This figure was adapted from Ratcliffe M. *et al.* ¹². 14
- Figure 5. Bursal development after hatch.** **A.** Structure of a bursal follicle, the follicles are separated by interfollicular connective tissue. **B.** After hatch, the FAE captures antigens from the bursal lumen and transports them into the follicle. **C.** Migration of B cells from the medulla across the basement membrane to the cortex, leading to the formation of the follicular cortex. **D.** Structure of the bursa after hatch, the B cells migrate to the periphery from the cortical zone. This figure was adapted from Ratcliffe M. *et al.* ¹². 16
- Figure 6. Experimental workflow to analyse by RNA-sequencing the B cells in ED12, ED14 and ED16, from the spleen, bursa and blood.** From these, single cell solutions, leucocyte fraction was isolated and B cells were stained for the sorting. RNA was extracted from B cells and converted into cDNA, the Illumina library pool was prepared and sequenced. The reads were mapped against the genome of reference, and the differential gene expression was investigated. This figure was created on Biorender.com. 23
- Figure 7. Representative images of the procedure to select a vein in the embryo to perform blood collection.** Triangle is drawn to indicate the direction of the chosen bloodstream to extract blood (left). The triangle was cut and removed without damaging the membrane (right). 25

Figure 8. Gating strategy for the identification of B cells. Cells were analysed in the CytoFLEX SRT Cell Sorter. **A.** PC7-A vs FSC-A permitted the elimination of dead cells, and a gate was drawn in the live cells, which are PC7⁻. **B.** SSC-A vs SSC-H were employed to eliminate the doublets, the gate contains the single cells. **C.** FITC-A vs FSC-A against was gated to select the Bu-1⁺ cells, which are the B cells. These figures were obtained from FlowJo™ v10.8 Software (BD Life Sciences) ¹⁰¹..... 28

Figure 9. MACS flow cytometrical data of Bu-1⁺ cells in ED12 splenic and bursal B cells sample. The spleens (n=113) **(A)** and the bursae (n=30) **(B)**, from ED12 embryos, were extracted, pooled and smashed, and the lymphocyte fraction was isolated by density gradient centrifugation on Ficoll. The B cells were stained with Bu-1-Biotin antibody and Streptavidin MicroBeads for MACS and subsequently stained with Fixable Viability Dye eFluor™ 780 and Mouse Anti-Chicken Bu-1-FITC for flow cytometry. The left panel shows the percentage of Bu-1⁺ cells before MACS, and the right panel illustrates the percentage of Bu-1⁺ cells after performing MACS. These figures were obtained from FlowJo™ v10.8 Software (BD Life Sciences) ¹⁰¹..... 34

Figure 10. MACS flow cytometrical data of Bu-1⁺ cells in ED12 spleen (A) and DT40 cells (B). A. The spleens from ED12 embryos (n=30) were extracted, pooled and smashed, and the lymphocyte fraction was isolated by density gradient centrifugation on Ficoll. The B cells were stained with Fixable Viability Dye eFluor™ 780 and Mouse Anti-Chicken Bu-1-FITC for flow cytometry. The left panel shows the percentage of Bu-1⁺ cells in the unstained fraction of cells, and the right panel illustrates the percentage of Bu-1⁺ cells after performing the staining. **B.** The DT40 cells were stained for B cells with Fixable Viability Dye eFluor™ 780 and Mouse Anti-Chicken Bu-1-FITC for flow cytometry. The left panel shows the percentage of Bu-1⁺ cells in the unstained fraction of the cells, and the right panel illustrates the percentage of Bu-1⁺ cells after performing the staining. These figures were obtained from FlowJo™ v10.8 Software (BD Life Sciences) ¹⁰¹..... 35

Figure 11. MACS flow cytometrical data of Bu-1⁺ cells in ED14 splenic B cells and in a broiler spleen. A. The spleens from ED14 embryos (n=30) and **B.** the spleen from a broiler (n=1), were extracted, pooled and smashed, and the lymphocyte fraction was isolated by density gradient centrifugation on Ficoll. The B cells were stained with Bu-1-FITC antibody and anti-FITC MicroBeads for MACS and stained with Fixable Viability Dye eFluor™ 780 for flow cytometry. The left panel shows the percentage of Bu-1⁺ cells before MACS, and the right panel illustrates the percentage of Bu-1⁺ cells after performing MACS. These figures were obtained from FlowJo™ v10.8 Software (BD Life Sciences) ¹⁰¹..... 36

Figure 12. MACS flow cytometrical comparing two MACS antibodies to isolate Bu-1⁺ cells in the blood of a broiler. The lymphocyte fraction was separated from the blood by density gradient centrifugation on Ficoll. **A.** The B cells were stained with Bu-1-FITC antibody and Anti-FITC MicroBeads for MACS and stained with Fixable Viability Dye eFluor™ 780 for flow cytometry. The left panel shows the percentage of Bu-1⁺ cells before MACS, and the right panel illustrates the percentage of Bu-1⁺ cells after performing MACS. **B.** The B cells were stained with Bu-1-AF647 antibody and Anti-Cy5/Anti-Alexa Fluor 647 MicroBeads for MACS and stained with Fixable Viability Dye eFluor™ 780 for flow cytometry. The left panel shows the percentage of Bu-1⁺ cells before MACS, and the right panel illustrates the

percentage of Bu-1⁺ cells after performing MACS. These figures were obtained from FlowJo™ v10.8 Software (BD Life Sciences) ¹⁰¹..... 36

Figure 13. MACS flow cytometrical data of Bu-1⁺ cells (A) and PC7⁻ cells (B) from ED12 splenic B cells. The spleens from ED12 embryos (n=37) were extracted, pooled and smashed, and the lymphocyte fraction was isolated by density gradient centrifugation on Ficoll. The B cells were stained with Bu-1-AF647 antibody and Anti-Cy5/Anti-Alexa Fluor 647 MicroBeads for MACS and stained with Fixable Viability Dye eFluor™ 780 for flow cytometry. **A.** Percentage of Bu-1⁺ cells in the ED12 splenic sample before and after MACS. **B.** Percentage of PC7⁻ cells in the splenic sample before and after MACS. The graphs correspond to the same as in sample A. These figures were obtained from FlowJo™ v10.8 Software (BD Life Sciences) ¹⁰¹..... 37

Figure 14. MACS flow cytometrical data of Bu-1⁺ cells (A) and PC7⁻ cells (B) from ED12 bursal B cells. The bursae from ED12 embryos (n=35) were extracted, pooled and smashed, and the lymphocyte fraction was isolated by density gradient centrifugation on Ficoll. The B cells were stained with Bu-1-AF647 antibody and Anti-Cy5/Anti-Alexa Fluor 647 MicroBeads for MACS, and after stained with Fixable Viability Dye eFluor™ 780 for flow cytometry. **A.** Percentage of Bu-1⁺ cells in the ED12 bursal sample before and after MACS **B.** Percentage of PC7⁻ cells in the bursal sample before and after MACS. These figures were obtained from FlowJo™ v10.8 Software (BD Life Sciences) ¹⁰¹..... 38

Figure 15. FACS flow cytometrical data of Bu-1⁺ cells from ED14 spleen (A) and bursa (B). The spleens (A) and bursae (B) from ED12 embryos (n=30) were extracted, pooled and smashed, and the lymphocyte fraction was isolated by density gradient centrifugation on Ficoll. The B cells were stained with Fixable Viability Dye eFluor™ 780 and Mouse Anti-Chicken Bu-1-FITC for flow cytometry. **A.** The left panel shows the percentage of live cells in the spleen sample before FACS, the middle panel represents the Bu-1⁺ cells in the spleen sample before FACS, and the right panel illustrates the percentage of Bu-1⁺ cells after performing FACS. **B.** The left panel shows the percentage of live cells in the bursa sample before FACS, the middle panel represents the Bu-1⁺ cells in the bursa sample before FACS, and the right panel illustrates the percentage of Bu-1⁺ cells after performing FACS. These figures were obtained from FlowJo™ v10.8 Software (BD Life Sciences) ¹⁰¹..... 39

Figure 16. FACS flow cytometrical data of live cells from ED12 spleen (A) and bursa (B). The spleen (A) and bursa (B) from ED12 embryos (n=30) were extracted, pooled and smashed, and the lymphocyte fraction was isolated by density gradient centrifugation on Ficoll. The B cells were stained with Fixable Viability Dye eFluor™ 780 and Mouse Anti-Chicken Bu-1-FITC for FACS. **A.** Percentage of PC7⁻ cells (live cells) in the spleen sample after FACS was performed. **B.** Percentage of PC7⁻ cells (live cells) in the bursa sample after FACS. These figures were obtained from FlowJo™ v10.8 Software (BD Life Sciences) ¹⁰¹..... 40

Figure 17. FACS flow cytometrical data of live cells from ED14 splenic (A) and bursal (B) B cells. The spleen (A) and bursa (B) from ED14 embryos (n=9) were extracted, pooled and smashed, and the lymphocyte fraction was isolated by density gradient centrifugation on Ficoll. The B cells were stained with Fixable Viability Dye eFluor™ 780 and Mouse Anti-Chicken Bu-1-FITC for FACS. **A.** Percentage of PC7⁻ cells (live cells) in the spleen sample after FACS was performed. **B.** Percentage of PC7⁻ cells (live

cells) in the bursa sample after FACS. These figures were obtained from FlowJo™ v10.8 Software (BD Life Sciences) ¹⁰¹. 40

Figure 18. FACS flow cytometrical data of Bu-1⁺ cells (A & B) and PC7⁻ cells (C & D) from an ED13 splenic (A,C) and bursal sample (B,D). The organs from ED13 embryos (n=15) were extracted, pooled and smashed, and the lymphocyte fraction was isolated by density gradient centrifugation on Ficoll. The B cells were stained with Bu-1-FITC and with Fixable Viability Dye eFluor™ 780 for flow cytometry. **A.** Percentage of Bu-1⁺ cells in the ED13 spleen sample before and after FACS. **B.** Percentage of Bu-1⁺ cells in the ED13 bursa sample before and after FACS. **C.** Percentage of PC7⁻ cells in the spleen sample before and after FACS. **D.** Percentage of PC7⁻ cells in the bursa sample before and after FACS. These figures were obtained from FlowJo™ v10.8 Software (BD Life Sciences) ¹⁰¹. 41

Figure 19. Flow cytometrical data of Bu-1⁺ cells from the spleen (left), blood (middle) and bursa (right) on ED12 (A), ED14 (B) and ED16 (C). The spleens and bursae (ED12: n=15, ED14: n=11, ED16: n= 30) were extracted from the embryos, pooled, smashed, and blood was collected. The lymphocyte fraction was isolated by density gradient centrifugation on Ficoll. The B cells were stained with Fixable Viability Dye eFluor™ 780 and Mouse Anti-Chicken Bu-1-FITC for FACS. These figures were obtained from FlowJo™ v10.8 Software (BD Life Sciences) ¹⁰¹. **A.** Percentage of Bu-1⁺ cells in ED12 spleen, blood and bursa, respectively. **B.** Percentage of Bu-1⁺ cells in ED14 spleen, blood and bursa, respectively. **C.** Percentage of Bu-1⁺ cells in ED16 spleen, blood and bursa, respectively. 44

Figure 20. Summary of the migration of B cells in their developmental stages. A. Percentage of Bu-1⁺ cells in the spleen, bursa and blood for the time points ED12 (blue), ED14 (green) and ED16 (red). **B.** Amplification of the data from the blood represented in A. Each dot corresponds to one experiment. For each location and time point, at least three replicates were obtained. The data was plotted in a scatter plot with the mean, and the error bars correspond to the standard deviation (SD). This figure was designed with GraphPad Prism ¹⁵³. 45

Figure 21. Heat map representation of the Pearson correlation test for the replicates of each sample in each time point, for spleen (A), bursa (B) and blood (C). Each square contains one R² value, and the darker the blue, the higher the value, hence the more similar the replicates are. The R² values presented were calculated in ArrayStar® ⁹⁶ and the heat maps were obtained with GraphPad Prism ¹⁵³. 47

Figure 22. Protein-Protein Interaction Network of the DEGs in ED12, ED14 and ED16 spleen. The list of DEGs obtained from ArrayStar® ⁹⁶ was subjected to a PPI analysis with the STRING® ¹⁰⁶ tool. The cytokine-cytokine receptor interactions (red), MAPK signalling pathway (blue), axon guidance (green) and the Wnt signalling pathway (yellow) were the most prevalent pathways. The edges represent the protein-protein associations, the known interactions (light blue and purple), the predicted interactions (green, orange, blue) and others (yellow, black, violet). A kmeans clustering was performed with the creation of 3 clusters shown by the dotted line between the proteins. 49

Figure 23. Protein-Protein Interaction Network of the DEGs in ED14 and ED16 bursa. The list of DEGs obtained from ArrayStar® ⁹⁶ was subjected to a PPI analysis with the STRING® ¹⁰⁶ tool. The cytokine-cytokine receptor interactions (red), MAPK signalling pathway (blue), calcium signalling pathway (green) and focal adhesion (yellow) were the most prevalent pathways. The edges represent

the protein-protein associations, the known interactions (light blue and purple), the predicted interactions (green, orange, blue) and others (yellow, black, violet). A kmeans clustering was performed with the creation of 3 clusters shown by the dotted line between the proteins. 50

Figure 24. Heat map of the DEGs between ED12, ED14 and ED16 splenic B cells (A) and ED14 and ED16 bursal B cells (B). Hierarchical clustering was performed with the list of DEGs and the corresponding samples. In blue are the low expressed genes, in yellow the medium expressed and in red the highly expressed. This figure was obtained with ArrayStar^{®96}. 51

Figure 25. Protein-Protein Interaction Network of the DEGs in ED12, ED14 and ED16 blood. The list of DEGs obtained from ArrayStar^{®96} was subjected to a PPI analysis with the STRING^{®106} tool . The cytokine-cytokine receptor interactions (red), MAPK signalling pathway (blue), axon guidance (green) and the Wnt signalling pathway (yellow) were the most prevalent pathways. The edges represent the protein-protein associations, the known interactions (light blue and purple), the predicted interactions (green, orange, blue) and others (yellow, black, violet). A kmeans clustering was performed with the creation of 3 clusters shown by the dotted line between the proteins. 52

Figure 26. Heat map of the DEGs between ED12, ED14 and ED16 blood B cells (A) and ED12 splenic and blood B cells (B). Hierarchical clustering was performed with the list of DEGs and the correspondent samples. In blue are the low expressed genes, in yellow the medium expressed and in red the highly expressed. This figure was obtained with ArrayStar^{®96}. 53

Figure 27. Protein-Protein Interaction Network of the DEGs in ED12 spleen and blood. The list of DEGs obtained from ArrayStar^{®96} was subjected to a PPI analysis with the STRING^{®106} tool. The cytokine-cytokine receptor interactions (red), MAPK signalling pathway (blue), axon guidance (green), the focal adhesion (yellow) and the Toll-like receptor pathway (purple) were the most prevalent pathways. The edges represent the protein-protein associations, the known interactions (light blue and purple), the predicted interactions (green, orange, blue) and others (yellow, black, violet). A kmeans clustering was performed with the creation of 3 clusters shown by the dotted line between the proteins. 54

Figure 28. Protein-Protein Interaction Network of the DEGs in ED14 spleen, bursa and blood. The list of DEGs obtained from ArrayStar^{®96} was subjected to a PPI analysis with the STRING^{®106} tool. The cytokine-cytokine receptor interactions (red), MAPK pathway (blue), axon guidance (green) and focal adhesion (yellow) were the most prevalent pathways. The edges represent the protein-protein associations, the known interactions (light blue and purple), the predicted interactions (green, orange, blue) and others (yellow, black, violet). A kmeans clustering was performed with the creation of 3 clusters shown by the dotted line between the proteins. 55

Figure 29. Protein-Protein Interaction Network of the DEGs in ED16 splenic, bursal and blood B cells. The list of DEGs obtained from ArrayStar^{®96} was subjected to a PPI analysis with the STRING^{®106} tool . The cytokine-cytokine receptor interactions (red), MAPK signalling pathway (blue), axon guidance (green), focal adhesion (yellow) and the intestinal immune network for IgA production (purple) were the most prevalent pathways. The edges represent the protein-protein associations, the known interactions (light blue and purple), the predicted interactions (green, orange, blue) and others (yellow,

black, violet). A kmeans clustering was performed with the creation of 3 clusters shown by the dotted line between the proteins..... 56

Figure 30. Heat map of the DEGs between ED14 splenic, bursal and blood B cells (A) and ED16 splenic, bursal and blood B cells (B) . Hierarchical clustering was performed with the list of DEGs and the correspondent samples. In blue are the low expressed genes, in yellow the medium expressed and in red the highly expressed. This figure was obtained with ArrayStar^{® 96}. 57

Figure 31. Heat map of the genes involved in cytokine-cytokine interaction. The genes involved in the cytokine pathway were selected and plotted in a heat map to compare the expression between the samples. In blue are the low expressed genes, in yellow the medium expressed and in red the highly expressed. This figure was obtained with ArrayStar^{® 96}. 58

Figure 32. Heat map representation of the differentially expressed between all samples involved in MAPK pathway. The genes that were differentially expressed between each sample and involved in the MAPK pathway were selected and plotted in a heat map to compare the expression between the samples. In blue are the low expressed genes, in yellow the medium expressed and in red the highly expressed. This figure was obtained with ArrayStar^{® 96}. 64

Figure 33. Heat map representation of the differentially expressed genes between the samples involved in Axon guidance. The genes that were differentially expressed between each sample and involved in Axon guidance were selected and plotted in a heat map to compare the expression between the samples. In blue are the low expressed genes, in yellow the medium expressed and in red the highly expressed. This figure was obtained with ArrayStar^{® 96}. 66

List of Tables

Table 1. The volume of blood (μL) possible to collect according to the age of the embryo regardless of survival, according to the internal standard operating procedure.	25
Table 2. Sample treatments performed in each experiment. UNS: unstained, L/D: live dead, AF: Alexa Fluor. Full stained is both L/D and FITC or AF.....	26
Table 3. Antibodies and MicroBeads tested in MACS and FACS. The name, dilution and supplier of the antibody are presented, as well as the name and supplier of the correspondent MicroBeads.....	26
Table 4. The volume of BL + TG Buffer and 100% isopropanol utilised according to the number of B cells in each sample. This table was retrieved from the ReliaPrep™ RNA Cell Miniprep protocol.	29
Table 5. List of the samples compared. Two types of comparisons were performed, first comparing the DEGs of B cells in the same location at different time points, and in distinct locations at the same time point.	32
Table 6. List of the definitive comparisons between samples. The list of DEGs of each isolated comparison was merged, and six global comparisons were achieved, each location (spleen, bursa and blood) in the three time points (ED12, ED14, ED16). The samples in red are missing.	32
Table 7. Data sent for Next Generation Sequencing. The embryonic day, date, origin of the B cells, RNA concentration measured in the bioanalyzer in $\text{pg}/\mu\text{L}$ and the RNA integrity number are displayed for the 27 samples selected for sequencing. For each time point and location three replicates were obtained.....	46
Table 8. Quantity and quality parameters of the library pool. A. Quantification via Qubit® dsDNA HS Assay Kit and the qPCR-based NEBNext® Library Quant Kit. The sample ID, library size in base pairs, the calculated concentration from Qubit® and the measured concentration from NEBNext® in nanomolar (nM) are shown. B. Quality parameters of the library pool by the SAV software. The ID of the run and sample, the yield in Gigabytes (Gb) and the percentage of Q30 bases.	46
Table 9. Summary of the mechanisms investigated that are involved in the cytokine receptor interaction. The receptor, ligand, importance and outcome as possible mechanisms for cell migration are shown.	63

Abbreviations

AID- Activation-induced cytidine deaminase

AF- Alexa Fluor

ALV- Avian leukosis virus

BAFF- B cell-activating factor

BAFFR- BAFF receptor

BCR- B Cell receptor

B_{mem}- memory B cells

BSA- Bovine serum albumin

BSDC- Bursal secretory dendritic cell

C- Constant region

CD- Cluster of Differentiation

cDNA- Complementary DNA

CSR- Class switch recombination

CSS- Schweigger-Seidel sheath

CXCR- CXC receptors

D- Diversity region

DEG- Differentially expressed genes

DSB- Double-strand break

dsDNA- Double strand DNA

ECM- Extracellular matrix

ED- Embryonic day

EGF- Epidermal growth factor

ERK- Extracellular-signal-regulated kinase

FACS- Fluorescence activated cell sorting

FAE- Follicle associated epithelium

FDR- False Discovery Rate

FGF- fibroblast growth factor

FITC- Fluorescein isothiocyanate

GC- Germinal Center

GO- Gene Ontology

H- Heavy chain

IBDV- Infectious bursal disease virus

IFE- Interfollicular epithelium

Ig- Immunoglobulin

IL- Interleukin

JAK- STAT- Janus kinase signal transducer and activator of transcription

JNK- Jun N-terminus kinase

L- Light chain

LD PCR- Long distance PCR

MACS- Magnetic activated cell sorting

MAPK- Mitogen-activated protein kinase

N nucleotides- Non-templated nucleotides

Nt- Nucleotide

P nucleotides- Palindromic nucleotides

PALS- Periarteriolar lymphoid sheaths

PBS- Phosphate-buffered saline

PC7- Phycoerythrin-cyanine 7

PCR- Polymerase chain reaction

PDGF- Platelet-derived growth factor

PPI- Protein-protein interaction

PWP- Periellipsoidal white pulp

qPCR- Quantitative PCR

RAG-1- Recombination Activating Gene 1

RAG-2- Recombination Activating Gene 2

RIN- RNA integrity number

RNA- Ribonucleic acid

RNA-seq- RNA-sequencing

RSS- Recombination Signal Sequences

SHM- Somatic hypermutation

Tdt- Terminal deoxynucleotidyl transferase

TGF- β - transforming growth factor β

TLR- Toll-like receptor

TNF- Tumour necrosis factor

TNFR- TNF receptor

UNG- Uracil DNA glycosylase

V- Variable region

VEGF- vascular endothelial growth factor

Ψ genes- Pseudogenes

1. Introduction

1.1. Poultry Industry

According to the Food and Agriculture Organization, in the succeeding years, the global consumption of animal protein will increase significantly ¹. Hence, the meat sector must grow accordingly to feed the entire population. Poultry is one of the livestock sectors with the highest growth rate. Chickens pose the advantage of producing two different products, meat and eggs. Besides, they have the lowest feed conversion rate and release the lowest amounts of carbon dioxide compared to other meat livestock sectors ². Therefore, chickens pose the wisest choice financially and environmentally.

In line with these advantages, the poultry industry has become more intense each year, which accelerates problems related to the welfare of the chickens. In poultry houses, animals are at high stock densities, and such unfavourable conditions lead to a high rate of pathogen propagation and, consequently, a higher mortality ³. This increase in disease spreading leads to enormous economic losses. One example of a pathogen contributing to massive financial losses, is the avian leukosis virus (ALV), where infected chickens have reduced weight and egg production ⁴. This virus has an enormous ability to overcome the chicken's vaccination and infect them, thus posing a global problem ⁵. Therefore, understanding the chicken's innate and adaptative system is of immense importance to provide them with more tools to fight and protect them against pathogens.

The role of B cells in the defence against pathogens is indisputable. These cells can produce antibodies and are an integral part of humoral immunity, vital for establishing immunological memory ⁶. However, not nearly as much is known about B cell development in chickens compared to mammals. In the last years, there has been a rising interest in studying the regulation mechanisms of the migration and development of B cells. Several approaches have been performed, such as quantitative PCR (qPCR) and RNA-sequencing (RNA-seq), to dissect the critical regulatory factors involved in developing B lymphocytes ⁷⁻¹⁰.

1.2. Structure of the Avian Immune System

There are several broad similarities between the avian and the human immune system. The general mechanisms and flow to establish an immune response are analogous. First, there needs to be antigen exposure and further uptake of this molecule, then mononuclear cells process and present it to lymphocytes. These trigger a specific immune response, and numerous effector mechanisms against the pathogen. There is rigorous control of these steps in both organisms to guarantee a suitable immune response ¹¹.

Nevertheless, looking at the details, it is noticeable that these two organisms have some differences. One of the main disparities regards the primary lymphoid organs. In humans and murine, the bone marrow is the primary lymphoid organ for B cell development. However, chickens' resort to the bursa of Fabricius, a unique organ for birds ¹². Another discrepancy is the absence of organized lymph nodes in birds, which were described in humans. Instead, chickens have developed diffuse lymphoid tissue, such

as the mucosa-associated lymphoid tissues, which includes the gut-associated lymphoid tissue (GALT), the respiratory-associated lymphoid tissue and the reproductive-associated lymphoid tissue¹³. Another critical distinction in the humoral immune system of these two organisms regards the period in which the antibody repertoire is formed. In humans and murine, the antibody repertoire can be diversified throughout life, whilst chickens are restricted to producing it entirely during embryonic stages¹⁴. Furthermore, for humans to generate a vast pre-immune antibody repertoire, B cells undergo one single process, designated as immunoglobulin (Ig) gene rearrangement. However, this gene rearrangement process in chickens does not contribute to antibody diversity. Therefore, avian B cells need to undergo an additional gene conversion mechanism to generate the wide variety, which occurs at the bursa of Fabricius¹⁴. Even so, despite existing considerable discrepancies between these organisms, most of the knowledge about human and murine immunology can be utilised to hypothesize how the chicken's mechanism occurs by homology.

Concerning the chicken's immune system, it is constituted by two primary lymphoid organs, the bursa of Fabricius, as mentioned, and the thymus, which is responsible for T cell development. Broadly, these organs are colonised by lymphoid precursor cells from the yolk sac, para-aortic foci, blood, spleen, and bone marrow, and are responsible for the maturation of B and T cells. Once mature, cells migrate to the secondary lymphoid organs, that is, the spleen, bone marrow and GALT. Following colonization, B and T lymphocytes are activated and become able to participate actively in immune responses^{14,15}.

Briefly, this project aims to investigate the early development stages of B cells in the chicken embryo, mainly focusing on how cell migration from the spleen to the bursa occurs. Hence, the main emphasis of the theoretical introduction are the multiple organs involved in B cell development and the mechanism responsible for generating and diversifying these cells.

1.2.1. Bursa of Fabricius

The name Bursa of Fabricius comes from the scientist Hieronymus Fabricius of Acquapendente, who identified the bursa in birds¹⁶. The chicken bursa has the size and shape of a chestnut and is located between the cloaca and the sacrum and is crucial to the progress of B cells and the generation of the antibody repertoire^{13,17}. The development of B cells initiates with hematopoietic cells (HSC) from the dorsal aorta that colonise the embryonic spleen. Afterwards, pre-bursal cells emigrate from here to occupy the bursa during the embryonic stage. Before hatch, there is antigen-independent differentiation and diversification of the B cells in the bursa. After hatch, the B cell development in the bursa is influenced by environmental antigens, thus becoming antigen-dependent¹². At this time, the B lymphocytes emigrate to the peripheral organs, participating in humoral immunity and antigen response⁶. The importance of the bursa in the humoral immune system was first suggested when Glick and its colleagues removed the bursa of embryonic chickens and inferred that, later in life, these birds had no specific antibody response to pathogens¹⁷. It was later realized that the antibody repertoire is assembled throughout a short period of time in this organ, more specifically, it is formed during late embryonic stages and in a short period after hatching. The bursa reaches its maximum size at 8 to 10 weeks, and then this organ undergoes involution at 6 to 7 months of age⁶. Consequently, when chickens are adults, they need to rely on post-bursal stem cells in the bone marrow as a source of B cells¹⁸. It is an elevated

risk to generate the entire antibody repertoire in such a short time and only one location. If the bursa is removed during embryonic development, as performed by Glick *et al.*, the humoral immunity is hampered¹⁷. This occurs because the organ where the antibody repertoire is produced is eliminated, hence these chickens have a nonspecific and weak adaptive immune response to pathogens¹⁹. Similarly, if the chicken embryo is infected by a pathogen that targets bursal cells, such as the infectious bursal disease virus (IBDV), a small RNA virus, the further humoral immune response is compromised²⁰. These findings illustrate the importance of the bursa of Fabricius as a primary lymphoid organ in birds where the repertoire of antibodies is formed.

The antibody repertoire's diversity is originated in the bursa through a process designated as gene conversion²¹. As mentioned, in humans, antibody diversity is achieved through Ig gene rearrangement (or designated also as V(D)J recombination). However, in chickens it does not contribute significantly to the variety of the antibody repertoire, because there is a diminished number of gene combinations possible in the chicken's heavy and light chain locus. While in humans, an enormous number of varieties are feasible, as there are multiple genes in the Ig locus. Consequently, after Ig gene rearrangement, chicken B cells undergo gene conversion in the bursa to generate Ig diversity¹². Once B cells are fully matured and diversified in the bursa, they start to emigrate to the spleen, bone marrow and other secondary lymphoid tissues. The period of B cell migration initiates before hatching and goes until sexual maturity, when bursal involution is practically complete⁶.

Briefly, regarding the constitution of the bursa (**Figure 1**), it is enclosed by a muscle layer essential for the movement of cells. Inner folds harbour the bursal follicles, which are colonised by B cells and its where the gene conversion process takes place¹³. As visible in **Figure 1**, each bursal follicle is composed of the medulla and the cortex, separated by blood and lymphatic vessels. Surrounding the follicles is the surface epithelium, comprising the interfollicular epithelium (IFE) and the follicle-associated epithelium (FAE). The FAE covers the upper part of the follicle and connects it to the bursal lumen. After hatch, antigens that arrive at the bursal lumen can be transported by the FAE into the medulla, which is a vital step for both B cell and bursal development^{13,22}. There are approximately 10,000 follicles per bursa, and each follicle is colonised by about 2 to 5 single B cell precursors. After, in this

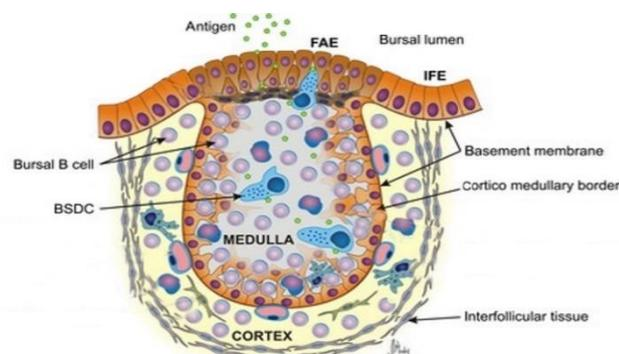


Figure 1. Schematic representation of a bursal follicle. Each follicle is constituted by a cortical and a medullary region, in the upper part is the follicular associated epithelium (FAE), the interfollicular epithelium (IFE) and the bursal lumen. Inside the medulla are the B cells and the bursal secretory dendritic cell (BSDC). Separating the medulla and the cortex is the basement membrane, and interfollicular tissue exists between each follicle. This figure was retrieved from Madej J. *et al.*¹⁵².

location occurs the B cell expansion and diversification. By this time, the number of B cells in each follicle increases to around 150,000 cells ^{23–25}.

1.2.1.1. Medulla and Cortex

The medulla comprises epithelial cells and hematopoietic cells, namely lymphoid cells, dendritic cells, and some macrophages ⁶. At ED10 to 13, BSDC precursors and B lymphocytes pass through the bursal epithelium and induce follicle formation. The colonization of the follicles by B cells occurs in two steps. First, dendritic cells and epithelial cells form the epithelial buds, and then it is colonised by the B cells that have entered the bursa, originating a bursal follicle ^{13,26,27}. Most of the lymphocytes in the medulla are B cells, which can proliferate between this location and the cortex. Around the hatch, as B cells are emigrating from this organ, the number of lymphocytes starts decreasing in the medulla and increasing in the cortex ⁶. And so, the cortical region begins its development around this period, with the formation of a surrounding outer cortex of cells. In this area occurs most cell division after hatch, and from here that B cells emigrate to the peripheric lymphoid tissues ¹². The cortical region's development is antigen-dependent since the migration and proliferation of B cells from the medulla to the cortex occurs in response to the presentation of gut antigens ^{28,29}.

1.2.2. The Spleen

Another vital organ in B cell development is the spleen. It is an oval structure situated near the proventriculus, and its development starts by the formation of a mass of mesenchymal cells at around 48 hours of life. The spleen begins to be colonised by HSC at ED6 to 7. It has a crucial role in B cell development, as the stem cells that have reached it can initiate Ig gene rearrangement, or designated as V(D)J recombination ⁶. In this process, the genes of the different Ig segments (variable, diversity and joining segments) of both heavy and light chains are rearranged. V(D)J recombination comprises two steps; the first involves the heavy chain only, and HSC that have undergone it become committed to the B lineage. The final step involves both Ig heavy and light chains and can either be completed in the spleen or later inside the bursa ¹². In the spleen, occurs the first step of V(D)J and some B cells may finish the second step, but it is not mandatory ¹³.

After hatching, the spleen fully develops and becomes a secondary lymphoid organ, yet for this to occur, it must be exposed to antigens ³⁰. This phenomenon was seen by Hedge *et al.*, in which germ-free chickens had spleen maturation hampered and no germinal centres inside it ³¹. It was suggested that since germ-free chickens lack antigen presentation to B cells, it may compromise their development and proliferation to the spleen, thus hampering this organ's growth. In normal conditions after hatch, the spleen is a site for antigen-dependent proliferation and differentiation of lymphocytes, contrasting with the bursa, which is primarily responsible for antigen-independent proliferation ³⁰. In the final stages of B cell development, the antigen-activated post-bursal B cells in spleen expand and become more diversified through class switch recombination (CSR), gene conversion and somatic hypermutation (SHM). The latter two occur in the germinal centres (GC), while CSR occurs prior in the spleen microenvironment ^{32,33}. Henceforth, this organ plays a crucial role in the early and final stages of B lymphocyte differentiation and recircularization, as it provides an environment for post-bursal modifications, the formation of memory and plasma cells, while contributing to the antigens' uptake and

presentation. These aspects sum up one of the two prominent roles of the spleen in vertebrates: disease resistance. The second key role of the spleen is assisting in oxygen supply, as this organ is responsible for removing from circulation damaged erythrocytes, and during early stages, it is also involved in erythropoiesis. However, the chicken spleen is not a blood reservoir as occurs in mammals ³⁰.

Regarding the structure of the spleen, there are two main divisions, the red and the white pulp.

1.2.2.1. Red pulp

In the early stages of splenic development, the red pulp functions as a hematopoietic organ. Once the chicken becomes an adult, the process of haematopoiesis decreases in this location and is thought to remain in the bone marrow. At this time, the red pulp becomes crucial to remove damaged erythrocytes from circulation, thereby becoming responsible for maintaining proper tissue oxygenation ³⁰. Besides these functions, the red pulp is also vital in lymphocyte development and the secretion of antibodies to circulation. Some antigens trapped by the spleen can be redistributed from the white pulp and other regions to the red pulp. Antigens are absorbed by red pulp macrophages and can be presented to B cells in this location ³⁴.

1.2.2.2. White pulp

The white pulp contains mostly lymphocytes and no erythrocytes, as the red pulp does. It surrounds the splenic vascular region and is morphologically subdivided into three lymphoid regions, the periarteriolar lymphoid sheaths (PALS), periellipsoidal white pulp (PWP) and the germinal centres (GC) ³⁰. The PALS region is the T-dependent zone of the spleen, whereas the PWP and the GC are the B-dependent zones. It is mainly in the GCs that B lymphocytes proliferate and undergo maturation processes after bursal development ^{30,35}. Now in more detail focusing on the different sections of the white pulp.

Periarteriolar lymphoid sheaths – PALS

The PALS region consists of a dense sheath of T lymphocytes surrounding the arterioles. It contains T helper cells, which play a crucial role in regulating immune responses and B cell development, as in mammals. The activation of these T helper cells is necessary for the response of B cells ¹³.

Periellipsoidal white pulp - PWP

Regarding the PWP, it contains ellipsoid cells, which are revested by a discontinuous capsule forming an antigen filtering system, preventing intravenous antigens from diffusing freely into the PWP ¹³. Surrounding the PWP is a ring of macrophage cells, and this area is classified as similar to the marginal zone of the mammalian spleen ³⁶.

1.2.2.3. Germinal centre

A germinal centre consists of aggregates of cells that arise after antigen stimulation, and in birds, these occur in defined locations within the peripheral tissues. Regarding the GCs of the spleen, these start developing near the blood vessel branching in the T cell zone, PALS ¹³. The activated post-bursal B cells emigrate from the bursa to the spleen, enter the GCs where they expand and proliferate heavily. In each GC of the spleen, 6 to 12 B cells are hypothesised to be initially expanding ³³.

In the GC of the spleen, B cells have their B cell receptor additionally modified by gene conversion and somatic hypermutation. These processes originated further diversity in the variable region of the heavy and light chain, originating antigen-specific immunoglobulins, resulting in a more robust and directed humoral response³³. Interestingly, B cells expressing different Ig isotypes, such as IgY and IgA, have been identified in GC. Hence class switch recombination events were suggested to take place in the GCs, nevertheless, recent studies revealed that CSR most likely occurs prior to B cell migration into the GCs³².

1.3. Generation of the antibody repertoire

For chicken B cells to generate a vast antibody repertoire, they must migrate from the spleen into the bursa. Generating a vast antibody repertoire is critical for further establishing specific and robust immune responses, as a diverse repertoire increases the probability of having an Ig specific for all the possible antigens that might arise from pathogens. Succinctly, in humans and murine, the diversity of the pre-immune antibody repertoire is entirely derived from V(D)J recombination events. Nevertheless, for the mature antibody repertoire, two other processes further diversify the rearranged Ig molecules, namely SHM and CSR events¹². These occur during secondary immune responses in the germinal centres of the peripheral lymphoid tissues.

Regarding chickens, the Ig structure is assembled by V(D)J recombination, however, this process does not create diversity, for a reason explained shortly. Therefore, chicken B cells must undergo a gene conversion process in the bursa to diversify the variable region of the previously assembled Ig. Similar to humans, SHM and CSR mechanisms occur after in the secondary lymphoid organs^{12,33}. SHM can occur in some extension in the bursa, nevertheless it is not as significant as in the secondary lymphoid tissues³⁷. The mechanism employed by chickens to generate diversified immunoglobulins is detailed in this next section.

1.3.1. Avian Immunoglobulins

Immunoglobulins are glycoproteins constituted by two light (L) and two heavy (H) chains that assemble and form a monomeric unit. Each chain is formed by a variable part (V) where the antigens bind, and a constant part (C) that defines the Ig class. The heavy chain also includes a diversity locus (D) located between the V and J segments. Every Ig class has distinct biochemistry characteristics, resulting in different abilities to migrate to cells or tissues; hence, all classes exert unique functions. Immunoglobulins can be in two distinct forms, either attached to the membrane of the B cell, being a B cell receptor (BCR), or in a soluble and secreted form, designated as antibody¹³.

Chickens only possess three distinct Ig classes, unlike mammals, which have five. More specifically, the chicken-heavy chain locus contains three constant regions. These C regions encode for the μ , α and u Ig heavy chains of IgM, IgA and IgY, respectively. Regarding the constitution of the light chain, mammals have two distinct loci, λ and κ . Whereas in chickens, there is only the λ locus, the other locus was probably eliminated during evolution¹². From a functional point of view, IgM and IgA share many characteristics with mammalian homologs. The avian IgM isotype is identical in function and structure to the mammalian IgM. This is the first class expressed, appearing early in embryonic development.

Additionally, IgM is the most expressed isotype after stimulation with a novel antigen and has a transient response. Regarding IgA, similarly to mammals, this isotype is the predominant one in secretions¹². In mammals this class is known to bind to a receptor in epithelial cells, facilitating its uptake and further secretion to the lumen of the organs, thus a similar function may be proposed for the avian isotype^{38,39}. Regarding the IgY isotype, it is equivalent to the mammalian IgG, as both have homologous roles, nevertheless they still differ in many biochemistry properties. However, further studies revealed that IgY also has similarities with human IgE. In chickens, the IgY is the main isotype present in the serum, and it is in the early stages transferred from the mother to the embryo via the egg yolk, being crucial in antigen responses before the immune system is fully established⁴⁰. In mammals, there are two more Ig isotypes, namely IgE and IgD, however in chickens, there is no evidence that these exist. IgY performs most IgE functions in mammals in chickens¹².

1.3.2. V(D)J recombination

The V(D)J recombination event is responsible for rearranging and assembling the segments of the Ig's heavy and light chain locus. This mechanism *per se* is virtually equal in humans and chickens, however, the sequence of events is fairly distinct. More specifically, in humans, the complete rearrangement of the heavy chain locus occurs before the light chain rearrangement. Whereas in chickens, the rearrangement of both chains co-occurs. Therefore, the Ig rearrangement in avian is defined as stochastic, and not sequential as in mammals⁴¹. Such distinction may result from the fact that in mammals, the V(D)J mechanism is responsible for generating all the Ig diversity. Consequently, it is crucial that mammals only amplify pre-B cells that harbour a successful rearranged heavy chain, to achieve the highest number of functional diversified B cells after light chain rearrangement. Some light chain rearrangements could be useless and eliminated if the heavy correspondent chain has not been successfully formed. However, birds do not have multiple genes for each Ig segment as humans do, hence the V(D)J recombination is incapable of generating vast Ig diversity (**Figure 2**). This event produces only 1 distinct light chain and 15 distinct heavy chains. Therefore, in chickens, the heavy chain rearrangement can occur simultaneously with the light chain since there is no possible increase in diversity by a sequential rearrangement⁴².

As visible in **Figure 2**, chickens have only 1 gene for each V and J and 15 distinct genes for the D_H region¹². In addition, the 15 D_H regions encode virtually the same amino acid, thus practically no diversity can be originated⁴³. As chickens have only one V_L and one J_L gene for the light chain, all rearrangements generate the same light λ chain. All these considerations justify the low diversity generated by gene rearrangement in birds¹². Nevertheless, the mechanism itself for V(D)J

recombination is identical in humans and chickens, and both light and heavy chains are rearranged by it ⁴⁴.

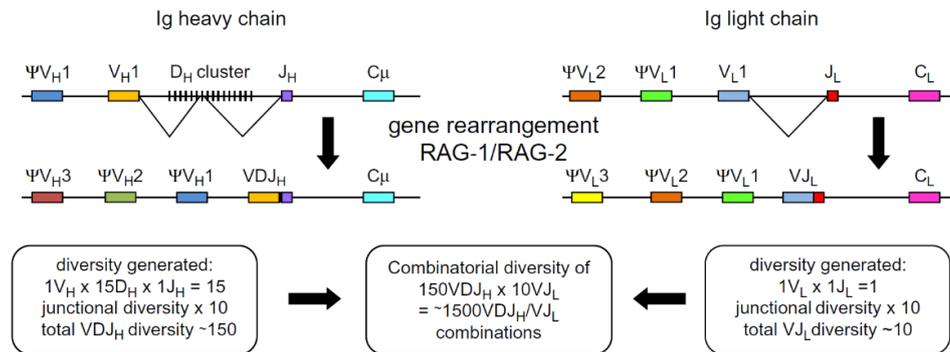


Figure 2. The mechanism involved in the Immunoglobulin gene rearrangement. On the left is illustrated the heavy chain rearrangement. The first step consists of rearranging the D_H and the J_H , and the second step is the junction of the V_H with the D_H . On the right is the Ig gene rearrangement of the light chain. The mechanism is alike, except that there is no D locus. This process involves the enzymes RAG-1 and RAG-2. The diversity generated is reduced, when combined the processes of the two chains there are around 1500 distinct Immunoglobulins. This figure was adapted from Avian Immunology (Third Edition) ⁴².

In the first step of V(D) recombination, chickens express the recombination activating gene 1 (RAG-1) and RAG-2, which generates a recombinase complex. This complex recognises and binds to the recombination signal sequences (RSS), that are directly flanking the gene segments undergoing recombination. This RSS sequence consists of a heptamer and a nonamer separated by a 12 or 23 nucleotide (nt) spacer. From the two Ig segments that are rearranged, one is flanked by an RSS containing a separator of 12 nt, and an RSS flanks the other with 23 nt. The RSS are recognised by the RAG-1/RAG-2 complex and are nicked, originating hairpins ¹². The opening of the hairpin occurs asymmetrically, resulting in the deletion of nt or in the addition of palindromic nt to the gene junction, which contributes to the junctional diversity also accounted in **Figure 2**. This last step of the opening of the hairpin is slightly different in mammals, as they have the addition of random non-templated (N) nucleotides by the terminal deoxynucleotidyl transferase (Tdt). In the avian Ig rearrangement, Tdt expression is absent, therefore the addition of the N nucleotides does not occur, which decreases the possible junctional diversity ^{13,45}. The V(D)J mechanism has low efficiency, only 1 in 3 light-chain and 1 in 9 heavy-chain rearrangements maintain the correct reading frame. Therefore, only 1 in 27 combinations of the two chains results in a rearranged and functional Ig molecule ⁴².

Another interesting variation in chickens is that the heavy chain rearrangement occasionally originates D_H -to- DJ_H or even $DDDJ_H$ rearrangements. These, however, can still rearrange with the V_H and generate a $VDDJ_H$ or $VDDDJ_H$. Many of these examples have been isolated from the bursa in the embryonic stage, nevertheless, after hatching, not more than one D region could be observed in chickens. This combination of D to D goes against the RSS12 and RSS23 principles, and does not occur in mammals. Nevertheless, it was thought that these rearrangements were relevant for diversity, and as the V(D)J event in chickens barely creates diversified Ig. Hence, it was thought that the avian immune system evolved in the sense of permitting these types of events to generate more Ig rearrangements ^{46,47}.

1.3.3. Gene conversion

As seen, the chicken Ig gene rearrangement does not contribute to the generation of antibody diversity. The same occurs in other avian species, also in horses, swine and rabbits, so they need to rely on a gene conversion process to diversify their BCR repertoire ⁴⁸.

This process was elucidated by Reynaud and his colleagues when studying the chicken Ig light chain complementary DNA (cDNA) in the spleen ⁴⁹. They identified that the majority of the V regions had modifications, and these were not found to be encoded in the V germline. Besides this, none of these mutations appeared in the J region, suggesting that a process was modifying the variable domain after the Ig rearrangement ⁴⁹. Additionally, it was found that the modifications were homologous to a set of genes upstream of the V region. In the light chain, these sequences are designated pseudo-V_L genes (ΨV_L) and are highly homologous to the V_L genes yet non-functional. Nevertheless, ΨV_L are crucial for the generation of diversity in the chicken Ig locus ^{21,50}. As visible in **Figure 3**, through gene conversion around 10⁹ combinations can be generated ⁴².

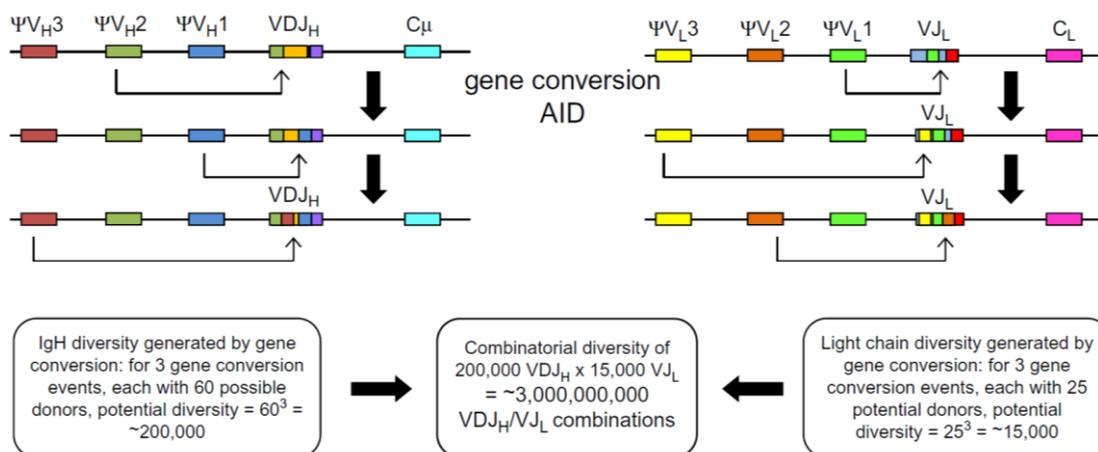


Figure 3. Gene conversion event in the heavy and light chain of an immunoglobulin. On the left is the gene conversion mechanism for the heavy chain. The arrows indicate the transfer of information from the pseudogenes to the V segment of the VDJ_H previously assembled. On the right is presented the same mechanism for the V segment of the light chain. The combinatorial diversity of three gene conversion events is much larger than the Ig gene rearrangement, it creates around 3,000,000,000 distinct combinations. The process of gene conversion is started by the AID enzyme stated. This scheme was adapted from Avian Immunology (Third Edition) ⁴².

Despite not being as well described for the heavy chain, the structure and line of thinking are the same ^{46,47}. There are also pseudogenes upstream of the heavy chain locus, although in this case, there are both pseudo-V_H and pseudo-D_H genes (**Figure 3**). As previously stated, during V(D)J recombination, Igs may harbour more than one D region, such as VDDJ or even VDDDJ. However, these rearrangements are not observed in adult birds, this happens because in the gene conversion process the transfer of segments from both V and D pseudogenes overwrites these bizarre combinations ⁴⁷. Regarding the number of pseudogenes in each chain, for the light chain, there are 25 ΨV_L and are found 20 kb immediately upstream of the functional V_L gene ⁴². For the heavy chain, there are more pseudogenes, about 80 for both ΨV_H and ΨD_H ⁵¹. These groups of segments are designated pseudogenes because they are non-functional genes, as they do not have a 5' region and leader

sequence. Additionally, they lack a functional recombination signal sequence, and many contain 5' and/or 3' truncations compared to the functional V or D gene. Therefore, these non-functional V genes cannot recombine with the J segment during the Ig gene rearrangement, which explains the observations made previously by Reynauld and his colleagues ⁴⁹. It was seen that some clusters of the ΨV_L segments harbour considerably more diversity. These sections are responsible for most of the transfer of segments to form the hypervariable or complementarity-determining regions (CDRs) of the V_L gene. The CDRs are the locations where the antigen binds, hence should be the most diverse regions in the immunoglobulin ¹².

The gene conversion event occurs in both heavy and light chains in the bursal environment and, with lower relevance, in splenic germinal centres ³³. In a summarised form, an event of gene conversion in the light chain are transferred nucleotide segments from the ΨV_L to the rearranged V_L gene, non-reciprocally. Meaning that the V_L gene does not transfer information back to the pseudogene, it is unidirectionally ^{21,52}. This is a highly variable process, not only because a single V_L gene can receive from 3 to 10 transferences, but also since the length of the segment transferred can vary enormously from one event to another ^{21,53}. Therefore, there are numerous possibilities of recombination events, permitting the formation of an undoubtedly diverse BCR repertoire ¹².

The frequency of usage of each pseudogene as a sequence donor depends on proximity, homology, and orientation to the V (or D) gene ⁵³. Regarding the first factor, ΨV_L that are closer to the V_L gene are used more often. This is reasonable since an alignment between the segments of the ΨV_L and the V_L gene needs to occur, thus the more proximal ΨV_L make an easier alignment. Subsequently, ΨV_L that have a higher degree of homology with the V_L gene can align more easily and then proceed to the recombination process. A minimum homology length is needed for the alignment, as the truncated ΨV_L are hardly used ^{21,53}. Interestingly, as each transfer of ΨV_L segments changes the sequence V_L gene, it affects the further usage of ΨV_L based on homology ⁵⁴. Lastly, ΨV_L that are in an antisense orientation to the V_L gene are more frequently used ⁵³. In the gene conversion process, the donor and recipient segments must be on the same DNA strand to align. Thus, for the antisense ΨV_L to align to the V_L gene, there only needs to occur a simple fold back of the DNA. Whereas if the ΨV_L is in the same orientation as the V_L gene, for them to align is much more complicated ⁵³.

Gene conversion appears to occur in a 5' to 3' directional matter relative to the V gene orientation. The 5' end begins the anneal in the pseudogene region with the highest homology to the variable gene. It extends until the 3' end, which is the position where the donor and the acceptor segments have less homology ⁵³. The gene conversion process occurs via homologous recombination via the synthesis-dependent strand annealing (SDSA) mechanism ⁵⁵. The first step for gene conversion is the formation of a DNA double-strand break (DSB), performed by the enzyme activation-induced cytidine deaminase (AID), which de-aminates cytosine residues forming uracil ⁵⁶. This results a base pair mismatch that is detected by the cell as an error. The uracil DNA glycosylase (UNG) eliminates these uracil mismatches, forming a DSB that is subjected to error repair. This results in a base pair mismatch detected by the cell as an error. The uracil DNA glycosylase (UNG) eliminates these uracil mismatches, forming a DSB subjected to error repair. For this, the pseudogene selected, based on the three criteria, is utilised and

homologous recombination between the latter and the Ig gene segment occurs. The final product consists of a rearranged Ig gene segment with modifications derived from the pseudogene sequence⁵⁵.

This process involves other enzymes, such as the paralogues of the RAD-51 gene, which is important for DNA homology search and the formation of the intermediate complexes between the donor and acceptor segment⁵⁵. Regarding AID, it is indispensable for gene conversion, as targeted disruption of AID in a chicken B cell line originates no diversity in the BCR. Hence deletion of this enzyme hampers gene conversion⁵⁶. The AID enzyme is also involved in SHM and CSR initiation steps. What differs in each process is the DNA repair mechanism employed and the presence or absence of a template⁵⁷. In chicken DT40 cells, a cell line with high expression of AID in the bursa that usually undergoes gene conversion *in vitro*, gene conversion occurs at a much higher frequency than SHM⁵⁶. Although, if pseudogenes are absent or if there is no activity of the RAD-51 enzyme in this cell line, the intense gene conversion is abolished, and SHM occurs instead. This compensation mechanism can be essential to guarantee that even in extreme cases where there are no gene conversion processes, there can still be generated some BCR diversity⁵⁵.

1.3.4. Immunoglobulin diversification

After B cells develop in the bursa, they migrate to the peripheral tissues in order to further mature and produce an immune response towards specific antigens. The GCs are responsible for subsequent proliferation after antigen contact and the diversification of the previously assembled Ig, through SHM and gene conversion⁴².

1.3.4.1. Immunoglobulin Isotype Switch

As mentioned, the first isotype to be expressed is the IgM; after a CSR process, B cells can express IgA and IgY¹². This process has recently been reported in mice that it occurs prior to the GC formation, during T cell-dependent immune responses³². Therefore, as this process in chickens is homologous to the mammalian one, it is likely that avian CSR also occurs before SHM in the GC³². During CSR, the previously obtained V(D)J rearrangement is maintained, and the constant region is the only section that suffers modification, hence no alteration of the antibody specificity towards antigens occurs⁵⁸. At the end of this process, three classes of immunoglobulins can be expressed in B cells. The affinity to proteins, the capacity of the Ig to diffuse into tissues and cells and the Ig half-life are characteristics of each class⁴².

1.3.4.2. Somatic hypermutation

To further diversify the immunoglobulins, B cells undergo somatic hypermutation followed by a selection of the cells in which the mutations increase the affinity for a specific antigen. The process of SHM consists of point mutations introduced in the V region of the heavy and light chain, which result in amino acid changes. Nevertheless, only some of these mutations lead to the production of more specific antibodies, these are the cells selected for further proliferation⁵⁹.

1.4. Development of B cells

Once one fully understands why B cells must migrate into the bursa, to become fully diversified and mature, creating a vast antibody repertoire, it becomes clear that the steps involving the emigration of the lymphocytes from the spleen towards the bursa are of extreme importance. In chickens, the development of B cells can be divided into three distinct periods, pre-bursal, bursal, and post-bursal. Briefly, the first period consists of the initiation of the V(D)J recombination and cell migration to the bursa. The process of gene conversion occurs in the second stage, where the repertoire is hugely diversified. Finally, the post-bursal phase initiates with the emigration of successfully rearranged and selected B cells from the bursa to the peripheral tissues ⁶.

1.4.1. Pre-bursal

Globally, in this first stage of development, the B cell precursors enter the spleen and can undergo a lineage commitment process, and in the final part of this phase they colonise the bursa ⁶.

The precursor cells, HSC, derive from the dorsal aorta of the chicken embryo early in ontogeny ⁶⁰. First, it was thought that HSC would only commit to the B cell lineage in the bursal environment ⁶¹. However, several studies identified pre-bursal cells committed to the B cell lineage before entering the bursa ⁶²⁻⁶⁵. In fact, the first cells committed to the B cell lineage are detected in the yolk sack on ED5 to 6. To become committed, B cell precursors go through the first stage of V(D)J recombination, which is the rearrangement of the D_H and J_H segment ¹⁵. This DJ_H rearrangement occurs first in the yolk sac and then in the blood and peripheral lymphoid organs, such as the spleen and bone marrow. More specifically, it is first detected from ED6 to 7 in the spleen, in the blood around ED8, and only later at ED10, in the bone marrow ¹⁵. The next Ig recombination step consists of rearranging the V_H to DJ_H segment at the same time of the V_L to J_H portion of the light chain. This rearrangement of the variable region was thought to be necessary for the B cells to enter the bursa ^{62,64,66}. Nevertheless, this hypothesis was disproved when B cells when Igs with incomplete V(D)J rearrangements were identified inside the bursa and follicles undergoing gene conversion, indicating that pre-bursal cells do not need to be fully rearranged to migrate. Thus, completion of the V(D)J rearrangement can occur in the bursa ¹⁵. Once this recombination process finalises, B cells have an Ig with a heavy and light chain formed and express the isotype IgM on the surface ¹². It is important to consider that pre-bursal B cells are restricted in ontogeny, meaning they only exist during embryogenesis and are no longer present after hatch ⁶⁷. Therefore, there is a brief window of time in which B cell precursors exist and can migrate to the bursa. Hence the first steps of B cell development are restricted to occurring during the early stages of life. Consequently, chickens are limited to producing the entire pre-immune antibody repertoire during embryonic periods. On the contrary, in mammals, the development of B cells and further generation and diversification of the antibody repertoire is ongoing through life ¹⁴. These characteristics demonstrate how crucial it is to have more knowledge on the migration of B cells to the bursa, as this is the only stage in which chickens can produce their entire antibody repertoire.

As mentioned previously, in humans and murine the Ig gene rearrangement confers vast diversity to the heavy and light chains. Nevertheless, chickens achieve practically no distinct combinations after V(D)J

recombination, thus B cells must go through gene conversion to generate the Ig diversity. As this event occurs in the bursa, the last step of the pre-bursal stage is the migration of the B cells to the bursa ¹². It is from the spleen that most B cells migrate, the number of cells compromised to the B lineage at this stage in the spleen is around 500,000 cells, whereas in the bone marrow are 100,000 cells. At this period in the bursa, already 3,000 pre-bursal cells have entered the mesenchyme ¹⁵.

Throughout the stages of development, B cells express different molecules on their surface. These for sure have an important role in cell migration and tissue adherence, additionally, permit the identification of each step based on B cell surface expression ⁶. Masteller and colleagues noticed that B cells express a carbohydrate epitope on the surface, by screening for known selectin ligands in these cells ⁶⁸. In the pre-bursal cells, the carbohydrate expressed was designated as sialyl-Lewis x or cluster of differentiation 15s (CD15s) ⁶⁸. This carbohydrate moiety is involved in white blood cell adhesion to endothelial cells via selectin binding ⁶⁹. Hence, such surface molecules may be relevant for migration and even entrance into the bursa. Further clusters of differentiation (CD) were identified in pre-bursal B cells, namely CD45 and CD1. Besides CDs, B cells in this stage also express the chicken B cell marker chB6, also designated as Bu-1 antigen ⁶³. This distinct expression of surface molecules throughout B cell development can be utilised to characterize a B population in a given period and organ ⁴². The mechanisms and molecules involved in the migration of B cells into the bursa are becoming increasingly popular, yet still not much is known about the necessary signals for bursal homing. The molecules expressed by the B cells during the migration period can provide hints on how it is regulated, which is crucial to understand B lymphocyte development in birds. Recently, it was proposed that the bursa creates an attractive microenvironment to recruit B cells via chemokines and chemoattract signals. Numerous reports indicate that the chemokine CXCL12 expressed by the bursa, and its receptor, CXCR4, expressed by B cells, play a role in this migration ⁷⁰. Besides, the granulocytes which are the first cells entering the bursa, are also believed to form an attractive microenvironment for B cells ¹². Nevertheless, a mechanism that is both sufficient and necessary for such migration is still unknown.

1.4.2. Bursal

The second stage was identified as taking place from ED8 to 14, with B cells exiting the spleen and entering the bursa via circulation ^{61,71}. The functional colonization of the bursa is divided into two distinct phases. First, pre-bursal B cells enter the bursal mesenchyme, and secondly they form and migrate into the bursal follicles ¹². Similarly, these migration processes are highly regulated, but little is known about them.

As previously specified, pre-bursal B cells initiate the V(D)J events outside the bursa, but there is no obligation to fully complete this rearrangement before entering this organ. B cells that have not completed this process can complete it in the bursal mesenchyme, as this organ contains the machinery necessary for this process ¹². The bursa expresses prominent levels of the enzymes RAG-1 and RAG-2, which are needed to the V(D)J recombination process ¹⁵.

B cells enter the bursal mesenchyme from the circulation, yet as there are many distinct cell types in the blood, there needs to be a selective regulation on which cells migrate into the bursa¹². As mentioned,

one example of a recently studied migration factor is the chemokine CXCL12 and its receptor CXCR4^{7,8}. Succinctly, resorting to this mechanism, the bursa can only attract certain cell types from the blood. The pre-bursal B cells are CXCR4 positive (CXCR4^{pos}) thus are attracted to the CXCL12^{pos} bursa. The same process occurs with granulocytes, as these cells also express the receptor CXCR4 they are attracted towards the CXCL12^{pos} bursa. The occurrence of the latter mechanism is of great importance since the bursal environment is also the site for granulopoiesis⁸. Once B cell precursors enter the bursa, the V(D)J recombination process can be finalised, if not previously completed¹⁵.

The next phase starts with the migration of BSDC precursors into the epithelium of the pre-follicle. Here, these trigger the development of a follicle bud (**Figure 4**). In the early follicular stage, the BSDCs become CXCL12^{pos} and attract the CXCR4^{pos} B cells⁸. Interestingly, the CXCR4^{pos} granulocytes are not attracted to the CXCL12^{pos} epithelial buds, which indicates that the signalling CXCL12/CXCR4 is not the only mechanism attracting B cells to the buds⁸. Hence, an additional cytokine and cytokine receptor mechanism was suggested to be crucial in this stage, the CXCL13/CXCR5 pair. This was suggested as bursal B cells express the receptor CXCR5 while granulocytes do not, thus B cells would be the only cell type to be attracted to the CXCL13^{pos} follicle⁸.

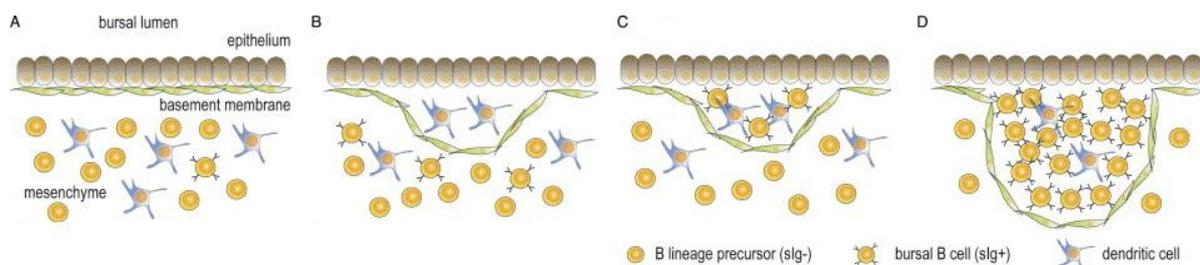


Figure 4. Schematic representation of the distinct stages of B cell development. **A.** Migration of granulocytes and B cells to the bursal mesenchyme. **B.** Dendritic cells enter first in the epithelial buds. **C.** The follicles are colonised by B cells. **D.** Rapid proliferation and gene conversion events occur in the follicle until the hatch. This figure was adapted from Ratcliffe M. *et al.*¹².

As visible in **Figure 4**, in the epithelial buds, the B cell precursors proliferate extensively, resulting in the development of the bursal follicles⁶¹. In here, gene conversion events occur to diversify the BCR. For a long time, it was assumed that only the B cells that productively completed V(D)J recombination and expressed a functional BCR complex were selected to colonise and proliferate in the follicles⁶⁶. Nevertheless, recent studies with B cells harbouring a deleted heavy chain showed contrary results. B cells with this characteristic lack BCR expression (BCR^{neg}), as for BCR expression on the surface, at least the heavy chain of the Ig must exist. Interestingly, BCR^{neg} B cells were observed inside the bursa and follicles, proliferating, and undergoing gene conversion, which abolished the initial hypothesis a necessary BCR expression^{72,73}. It is important to consider that a functional BCR consists of the non-covalently association of the Ig with the Igα/β heterodimer. In mouse models, it has been reported that the Igα/β heterodimer is essential for expressing IgM on the surface of early B cells. Nevertheless, in chickens lacking the Igα/β heterodimer, the IgM is still expressed in the surface. However, the dimer is necessary for the Ig to transduce signals efficiently, thus, without the Igα/β heterodimer, the IgM is

considered biologically inert. Therefore, both surface Ig and Ig α / β heterodimer expression are crucial to guarantee a correct BCR complex^{73,74}.

Afterwards, each follicle bud is colonised by, on average, 3 B cell precursors, and as there are around 10,000 follicles in the bursa, approximately 30,000 B cells start the gene conversion process²⁵. In this stage, intense proliferation occurs, correlated with the gene conversion period. The regulatory mechanism for this intense proliferation are still not fully understood, nevertheless a homolog of the mammalian B cell activating factor (BAFF) was reported to be relevant in this stage⁷⁵. This molecule is highly expressed in this period, and is suggested to be important for maintaining intense B cell proliferation. It was demonstrated that neutralisation of BAFF significantly reduced the size of the follicles and the number of B cells, thus validating that this factor is relevant in B cell proliferation in the follicles⁷⁶. In the final week of embryonic development, there is an exponential increase in the number of B cells in the follicles. The rate of B cell death is much less than the rate of cells emerging from the expansion. From the initial 3,000 non-diversified B cells, around 10⁷ diversified cells are obtained at the end of the bursal stage¹⁵.

Before hatch (ED 21), the bursa suffers a morphologic change (**Figure 5**), and the follicle-associated epithelium (FAE) is formed by differentiation of the epithelium. The FAE is in contact with the follicle and the bursal lumen, and contains dendritic-like cells that transfer the content arriving at the lumen into the follicles, such as the gut-associated antigens⁷⁷. As the bursal lumen is connected to the gut lumen, the antigens and other pathogen-derived molecules present in the gut can be transported to the bursal lumen. Once in the bursal lumen, the dendritic-like cells of the FAE translocate them into the follicles, where are the B cells²⁸. The antigen presentation to the lymphoid cells is crucial in both B cell and bursal development. The ablation of this mechanism leads to failure in lymphocyte development after hatch, and compromises the peripheral population of B cells. Additionally, the presentation of the antigens to these lymphocytes induces their migration from the medulla to an outer region, starting the development of the cortex²⁸. Again, this migration to the follicular cortex is probably well regulated by attractant chemokines and their receptors, as the cortex expresses high levels of CXCL12 compared to the medulla⁸.

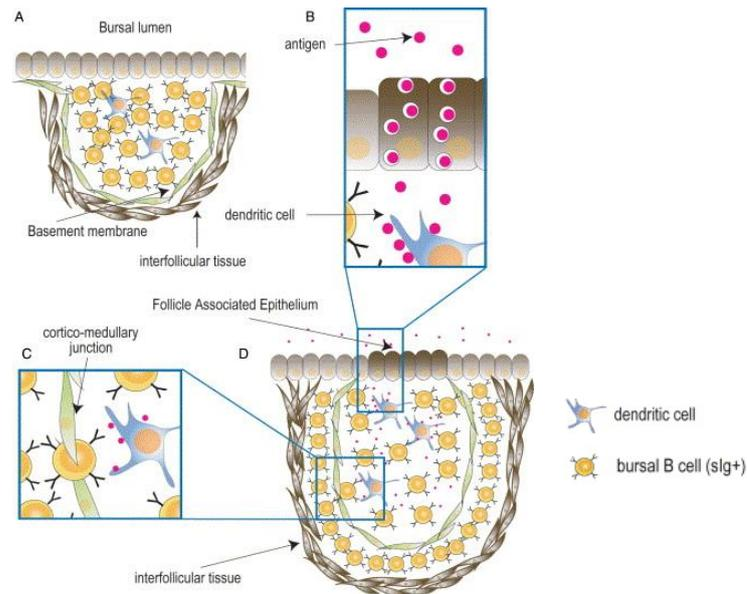


Figure 5. Bursal development after hatch. **A.** Structure of a bursal follicle, the follicles are separated by interfollicular connective tissue. **B.** After hatch, the FAE captures antigens from the bursal lumen and transports them into the follicle. **C.** Migration of B cells from the medulla across the basement membrane to the cortex, leading to the formation of the follicular cortex. **D.** Structure of the bursa after hatch, the B cells migrate to the periphery from the cortical zone. This figure was adapted from Ratcliffe M. *et al.*¹².

B cells from the cortical region emigrate to the peripheral secondary lymphoid organs after hatch²⁸. Nevertheless, only the B cells that express CXCR4^{low} migrate to the periphery, whereas the CXCR4^{pos} remain in the cortex. This distinct migration possibly occurs since B cells that express low levels of CXCR4 are not as attracted to the CXCL12^{pos} cortex when compared to the cells that express high levels of CXCR4, hence the first ones tend to migrate to the periphery⁸. B cells leave the bursa and reach the peripheral lymphoid organs via circulation. However, most B cells produced in the bursa are eliminated by apoptosis prior to migration, and only 5 % of the B cells generated per day migrate to the periphery⁷¹. This low percentage of migrating cells was first thought due to non-functional rearrangements of the Ig, analogous to what occurs in humans^{71,78}. It was then suggested that the gene conversion process was very error-prone, however, later reports indicated that it only generates 2-3 % non-functional gene conversions⁷⁹. Now it is hypothesised that the gene conversion process generates diversified V_H and V_L regions that fail to assemble to form a functional Ig, leading to the elimination of these B cells by apoptosis¹³.

Analogous to the pre-bursal stage, bursal cells express cell surface markers characteristics of this period. The entrance of pre-bursal cells in the bursa can be identified by an accumulation of sialyl-Lewis x expressing cells in this organ. From ED15 to 18, which is the gene conversion period, there is a switch from sialyl-Lewis x expression to Lewis x, and B cells express the chB1 gene, a pro-apoptotic receptor^{68,69}. This decrease in sialyl-Lewis x correlates with the period when bursal cells lose their ability to migrate into the bursa⁶. Around the day of hatch (ED 21), B cells begin to emigrate from the bursa. In this stage, there is a significant reduction of the Lewis x expression, which correlates with the termination of B cell proliferation⁶⁸.

1.4.3. Post-bursal

The last stage of B cell development starts around the hatch and continues until bursal involution. The B cells that generated a diversified, fully functional BCR and were positively selected cease their heavy proliferation and migrate out of the bursa, to the secondary lymphoid organs⁸⁰. At this period, B cells in the bursa begin to accumulate in the G0/G1 phase of the cell cycle, which corresponds to a resting phase. This transition from cells that proliferate extensively to almost quiescent cells can be accounted for another maturation or selection step in B cell development. Consequently, only B cells that become quiescent can exit the bursa⁶. Once in the secondary organs, B cells can encounter antigens and differentiate into antibody-secreting cells (plasma cells) and memory cells (B_{mem})^{6,81}. Nevertheless, before becoming a crucial component of the immune system, B cells need to undergo SHM and CSR. These events are essential to creating a specific and efficient antigen response by increasing the affinity and changing the Ig isotype¹³.

In this final stage, the post-bursal B cells shift their surface expression towards the emigration of the bursa. More specifically, there is a decrease in the Lewis x expression, and at this time an accumulation of cells expressing low levels of Lewis x is visible in the secondary organs. Therefore, low levels of Lewis x are suggested to be required for B cells to exit the bursa and colonise the secondary organs⁶⁸. After migration from the bursa, the post-bursal B cells become an integrated part of the humoral immune responses throughout the chicken's life^{6,18}.

1.4.4. Factors involved in B cell development

The migration, maturation, and further survival of lymphocytes require extensive regulation. Cytokines and chemoattractants are key elements in regulating the migration of B cells throughout the various locations of their development¹³. In mammals, B lymphocytes are generated firstly in the bone marrow, where the antibody repertoire is formed, and then migrate to the peripheral tissues. On the contrary, chickens have a much more complex "path" of B cell development¹². Succinctly and as mentioned during this project, B cells first rearrange their Ig in the spleen, then migrate into the bursa to diversify generated Ig, and finally, in the secondary lymphoid organs the Ig maturation occurs. Therefore, this involves much more migration steps compared to the B cell development in humans, hence chickens' resort to a larger number of highly regulated mechanisms to guarantee proper lymphocyte movement and development^{9,12}. Additionally, the migration of B cells to the bursa can be classified as a homeostatic process. As only a restricted number of B cells enter the bursa, and only after this colonisation is finished, there are signals for more B cells to migrate from the peripheral organs^{10,82}. Thus, the migration of cells to the bursa is an extensively regulated process¹³. Nevertheless, most of these regulatory mechanisms and molecules have only recently begun to be elucidated, yet the majority still remain unknown. A succinct description of the most important mechanisms involved in B cell migration are presented below.

B cell-activating factor of the TNF family (BAFF)

Most migration factors and mechanisms identified in chickens arise from previous knowledge of mammalian B cell factors involved in B cell development¹³. It is the case for the B cell-activating factor of the TNF family (BAFF), which was discovered in chickens and is homologous to the human BAFF^{13,75,83}. It has been shown in mammals that BAFF plays a crucial role in the proliferation, survival and maturation of peripheral B cells, mainly in the marginal zone⁷⁶. In chicken, the cytokine BAFF is mostly expressed in the spleen and the bursal follicles, concordant to the mammalian BAFF expression^{13,75,84}. However, most BAFF-expressing cells in chickens are B cells in an autocrine way. This does not occur in mammals and mice, the only cells that express BAFF are malignant cells⁷⁶. The BAFF receptor (BAFFR) is expressed in B cells in different stages, such as early in the spleen and then in the bursa, increasing continuously in this organ until the hatch. During development, the levels of BAFFR expression in the bursa increase as the number of B cells migrating to the follicles is higher. At hatch, there is a second wave of BAFFR expression, now in the peripheral organs, due to the migration of mature B cells⁷⁶. BAFF neutralisation leads to a decrease in the bursal follicle size and the number of cells seeding in this location, which means that in contrast to mammals, this factor is also required for the development of immature B cells⁷⁶. As expected, high levels of BAFF permit a maximal migration of B cells towards the follicles. These results suggest that the BAFF cytokine and its receptor have a crucial role in the migration of pre-bursal and bursal cells⁷⁶. Such evidence is essential to obtain insights into the distinct mechanisms of B cells before and after hatch, when compared to the mammal mechanisms.

CD40 and CD40 Ligand

Additionally, based on similarity with factors involved in B cell development in humans, the CD40-CD40 ligand (CD40L) pair was identified in chickens. This mechanism is known to be important in both T and B cell response regulation. In mammals, the CD40 expressed by B cells must bind to the CD40 ligand to seed and maintain the germinal centre reaction. More specifically, the CD40L is expressed by T cells, which is then present to B cells, providing crucial signals for these cells. This co-stimulatory molecule regulates B cell effector functions, such as proliferation, somatic hypermutation and immunoglobulin isotype switch^{13,85}. It is still unknown if the CD40-CD40L pair is important in immature stages of B cell development, such as B cell migration to the bursa⁴².

Interleukin 7

In mammals, the interleukin 7 (IL-7) signal is involved in the early development of B cells in their proliferation, survival and further differentiation⁸⁶. In chickens, it was observed that B cells under robust proliferation in the bursa express higher levels of IL-7, thus suggesting that this interleukin is relevant in the gene conversion, and expansion period¹⁰. Nevertheless, the role of this interleukin in pre-bursal migration has not yet been established, and further studies are necessary.

AID, RAG-1, RAG-2 and Ikaros

It is also interesting to study the factors expressed in the bursal B cells, during the immunoglobulin diversification process via gene conversion, as these may also provide leads on novel mechanisms of bursal cell migration. As previously mentioned, the enzyme AID is necessary for gene conversion, B cells with an increased proliferation express higher level of this enzyme⁵⁶. The same applies to the recombination activating genes involved in gene conversion, RAG-1. However, RAG-2 has not been reported to be more expressed in the cells that proliferate and migrate more¹⁰. Additionally, the Ikaros family factors were reported to be present in B cells of the embryonic bursa. This family of transcription factors has a critical role in the expansion and maturation of bursal B cells²⁴. Ikaros was suggested to have a role in regulating AID expression, as binding sites for this transcription factor were identified in the regulatory elements of the AID gene⁸⁷. Besides, the lack of Ikaros was reported to impair the expression of the BCR. Hence, Ikaros family members appears crucial for B cell development⁸⁸.

Signalling pathways

Lastly, many signalling pathways are known to be involved in the initial stages of B cell development, such as the cytokine-cytokine receptor interactions, the MAPK, Wnt, Notch and JAK-STAT signalling pathways⁹. Transcriptomic analysis uncovered that these signalling pathways are crucial in different stages of B cell development, which was proposed due to their high and varied gene expression among the developmental phases^{9,70}.

1. Cytokine-cytokine receptor interactions

Besides these two factors, important chemoattractant cytokines and receptors are involved in the migration of the B cells to the bursa and into the follicles. One of these examples are the, already mentioned throughout this work, CXC receptors and chemokines, designated this way due to a Cysteine-X-Cysteine motif at their C-terminal⁸⁹. Two CXC receptors (CXCR) are proposed to be important for bursal colonisation, the CXCR4 and CXCR5^{8,13,90}. These receptors are expressed by B cells and respond to chemoattractant cytokines present in the bursa, thus directing the migration of these cells⁴². More specifically, in embryonic stages, pre-bursal cells express CXCR4 and are attracted to the bursa expressing the cytokine CXCL12⁷. Two recent studies, by M. Laparidou *et al.* and Nagy *et al.*, reported that the CXCR4/CXCL12 mechanism indeed mediates B cell migration to the bursa, yet both concluded that additional factors must be involved in this migration^{7,8}. The first study, by M. Laparidou *et al.*, discloses that BCR expression is necessary for the B cells to migrate via the CXCR4/CXCL12 mechanism. Interestingly, however, the BCR^{neg} B cells that have failed to migrate towards the CXCL12 were still migrating into the inside of the bursa⁷. This result suggests that more factors are driving the migration of B cells to the bursa, as the BCR^{neg} cells can still migrate to the bursa without the CXCR4/CXCL12 signalling. The second study, by Nagy *et al.*, detected that both granulocytes and B cells had a similar CXCR4 expression. However, in the migration to the CXCL12^{pos} follicle buds only the B cells migrated⁸. This suggests that further signals, such as the CXCR5/CXCL13 mechanism, are necessary to this B cell migration step, and not only the pair CXCR4/CXCL12 per se, since the granulocytes failed in migrating⁸.

Focusing on the CXCR5/CXCL13 pair, a similar mechanism occurs, in this case, bursal B cells express the CXCR5 and migrate towards the chemokine CXCL13, which is expressed in the follicles¹³. Hence, the first mechanism by CXCR4/CXCL12 is suggested to be important for the colonization of the bursal mesenchyme by B cells from the peripheral organs, whilst the CXCR5/CXCL13 mechanism is suggested to be also relevant for directional migration inside the bursa, to the developing follicles. Interestingly, chickens evolved a more extensive range of homeostatic B cell chemoattractants than humans and murine. This was expected as the migration of the B cells during their development in chickens is much more complex than in mammals, thus it is beneficial for birds to have more regulation mechanisms¹³.

2. MAPK signalling pathway

The mitogen-activated protein kinase (MAPK) signalling pathway is relevant in the migration and differentiation of B cells during their development. Based on human homology, the receptors CXCR4 and CXCR5 are thought to encode G-protein-coupled receptors (GPCR), which are seven transmembrane-domain proteins. Once these receptors bind to the correspondent chemokine, the G-protein becomes active, and signal transduction occurs via the MAPK pathway^{70,91}. Hence these receptors are possible activators of this pathway and, as previously mentioned, are involved in the migration to and inside the bursa⁸. Therefore, the MAPK pathway is most likely important in migrating pre-bursal and bursal cells.

3. Wnt signalling pathway

The Wnt signalling pathway consists of secreted cysteine-rich glycosylated and lipid-modified proteins⁷⁰. The Wnt canonical pathway is relevant in primordial germ cell development and cell line specification⁹². The canonical path includes Wnt proteins, frizzled receptors, and lymphoid-enhancing factors, and the latter are expressed in B cell progenitors⁹. Additionally, the bursa was recently reported to express Wnt ligands and receptors, thus this pathway is most likely important for B cell migration and development in this organ. It was suggested that Wnt could function as a cell-bound or a free ligand that stimulates B cell differentiation⁷⁰. In mammals, the canonical pathway is crucial to generate proliferating signals for B lymphocytes⁹². In chickens, a similar role is suggested⁹³.

4. JAK-STAT signalling pathway

The JAK-STAT pathway is involved in the B cell development inside the bursa. The interleukin-4 (IL-4) receptor expressed in the bursa is an activator candidate for the JAK-STAT pathway⁷⁰. When IL-4 is expressed in the bursa during B cell development, it can initiate a signal transduction mechanism via the JAK-STAT pathway, stimulating B cells to proliferate. More specifically, the IL-4 receptor activates JAK-1 and JAK-2, phosphorylating STAT6, which forms heterodimers and can enter the nucleus. Once in the nucleus, STAT6 dimers lead to gene transcription related to cell proliferation and germinal centre events⁷⁰.

5. Notch signalling pathway

Finally, the Notch signalling pathway is involved in cell developmental processes, such as lymphocyte fate differentiation into T or B cells⁹. It also has a role in B cell development, as B cells of distinct stages

express the Notch receptor, and the bursa expresses Notch ligands⁹⁴. The expression of these factors in the bursa is differential, the receptor Notch 1 is expressed in medullary B cells, whereas the Notch ligand Serrate2 is expressed only in the epithelia surrounding the medulla. Constitutive expression of any of these molecules leads to a reduction in the expression of surface IgM⁹⁴. This suggests that the Notch pathway is involved in the inhibition of B cell development, and therefore it has an important role in the selection process that occurs in the bursa before B cells migrate to the periphery^{9,95}.

6. BCR signalling

Besides these, another crucial mechanism in B cell development is the BCR signalling pathway. As mentioned, the BCR complex consists of a light and heavy chain that are non-covalently bound to an Ig α / β dimer. It was first thought that the presence of a functional BCR complex was an essential signal for cells to migrate into the bursa, meaning that BCR^{neg} would be selected for elimination at the entrance of the bursa. Then this hypothesis was disproven with the observation of BCR^{neg} B cells inside the bursa¹⁵. It was then suggested that BCR signalling was necessary for B cells to enter the follicles, undergo gene conversion, and later emigrate from the bursa^{71,78}. Nevertheless, additional recent observations in BCR^{neg} chicken B cells, which were obtained by deletion of the J_H segment, revealed that these cells can still enter the follicles and undergo gene conversion on the light chain. The BCR appears unnecessary for B cells to enter the bursa and the follicles and to further proliferate inside these⁷³. However, after hatch, the expression of a heavy chain and consequently BCR is mandatory for further B cell development. Therefore, as B cells of the J_H^{-/-} chickens cannot express surface immunoglobulins and thus cannot migrate to the periphery, there is a total lack of antibodies and peripheral B cells in this population⁷³. This occurs due to BCR^{neg} B cells being eliminated by apoptosis prior to migration from the bursa. Additional studies performed in chickens harbouring Ig light chain deletions revealed that the heavy chain is sufficient to maintain BCR signalling. The deletion of the light chain did not abrogate B cells in the periphery, whereas the heavy chain hampered B cells in the periphery due to abolishing BCR expression^{72,73}. Therefore, such results confirm that BCR signalling is in fact crucial to the later development of B cells, as when this signalling is hindered B cells in the periphery are absent⁷³. Additionally, the BCR signalling is also essential to B cell migration resorting to chemokine signalling. More specifically, the BCR complex is necessary for B cells to migrate towards the CXCL12 in the bursa, as B cells with deleted BCR fail to migrate towards this chemokine⁷. Thus, it suggests that the BCR is not only important to the bursal stages of development but is also crucial in the pre-bursal cell migration⁷.

In conclusion, it is perceivable that proper migration of B lymphocytes and further development in the bursa requires extensive regulated mechanisms, some achieved by the cytokines and signalling pathways mentioned¹³. Nevertheless, the question regarding which signals are both necessary and sufficient for B cell migration remains. To answer this question, this project aims to establish a methodology to analyse embryonic B cells in a high-throughput fashion resorting to RNA-sequencing, thus permitting investigation of the mechanisms that are necessary and sufficient for cell migration.

2. Objectives and Motivation

In recent years, there has been an increased interest in studying the chicken's immune system. As this animal becomes increasingly important in the food system, a global concern for the health and welfare of poultry arises. To overcome these obstacles, enhanced knowledge of poultry immunology is vital¹³.

Lately, some studies focused on analysing the transcriptome of the chicken to dissect which mechanisms and factors are essential for the immune system development. In 2016, Xiao-dong Liu *et al.* conducted a study using RNA-sequencing (RNA-seq), to analyse changes in gene expression during different B developmental stages in the bursa⁹. Until then, no other RNA-seq approach was performed to understand the development phases of B cells in chickens. Their findings contributed to the elucidation of many signalling pathways involved in B cell development, such as the Wnt, MAPK, JAK-STAT, and other signals. This study accelerated the research on B cell development in chickens. In 2018, Kwang Hyun Ko and colleagues identified more molecules expressed by B cells during pre- and bursal stages. Besides, they showed that B cells migrating and proliferating more extensively in the bursa have a bigger size than less active B cells¹⁰. Afterwards, in 2019 Nuthalapati N. *et al* published a study where deep sequencing of the B cell population by RNA-seq between ED16-19 was performed⁷⁰. In this far more reduced period of development, some molecules expressed by the B cells, and suggested to be important in the migration to the bursa, were identified, namely, the chemokines receptors CXCR4 and CXCR5. Respectively, these receptors bind to the chemokines expressed by the bursa and follicles, the CXCL12 and CXL13. Such discoveries enabled further dissection of the regulation factors in the migration processes, and more studies have been developed in this sense. In 2020 two distinct studies were performed, one by M. Laparidou *et al* and the other by N. Nagy *et al*, which focused on understand the roles of the CXCR4/CXCL12 mechanism in the migration of B cells towards the bursa^{7,8}. It was concluded that this mechanism is important to the migration of B cells to the bursa, nevertheless, not sufficient, thus suggesting that other factors and signals contribute to this migration as well^{7,8}. Therefore, the question remains: What signalling mechanisms are both necessary and sufficient for B cell migration into the bursa?

To answer this question, this project aimed to develop a methodology for isolating, extracting and sequencing the RNA from B cells in their early stages and from the locations involved in their development, namely on ED12,14 and 16, from the spleen, bursa and blood. Until this date, no method has been established isolate B cells in these stage and in such three locations. It is vital to have a defined protocol as the number of B cells in this stage is very low since these cells have not yet undergone expansion and proliferation in the bursa. Therefore, an optimized method is crucial to determine the amount of starting material needed, and to guarantee that the employed techniques permit to obtain enough quantity and of good quality for sequencing. The study of B cells in this stage has been widely performed on a non-high throughput scale, using for instance, quantitative PCR (qPCR) to analyse specific genes^{7,8,10}. However, no high throughput analysis of ED12 B cells has been reported, the closest approach was the study of bursal B cells on ED16 employing RNA-seq⁷⁰. Nevertheless, the methodology utilised by the latter study is to isolate B cells already in the bursal stage, hence these cells

have most likely already undergone gene conversion and cell expansion, thus, are at a much higher number, and are not so sensitive ¹³.

The proposed methodology is represented in **Figure 6**, and consisted in first isolating the B cells from the spleen, bursa and blood at ED12, ED14 and ED16 via FACS, then extracted the RNA. After, RNA was converted into cDNA, and an Illumina library was prepared for further sequencing. The last step was the RNA-sequencing analysis, in the ArrayStar[®] ⁹⁶ software, where the differentially expressed genes between samples were examined, to further dissect the mechanisms involved in B cell migration to the bursa.

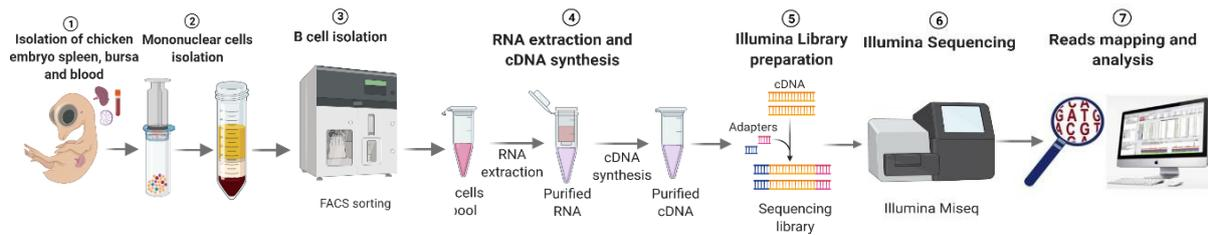


Figure 6. Experimental workflow to analyse by RNA-sequencing the B cells in ED12, ED14 and ED16, from the spleen, bursa and blood. From these, single cell solutions, leucocyte fraction was isolated and B cells were stained for the sorting. RNA was extracted from B cells and converted into cDNA, the Illumina library pool was prepared and sequenced. The reads were mapped against the genome of reference, and the differential gene expression was investigated. This figure was created on Biorender.com.

3. Materials and Methods

3.1. Buffers and media

PBS: 40 g NaCl (#131659, AppliChem), 5.75 g Na₂HPO₄ (#A1046, AppliChem), 1 g KCl (# A2939, AppliChem), 1 g KH₂PO₄ (#A1043, AppliChem), ddH₂O to a total volume of 5 L

PBS+BSA: 5 g Albumin (BSA) Fraction V pH 7.0 (#A1391, AppliChem), 500 mL PBS

Fluo-buffer: 500 mL PBS, 50 mg NaN₃ (#A1430, AppliChem), 5 g Albumin Fraction V (#A1391, AppliChem)

Labelling Buffer: 50 mL PBS, 200 µL EDTA (#A3145, AppliChem)

Separation Buffer: 100 mL PBS, 400 µL EDTA (#A3145, AppliChem), 0.5 g Albumin Fraction V (#A1391, AppliChem)

3.2. Animals

Wild-type white leghorn chickens were bred and maintained under specific-pathogen-free (SPF) conditions in the animal facility at the Technical University of Munich (School of Life Sciences, Weihenstephan, Freising, Germany). Chickens were kept and provided free water access and a standard diet *ad libitum*. Fertilised eggs were incubated at 37.8 °C and 55 % humidity, and were rocked three times per day.

3.3. Isolation of embryonic spleens and bursae

At embryonic day (ED) 12, ED14 and ED16, the eggs were opened, and the embryos were euthanised by decapitation. Spleen and bursa were harvested and transferred into a FACS tube with 500 µL of PBS+BSA on ice. One single cell suspension was obtained by disaggregation of the organs through a 40 µm nylon cell strainer in a Petri dish. Per every 5 embryos, organs were mashed and then pooled in one single suspension per experimental group. The Petri dishes were washed with 500 µL PBS, and this volume was transferred to FACS tubes.

3.4. *In ovo* Blood Collection

Blood collection was performed on ED12, ED14 and ED16. Depending on the embryonic age, the maximum volume possible to be retrieved from a single embryo varies (**Table 1**). The anticoagulant was prepared by diluting Heparin (Heparin-Natrium-25000-ratiopharm) 1:100 in RPMI (Roswell Park Memorial Institute), and for every 50 embryos, 1 mL of this solution was divided to coat all syringes.

Table 1. The volume of blood (μL) possible to collect according to the age of the embryo regardless of survival, according to the internal standard operating procedure.

Embryonic day	ED12	ED14	ED16
Maximum volume of blood	500 μL	650 μL	800 μL

Each egg was placed in a holder with the air bubble towards the light, and a triangle was drawn to indicate the location and direction of the selected bloodstream to extract blood (**Figure 7**). A Dremel was employed to cut the triangles marked without damaging the membrane. The triangle was removed, and a drop of paraffin oil was placed in the membrane. With the egg set in a position where the vein was pointing away from the light source, the blood was extracted resorting to 1 mL syringes (I010033, MarMed) with 27G needles (I023001, MarMed), and it was placed inside EDTA tubes (NC9990563, Fisher Scientific) to avoid coagulation. The blood was pooled in a 15 mL Falcon[®] tube and diluted 1:1 with ice-cold PBS.

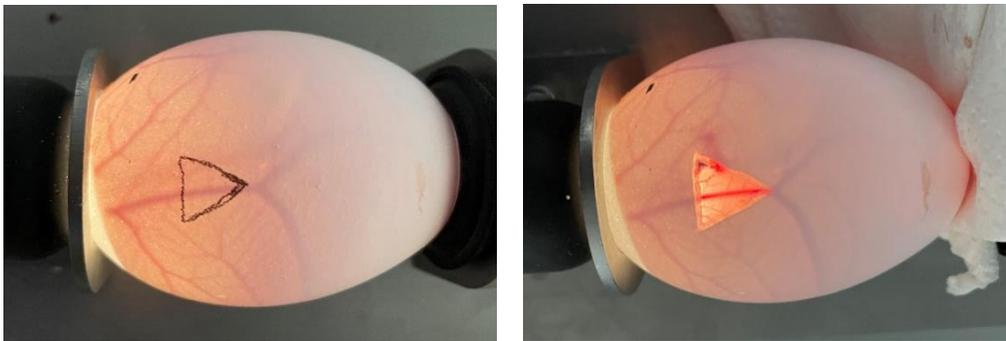


Figure 7. Representative images of the procedure to select a vein in the embryo to perform blood collection. Triangle is drawn to indicate the direction of the chosen bloodstream to extract blood (left). The triangle was cut and removed without damaging the membrane (right).

3.5. Mononuclear Leucocytes Isolation

To isolate the mononuclear leucocyte fraction from the single cell suspensions of the spleen, bursa and blood, a density gradient centrifugation was performed with a 1:1 volume of Histopaque[®] 1077 Hybrid-Max medium (H8889-100 mL, Sigma-Aldrich[®]). The cell solution was layered on top and centrifuged at 650 x g for 12 min at 4 °C without acceleration/deceleration. The (white) cell layer was collected from the interface and transferred into a FACS tube with 1 mL PBS+BSA. The cells were washed 222 x g for 5 min at 4 °C, the supernatant was discarded, and 2 mL of Fluo-buffer was added to disperse the cell pellet.

3.6. Cell Counting

Cell counting was performed with a Neubauer chamber (0.1 mm, 0.0025 m³, Paul Marienfeld GmbH & Co.KG) and an inverted light microscope with phase contrast (Labovert FS/Biomed, Leica

Microsystems). Cells were counted in a 1:10 dilution of trypan blue (T8154, Sigma-Aldrich®), and live cell concentrations were calculated according to **Equation 1**. Cells were concentrated to 5×10^6 cells/mL by centrifuging at $222 \times g$ for 5 min at 4°C and resuspending with the appropriate volume of Fluo-buffer. **Equation 1. Total number of live cells in the initial volume of the sample, from the number of cells counted in the Neubauer chamber.**

$$\frac{96}{2} \times 10 \times 10^4 = 4.8 \times 10^6 \text{ cells. mL}^{-1} \times 3 \text{ mL} = 14.4 \times 10^6 \text{ cells}$$

1:10 Dilution w/ Trypan Nr of cells/mL Total nr of cells
 ↓ ↓ ↓
 Nr cells/ Nr square From counting the chamber's large squares Volume of FACS buffer used (total volume of our sample)

3.7. MACS-based cell sorting

Two different procedures were tested to isolate B cells, MACS (Magnetic associated cell sorting) and FACS (Fluorescence associated cell sorting), as these are the most employed techniques in isolating B cells and yield good results⁹⁷. The procedure for B cell isolation via MACS was adapted for ED12 chicken embryos from a previous protocol established by Miltenyi Biotec for Streptavidin MicroBeads cell separation⁹⁸. The labelling buffer, separation buffer and Fluo-buffer were prepared the day before, stored at 4 °C and were de-gas shortly before use. The volume of cells obtained in the previous step was split between FACS tubes to perform different treatments (**Table 2**). The single cell suspensions were centrifuged at $300 \times g$ for 10 min at 4 °C. For the MACS staining, three AV20 antibody clones and their respective beads were tested to infer which allowed for a higher enrichment of B cells (**Table 3**).

Table 2. Sample treatments performed in each experiment. UNS: unstained, L/D: live dead, AF: Alexa Fluor. Full stained is both L/D and FITC or AF.

Treatments	UNS	L/D Single Stain	FITC or AF Single Stain	Full Stained without MACS/FACS	Full Stained undergoing MACS/FACS

Table 3. Antibodies and MicroBeads tested in MACS and FACS. The name, dilution and supplier of the antibody are presented, as well as the name and supplier of the correspondent MicroBeads.

Antibody	Antibody dilution	Antibody Supplier	MicroBeads	MicroBeads Supplier
Mouse Anti-Chicken Monoclonal Bu-1-Biotin antibody	1:200 dilution	#MA5-28700 Thermo Fisher Scientific	Streptavidin MicroBeads	# 130-048-102 Miltenyi Biotec
Mouse Anti-Chicken Monoclonal Bu-1-FITC antibody	1:200 dilution	#MA5-28701 Thermo Fisher Scientific	Anti-FITC MicroBeads	# 130-048-701 Miltenyi Biotec
Mouse Anti-Chicken Monoclonal Bu-1-AF647 antibody	1:200 dilution	#8395-31 Southern Biotech	Anti-Cy5/Anti-AF647 MicroBeads	# 130-091-395 Miltenyi Biotec

The protocol followed for the three cases was identical. Each volume was resuspended in 500 μ L of the antibody, vortexed shortly and placed for 20 min on ice in the dark. Cells were washed to remove unbound primary antibody with 500 μ L of labelling buffer and centrifuged at 350 x g for 7 min at 4 °C. The cell pellet was resuspended in 180 μ L labelling buffer, 20 μ L of MicroBeads were added and the solution was refrigerated for 15 minutes at 4 °C in the fridge. Cells were washed, the MACS magnet and column were set up, and the latter was primed with 3 mL separation buffer. In the stained samples for MACS, the pellet was resuspended in 750 μ L of separation buffer and applied to the MACS® LS column. The unlabelled cell fraction was collected, and the column was washed 3 times with 4 mL separation buffer. The column was removed from the separator and placed in a 15 mL falcon tube, 5 mL of separation buffer was added, and the plunger was pushed to flush out the labelled cells. The cells exiting the column and the non MACS-sorted cells (control) were washed and resuspended 1 mL of Fluo-buffer. In the next step, a UNS control and single stains (L/D and FITC or AF) for the detection in the Invitrogen Attune NxT Flow Cytometer were defined, and the volumes were transferred to wells in a 96-well round bottom plate (Thermo Scientific™). The plate was centrifuged at 700 x g for 1 min at 4 °C, and the supernatant was discarded. For the Live/Dead staining, 50 μ L of Fixable Viability Dye eFluor™ 780-staining (1:1000 dilution) (#65-0865-14, Invitrogen™) was added to each well, and the pellets were resuspended carefully, the plate was incubated for 20 min on ice in the dark. For the unstained wells, 200 μ L Fluo-buffer was added. After incubation, 150 μ L of Fluo-buffer was added to the stained wells and the plate was centrifuged at 700 x g for 1 min at 18 °C. Next, MACS cells sorted with the Bu-1-Biotin antibody were additionally stained with Bu-1-FITC to be able to detect them with the flow cytometer. For this, 50 μ L of Bu-1-FITC antibody (1:200 dilution) (#MA5-28701, Thermo Fisher Scientific) was added to each well, and incubated for 20 min on ice in the dark. Cells sorted with Bu-1-FITC antibody and Bu-1-AF647 antibody did not require additionally staining for detection, as they were already stained with FITC and Alexa Fluor, respectively. Cells were washed, and the pellet was resuspended in 300 μ L of Fluo-buffer, ready to be analysed in the Invitrogen Attune NxT Flow Cytometer.

3.8. FACS-based cell sorting

Alternatively, FACS was also tested to isolate the B cells. To the leucocyte suspension obtained after cell counting, the staining with Fixable Viability Dye eFluor™ 780 and Bu-1-FITC for FACS detection was performed as described for MACS. Briefly, the treatment conditions were defined (**Table 2**), 200 μ L of the samples were transferred to a 96-well round bottom plate and centrifuged at 700 x g for 1 min at 4°C. For the live/dead staining, 200 μ L of Fixable Viability Dye eFluor™ 780-staining was used and the plate was incubated for 20 min on ice in the dark. After the 20 min incubation, 150 μ L of Fluo-buffer were added to the stained wells and the plate was centrifuged at 700 x g for 1 min at 18 °C. Then, 50 μ L of Bu-1-FITC antibody was added to each well and incubated for 20 min on ice in the dark. Cells were washed, and the pellet was resuspended in 300 μ L of Fluo-buffer, ready to be analysed in the CytoFLEX SRT Cell Sorter. B cells were directly sorted into a tube with 1-Thioglycerol (TG) + BL buffer, for further RNA extraction.

3.9. Invitrogen Attune NxT Flow Cytometer and CytoFLEX SRT Cell Sorter

In the Invitrogen Attune NxT Flow Cytometer, a volume of 100 μ L of each treatment was set to be analysed. The voltage of the FSC laser was set to 190 volts and the SSC to 380 volts, to obtain the best visualisation of the data. Regarding the CytoFLEX SRT Cell Sorter, this equipment was utilised for the FACS assays, as it allowed the selection and sorting of the desired population. In here, one defined the population to sort (based on the gating), the sorting mode (based on purity) and the volume of the sample and the target count, which was set as unlimited to sort all the B cells in the volume.

The gating strategy was the same in both instruments. One representative example is shown in **Figure 8**. The first gate corresponds to the selection of the live cells, with the forward scatter plotting against the PC7 channel (**Figure 8 A**). The PC7 channel detects the peak emission at 780nm from the Fixable Viability Dye eFluor™ 780, the gated cells must be negatively stained to correspond to the alive cells⁹⁹. Next, all the events that consisted of two independent particles, designated doublets, were excluded by plotting side scatter height against side scatter area. Doublets have increased area while maintaining a similar height to single cells, so to exclude them, a gate was made in the diagonal zone of the square (**Figure 8 B**)¹⁰⁰. Finally, the forward scatter was plotted against the FITC channel to target the B cells, and a gate was drawn for the Bu-1⁺ cells (**Figure 8 C**). All the results from the flow cytometer and the sorter were analysed using FlowJo™ v10.8 Software (BD Life Sciences)¹⁰¹. The total number of isolated B cells in the sample could be estimated from both instruments.

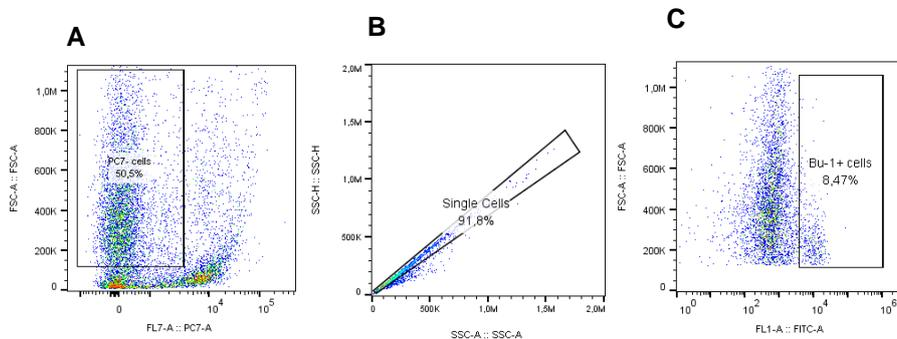


Figure 8. Gating strategy for the identification of B cells. Cells were analysed in the CytoFLEX SRT Cell Sorter. **A.** PC7-A vs FSC-A permitted the elimination of dead cells, and a gate was drawn in the live cells, which are PC7-. **B.** SSC-A vs SSC-H were employed to eliminate the doublets, the gate contains the single cells. **C.** FITC-A vs FSC-A against was gated to select the Bu-1⁺ cells, which are the B cells. These figures were obtained from FlowJo™ v10.8 Software (BD Life Sciences)¹⁰¹.

3.10. RNA Extraction

The procedure to extract RNA was dependent on the number of B cells isolated. If the number of B cells was higher than 1,000, then RNA was extracted according to the described in this point. On the other hand, if the number of B cells were inferior to 1,000, then cDNA would be directly synthesised via a

SMART-Seq v4 PLUS Kit. However, the number of B cells was always superior to 1,000, so the second case never happened, and RNA was always extracted as reported here.

To extract total RNA from the isolated B cells, the ReliaPrep™ RNA Cell Miniprep kit (#Z6010, Promega Corporation) was employed according to the manufacturer 's instructions. Briefly, cells were centrifuged at 300 x g for 5 min, and the supernatant was discarded. The cell pellet was washed with ice-cold, sterile 1 x PBS and centrifuged at 300 x g for 5 min. Depending on the concentration of B cells, different ratios of 1-Thioglycerol (TG) + BL buffer were prepared according to the protocol (**Table 4**). The corresponding volume of 100 % isopropanol was added (**Table 4**), and the solution was vortexed for 5 sec. The lysate was transferred to a Minicolumn in a collection tube, centrifuged at 14,000 x g for 1 min at 20 °C, and the liquid in the collection tube was discarded. 500 µL of RNA wash solution was added to the Minicolumn and it was centrifuged. DNase I incubation mix was prepared according to the ReliaPrep™ RNA Cell Miniprep protocol, and 30 µL were added to the column and incubated for 15 min at 20 °C. After 200 µL of Column wash solution (with ethanol) was added, the column was centrifuged for 30 sec at 14,000 x g. Similarly, 500 µL of RNA wash solution (with ethanol) was added and centrifuged at 14,000 x g for 1 min. 300 µL of RNA wash solution was added, the column was centrifuged at 23,000 x g for 2 min, and the collection tube was discarded. The column was transferred to a 1.5 mL Eppendorf tube, and 15 µL of Nuclease-free water was added, followed by centrifugation at 14,000 x g for 1 min, and the RNA was stored at -80 °C.

Table 4. The volume of BL + TG Buffer and 100% isopropanol utilised according to the number of B cells in each sample. This table was retrieved from the ReliaPrep™ RNA Cell Miniprep protocol.

Number of B cells	BL + TG Buffer	100% Isopropanol
1×10^2 to 5×10^5	100µl	35µl
$> 5 \times 10^5$ to 2×10^6	250µl	85µl
$> 2 \times 10^6$ to 5×10^6	500µl	170µl

3.11. Bioanalyzer

The total RNA was analysed using the Agilent 2100 Bioanalyzer instrument with the Agilent RNA 6000 Pico kit. This kit was selected as it allows to analyse RNA in low concentrations (50 - 5000 pg/µL in water). The chip priming station was set for RNA analysis by replacing the syringe and adjusting the base plate and syringe clip. The RNA ladder, the gel and the gel-dye mix were prepared according to the protocol for the Pico kit, and the gel-dye was loaded into an RNA chip. The conditioning solution and the marker were loaded in the RNA chip defined spots, and 1 µL of the ladder and samples were loaded. With this procedure, it was possible to determine the RNA integrity number (RIN), quality and concentration of total RNA, as well as identify and calculate the ratio of the ribosomal peaks (18S/28S or 16S/23S), relevant for determining the level of sample degradation. Only RNA samples with a minimum RIN of 8.0 were used for further analysis.

3.12. cDNA Synthesis

The cDNA synthesis and all the further steps until the library sequencing were performed by Christine Wurmser (TU München, Freising). The cDNA synthesis from total RNA was performed with the SMART-Seq[®] v4 PLUS Kit from Takara Bio USA, Inc. The SMART (Switching Mechanism at the 5' End of RNA Template) technology relies on the template-switching activity of the reverse transcriptase (RT) to enrich for full-length cDNAs and to add defined PCR adapters directly to both ends of the first-strand cDNA. With this, one can guarantee that the final cDNA libraries contain the 5' end of the mRNA, thus maintaining an accurate representation of the original transcripts, critical for an unbiased gene expression analysis ¹⁰².

Briefly, lysis buffer and RNase inhibitor were added to the purified RNA samples, according to the concentrations in the protocol. Then the 3' SMART-Seq CDS Primer II A was added and samples were mixed. The following step was the synthesis of the first strand of cDNA, which was primed with the 3' SMART-Seq CDS Primer II A. In the synthesis, the reverse transcriptase SMARTScribe used the SMART-Seq v4 Oligonucleotide for template switching at the 5' end of the transcript. Next cDNA was amplified by long distance PCR (LD-PCR), where the PCR Primer II A amplified the cDNA by priming to the sequences introduced by the 3' SMART-Seq CDS Primer II A and the SMART-Seq v4 Oligonucleotide. In this step, the number of PCR cycles ran depended on the total RNA input amount, according to the SMART-Seq[®] Kit protocol. Then, the amplified cDNA was purified by immobilisation on NucleoMag NGS Clean-up and Size Select beads (available from Takara Bio, Cat. No. 744970). The beads were washed with ethanol, and the cDNA was eluted with Elution Buffer. Finally, the cDNA quality and quantity were determined with the Agilent 2100 Bioanalyzer and Agilent 's High Sensitivity DNA Kit (Agilent, #5067-4626). A successful high sensitivity cDNA sample run is identified by all the sample peaks appearing between the lower and upper marker peaks, a flat baseline with readings of at least 5 fluorescence units (FU), the marker readings being at least 3 FU higher than the baseline and if both marker peaks are well resolved from sample peaks ¹⁰³. Once determined that the quality and quantity of samples were good, the library preparation step was followed.

3.13. Library Preparation and Illumina Next-Generation Sequencing

A cDNA dilution was performed with the buffers indicated in the SMART-Seq[®] v4 PLUS Kit protocol, and a Stem-Loop adapter was bound. For the library preparation, a master mix was assembled and added to each containing the cDNA and Stem-Loop Adapter mix, and a library preparation reaction PCR program was run according to the protocol. The prepared library was then amplified by a PCR amplification program, where the number of cycles varied with the amount of cDNA. Finally, the amplified libraries were pooled and purified by immobilisation on NucleoMag NGS Clean-up and Size Select beads (available from Takara Bio, Cat. No. 744970), similarly to what was done with the cDNA. The beads were washed with ethanol, and the library was eluted with Nuclease-Free Water. The library pool was quantified with the highly sensitive fluorescent dye-based Qubit[®] dsDNA HS Assay Kit (Thermo

Fisher Scientific) and the NEBNext® Library Quant Kit for Illumina (New England Biolabs), utilizing the ViiA7™ Real-Time PCR System (Thermo Fisher Scientific). To avoid overestimating the library concentration, dilution and sequencing were performed based on a balanced estimation of both Qubit® and NEBNext® measurements. All quantification steps were carried out according to the manufacturer's instructions. The High Sensitivity DNA Kit (Agilent Technologies) 2100 Bioanalyzer (Agilent Technologies) was employed for quality determination. After these procedures, the library was diluted and denatured it with NaOH to ensure the presence of only single-stranded cDNA fragments for cluster generation. At this stage, the final library pool consisted of single-stranded fragments with adapters, sequencing primers binding sites and indices.

Sequencing was performed by the IMG/M Laboratories (TU München, Freising), resorting to the Illumina NovaSeq® 6000 SP Next-Generation Sequencing system in XP mode in 100-cycle run, with single-reads chemistry, a read length of 1x100 bp, 25 M reads per sample and 400 M of total reads. Raw data were quality-controlled, demultiplexed and transferred without further processing. Technical quality parameters were evaluated using the SAV software. The main quality parameter for assessing the run quality is the percentage of the Phred score (Q), specifically the Q30. Here each base was assigned with a quality Phred score, where a base with a Q of 30 has a probability of 1 in 1,000 to have been called incorrectly, thus 99.9% probability of a correct base call. The specifications provided by Illumina to classify this sequencing run type as fine quality is Q30 bases $\geq 85\%$ ¹⁰⁴.

3.14. RNA-Sequencing Analysis

The RNA-sequencing analyses were run with the default settings of the DNASTAR Lasergene Genomics® ⁹⁶ software. Briefly, after the sequencing of the library fastq.gz files were obtained for each experiment, and were analysed with the DNASTAR Lasergene Genomics® ⁹⁶ software. In the DNASTAR Navigator, the RNA-seq workflow was selected, and a quantitative analysis was performed resorting to the SeqMan NGen® ⁹⁶ application. Assembly of the genes was performed against the most annotated *gallus gallus* reference genome, which was GRCg6a (GCA_000002315.5), and was downloaded from NCBI ¹⁰⁵. The experiments were set as multi-sample, with replicates defined manually. The normalisation method utilised was RPKM (Reads per kilobase of transcript per million reads mapped) since a proper control sample could not be defined.

The assembly project was run, and the results were imported to ArrayStar® ⁹⁶. First, the replicate's similarity was accessed by performing a Pearson correlation test. Then, to compare the gene expression between the samples gene sets of interest were created by filtering the samples. Three workflows were available for comparing the samples based on: 1- experiments compared individually, 2- experiments compared to a baseline and 3- experiments compared pairwise. The second workflow was used to compare the gene expression between the samples. Here a gene expression fold change of 10, up and down, between samples was the criteria selected, as this project aimed to identify the differentially expressed genes (DEGs) between samples. This value of 10-fold was selected as it generated gene sets with a more reduced number of genes, containing only the most differentially expressed ones. No

selection for $p_value < 0.05$ was performed, as the RPKM method does not calculate this value. Two types of comparisons were performed, first comparing the DEGs of B cells in the same location at different time points, and then cells in distinct locations at the same time point (**Table 5**).

Table 5. List of the samples compared. Two types of comparisons were performed, first comparing the DEGs of B cells in the same location at different time points, and in distinct locations at the same time point.

Same location of B cells			Same ED of B cells		
ED12 spleen	vs	ED14 spleen	ED12 spleen	vs	ED12 blood
ED12 spleen	vs	ED16 spleen	ED14 spleen	vs	ED14 bursa
ED14 spleen	vs	ED16 spleen	ED14 spleen	vs	ED14 blood
ED14 bursa	vs	ED16 bursa	ED14 bursa	vs	ED14 blood
ED12 blood	vs	ED14 blood	ED16 spleen	vs	ED16 bursa
ED12 blood	vs	ED16 blood	ED16 spleen	vs	ED16 blood
ED14 blood	vs	ED16 blood	ED16 bursa	vs	ED16 blood

Once a gene set was created for each comparison, the DEGs were clustered based on their gene ontology (GO) terms. In this step, the GO term “Locomotion” was selected in each comparison, and new gene sets were created. This term was selected as it comprises the DEGs that participate in the migration of the B cells, which is in line with the aim of this thesis. With this, it is possible to investigate the role of these DEGs in the early stages of chicken development and perhaps elucidate novel genes that are essential for this migration. After obtaining the locomotion gene sets for each comparison of **Table 5**, some gene sets were merged to form the comparisons shown in **Table 6**. This was done to obtain a list of the DEGs involved in locomotion for each time point and location. To further visualise and examine this data, heat maps in ArrayStar^{®96} and protein-protein interaction (PPI) network analysis with the STRING^{®106} tool were performed with default settings and selecting *gallus gallus* as the target organism. Active interaction sources with a minimum interaction score of 0.4 were applied, and three clusters were defined based on kmeans clustering to create the PPI networks. The KEGG¹⁰⁷ database and the local network cluster of STRING^{®106} were employed to perform the functional pathway enrichment in the network, where pathways were ordered based on their count in the network. From the STRING^{®106} results, the interactions and pathways involved in the locomotion of B cells in each comparison were assessed and further analysed.

Table 6. List of the definitive comparisons between samples. The list of DEGs of each isolated comparison was merged, and six global comparisons were achieved, each location (spleen, bursa and blood) in the three time points (ED12, ED14, ED16). The samples in red are missing.

Location / Time-Point	Comparisons		
Spleen	ED12 Spleen	ED14 Spleen	ED16 Spleen
Bursa	ED12 Bursa	ED14 Bursa	ED16 Bursa
Blood	ED12 Blood	ED14 Blood	ED16 Blood
ED12	ED12 Spleen	ED12 Bursa	ED12 Blood
ED14	ED14 Spleen	ED14 Bursa	ED14 Blood
ED16	ED16 Spleen	ED16 Bursa	ED16 Blood

4. Results and Discussion

4.1. Methodology optimisation and establishment of the procedure to isolate B cells

The aim of this project was to establish a methodology to isolate B cells in their early stages of development and to perform an RNA-sequencing analysis to identify the mechanisms involved in their migration to the bursa. Therefore, lymphocytes were isolated from embryonic days 12, 14 and 16 in the three locations involved in the embryonic B cell development, the spleen, bursa and blood.

Until this date, no procedure to isolate B cells for RNA-seq from such early stages of embryonic development has been elucidated. So far, only a methodology for more later stages was defined, from embryonic day 16 to ED19⁷⁰. However, in ED16, the embryo is more structured than in ED12. At such an early time, the B cells are in a significantly reduced number and the organs are in their initial growth, so the amount of B cells per embryo is low. Henceforth, it is crucial to define a procedure that identifies the amount of embryos and the time needed to obtain enough high-quality RNA from the isolated B cells¹³. Even though there are methodologies defined to obtain cell suspensions from the splenic and bursal tissue at ED10, these do not focus on isolating the B cells but aim to analyse only the tissue⁸. Two different cell sorting techniques were tested and compared to establish an embryonic B cell isolation. These were magnetic-activated cell sorting (MACS) and fluorescence-activated cell sorting (FACS), as they allow for selection and sorting of B cells⁹⁷. Nevertheless, the existing protocols for isolating B cells that resorted to MACS and FACS had to be optimised, as ED12 B cells are susceptible and in reduced numbers^{8,10}. Once the methodology was established for ED12, it was applied to ED14 and ED16 time points. A reproducible procedure to isolate alive B cells from the embryonic spleen, bursa and blood at ED12 was successfully established.

4.1.1. Magnetic-activated cell sorting

The first approach assessed to isolate the B lymphocytes was magnetic-activated cell sorting (MACS). This technique was evaluated first as, compared to FACS, it was reported to process cells faster, obtain higher yields and more viable cells. Additionally, MACS is a more straightforward procedure and requires no previous training. Nevertheless, this technique is known to have more false negatives and may require the usage of more volumes of antibodies and beads than recommended in the manufacturer protocols, thus increasing its cost⁹⁷. The most challenging time point is ED12, so most tests and comparisons were performed in embryos at this age. To isolate B lymphocytes via MACS, the antibodies employed were against the Bu-1 receptor (**Table 3**), which is expressed in B lymphocytes since ED9^{7,10,13,108}.

The first antibody evaluated was the Bu-1-Biotin and the Streptavidin MicroBeads. Once MACS was performed in splenic B cells of ED12, and the complex B cells-antibody-beads was isolated, the cells were analysed in the Invitrogen Attune NxT Flow Cytometer. The percentage of B cells (Bu-1⁺), in the ED12 splenic sample before performing MACS was 0.30 %, and after MACS decreased to 0.26 % (**Figure 9 A**). For the bursa, the percentage of Bu-1⁺ cells before MACS was 0.04 %, and after isolation, it was 0.03 % (**Figure 9 B**). These results indicate that the Bu-1-Biotin antibody and Streptavidin MicroBeads are unsuitable for isolating B cells, as most of the cells died.

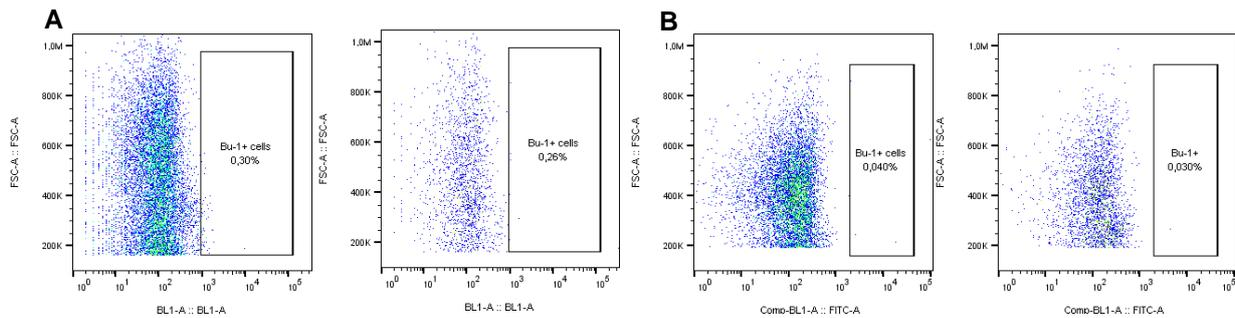


Figure 9. MACS flow cytometrical data of Bu-1⁺ cells in ED12 splenic and bursal B cells sample. The spleens (n=113) (**A**) and the bursae (n=30) (**B**), from ED12 embryos, were extracted, pooled and smashed, and the lymphocyte fraction was isolated by density gradient centrifugation on Ficoll. The B cells were stained with Bu-1-Biotin antibody and Streptavidin MicroBeads for MACS and subsequently stained with Fixable Viability Dye eFluor™ 780 and Mouse Anti-Chicken Bu-1-FITC for flow cytometry. The left panel shows the percentage of Bu-1⁺ cells before MACS, and the right panel illustrates the percentage of Bu-1⁺ cells after performing MACS. These figures were obtained from FlowJo™ v10.8 Software (BD Life Sciences) ¹⁰¹.

However, the low percentages of B cells may also be due to the antibodies utilised in MACS and then in the flow cytometer staining, the Bu-1-Biotin and the FITC, both bind to the Bu-1 receptor. Hence, some steric hindering effects may have occurred, or even the occupation of the receptor by, for instance, the Bu-1 antibody, thus hampering the subsequent ligation of the FITC antibody, resulting in a decreased number of labelled cells. On the other hand, B cells could have already been dead before MACS, compromising the results with any antibody/beads pair. The damaging of the cells before MACS could be related to the duration of the protocol, the smashing of the cells being too harsh, or the cells being under deteriorating conditions.

To discard the option of the B cells being dead already before MACS, a control cell line was used and treated in the same conditions as the B cells in the staining. The cell line utilised was the embryonic and cancer chicken B cell line DT40 (**Figure 10 B**). However, as this control is a bursal B cell line, it probably not as sensitive as ED12 B cells, nevertheless it is the best cell line control available. The procedure until MACS was performed equally in both cell lines, and the percentage of B cells was measured to assess if it was in these steps that B cells were dying. For the spleen, the percentage of B cells in the control unstained sample was 0.53 % and in the stained sample was 2.07 % (**Figure 10 A**). For the DT40 cell line, the percentage of B cells in the control unstained sample was 0.10 % and for the stained sample was 80.70 % (**Figure 10 B**). The high percentage of B cells in the control line (80.70 %)

compared to the splenic sample (2.07 %), suggests that the reduced value of B cells in the spleen and bursa after MACS (**Figure 9**) was not related to incorrect handling or unfavourable conditions to the cells, as the control B cell line DT40 was treated equally and achieved a high percentage of stained B cells. Hence, this indicates that the reason why cell isolation failed was not due to the procedure before MACS, but was instead due to the antibody/bead pair employed. To overcome this, further optimisation and selection of better antibodies/beads were performed.

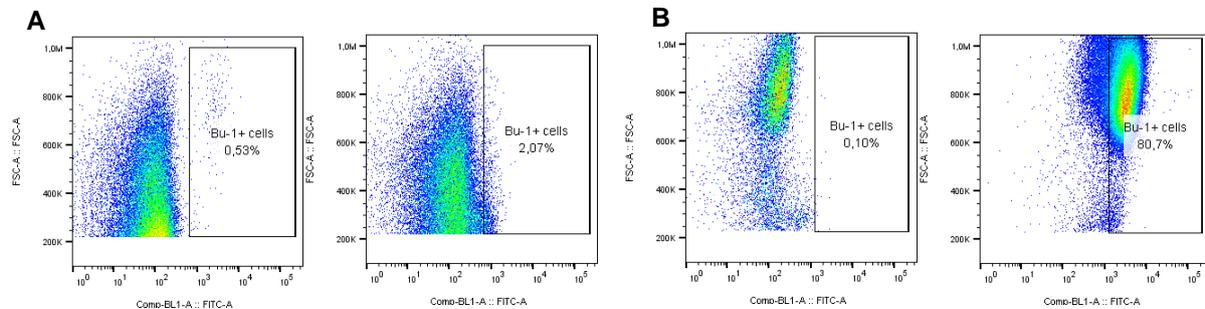


Figure 10. MACS flow cytometrical data of Bu-1⁺ cells in ED12 spleen (A) and DT40 cells (B). **A.** The spleens from ED12 embryos (n=30) were extracted, pooled and smashed, and the lymphocyte fraction was isolated by density gradient centrifugation on Ficoll. The B cells were stained with Fixable Viability Dye eFluor™ 780 and Mouse Anti-Chicken Bu-1-FITC for flow cytometry. The left panel shows the percentage of Bu-1⁺ cells in the unstained fraction of cells, and the right panel illustrates the percentage of Bu-1⁺ cells after performing the staining. **B.** The DT40 cells were stained for B cells with Fixable Viability Dye eFluor™ 780 and Mouse Anti-Chicken Bu-1-FITC for flow cytometry. The left panel shows the percentage of Bu-1⁺ cells in the unstained fraction of the cells, and the right panel illustrates the percentage of Bu-1⁺ cells after performing the staining. These figures were obtained from FlowJo™ v10.8 Software (BD Life Sciences) ¹⁰¹.

Next, the Bu-1-FITC antibody and Anti-FITC MicroBeads were evaluated. This antibody poses the advantage of skipping the FITC staining step necessary to visualise the cells in the flow cytometer after MACS. The procedure was evaluated on ED14 splenic B cells, where the percentage of Bu-1⁺ cells before MACS was 12.40 %, and after MACS decreased to 2.72 % (**Figure 11 A**). Thus, MACS with Bu-1-FITC antibody and anti-FITC MicroBeads was also not working in the embryonic stages. Another test with this antibody/beads was performed on a spleen from a broiler, (**Figure 11 B**), as the B cells and the organs of a hatched chicken are more resistant than in an embryo, as well as the number of B cells is higher ¹³. With this test one could evaluate if the antibody/beads pair worked in a more favourable sample, with a much higher number of cells. In this experiment, the percentage of B cells before MACS was 39.10 %, and after performing MACS was 38.80 % (**Figure 11 B**). These values indicate that even

in conditions where B cells were abundant and more resistant, MACS with Bu-1-FITC antibody and Anti-FITC MicroBeads barely did not increase the B cell purity.

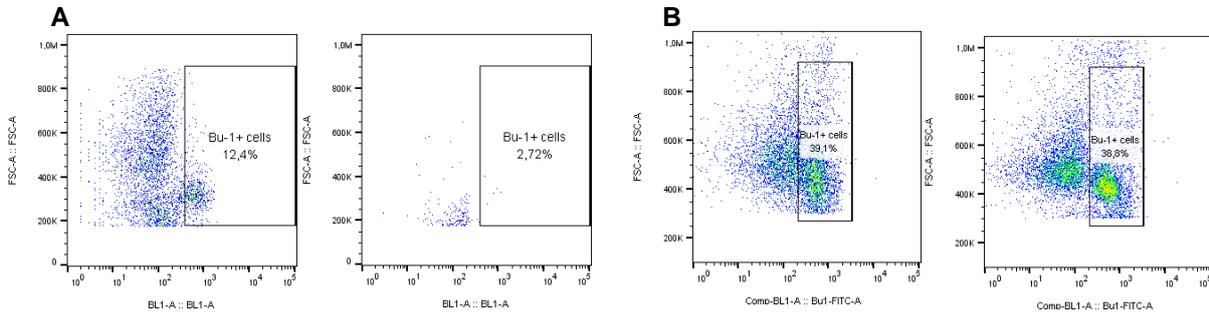


Figure 11. MACS flow cytometrical data of Bu-1⁺ cells in ED14 splenic B cells and in a broiler spleen. **A.** The spleens from ED14 embryos (n=30) and **B.** the spleen from a broiler (n=1), were extracted, pooled and smashed, and the lymphocyte fraction was isolated by density gradient centrifugation on Ficoll. The B cells were stained with Bu-1-FITC antibody and anti-FITC MicroBeads for MACS and stained with Fixable Viability Dye eFluor™ 780 for flow cytometry. The left panel shows the percentage of Bu-1⁺ cells before MACS, and the right panel illustrates the percentage of Bu-1⁺ cells after performing MACS. These figures were obtained from FlowJo™ v10.8 Software (BD Life Sciences) ¹⁰¹.

The third attempt to isolate B cells with MACS was employing the Bu-1-AF647 antibody and Anti-Cy5/Anti-AF647 MicroBeads. This antibody was assessed as it was reported to be successful in numerous studies in isolating B cells ^{109,110}. A broiler blood sample was utilised to compare the Bu-1⁺ percentage obtained after performing MACS with: Bu-1-FITC antibody + Anti-FITC MicroBeads (**Figure 12 A**) and MACS with Bu-1-AF647 antibody + Anti-AF647 MicroBeads (**Figure 12 B**). When utilising the Bu-1-FITC antibody and anti-FITC MicroBeads, an increase from 2.54 % to 7.35 % B cell percentage was obtained (**Figure 12 A**). This not substantial increase in the B cell purity could be related to Bu-1-

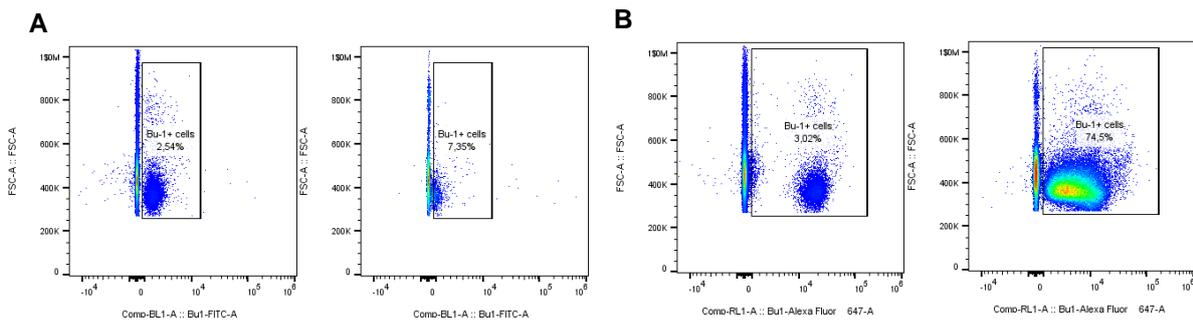


Figure 12. MACS flow cytometrical comparing two MACS antibodies to isolate Bu-1⁺ cells in the blood of a broiler. The lymphocyte fraction was separated from the blood by density gradient centrifugation on Ficoll. **A.** The B cells were stained with Bu-1-FITC antibody and Anti-FITC MicroBeads for MACS and stained with Fixable Viability Dye eFluor™ 780 for flow cytometry. The left panel shows the percentage of Bu-1⁺ cells before MACS, and the right panel illustrates the percentage of Bu-1⁺ cells after performing MACS. **B.** The B cells were stained with Bu-1-AF647 antibody and Anti-Cy5/Anti-Alexa Fluor 647 MicroBeads for MACS and stained with Fixable Viability Dye eFluor™ 780 for flow cytometry. The left panel shows the percentage of Bu-1⁺ cells before MACS, and the right panel illustrates the percentage of Bu-1⁺ cells after performing MACS. These figures were obtained from FlowJo™ v10.8 Software (BD Life Sciences) ¹⁰¹.

FITC antibody inability to bind strongly enough to the magnetic field of the column, which may lead to the stained B cells eluting in the fraction before the desired, hence resulting in low percentages of B cells obtained. Regarding the results obtained for MACS with the Bu-1-AF647 antibody and Anti-AF647 MicroBeads, a cell enrichment from 3.02 % to 74.50 % was achieved (**Figure 12 B**). The Bu-1-AF647 antibody and Anti-AF647 MicroBeads allowed for a much higher enrichment in the B cell purity after MACS. Therefore, in line with these results, all further MACS procedures were performed employing the Bu-1-AF647 antibody and Anti-AF647 MicroBeads.

4.1.1.1. MACS enriched B cells in the ED12 spleen but failed in the bursa

Once the MACS methodology that achieved the highest enrichment in B cell purity (with Bu-1-AF647 antibody and Anti-AF647 MicroBeads) was defined, the next step was to employ it to isolate the cells from the spleen and bursa in ED12.

In line with this, several MACS assays were performed, using to the Bu-1-AF647 antibody and Anti-AF647 MicroBeads to stain and isolate the ED12 B cells. The methodology was executed in the ED12 splenic B cells, and the percentage of Bu-1⁺ cells obtained after MACS went from 13.90 % Bu-1⁺ cells to 71.50 % (**Figure 13 A**). Previous studies that employed equal antibody and beads for MACS reported an achieved purity of B cells of around 80 % for the whole blood of humans ¹¹¹. Nonetheless, a purity of 71.50 % obtained by MACS in ED12 splenic B cells was good, as cells in such an early stage are extremely difficult to isolate alive compared to the whole blood of an adult individual ^{13,111}. Concerning

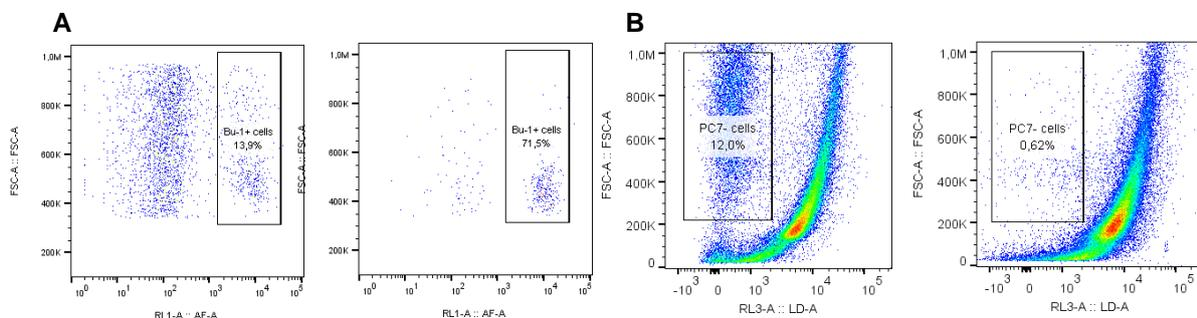


Figure 13. MACS flow cytometrical data of Bu-1⁺ cells (A) and PC7⁻ cells (B) from ED12 splenic B cells. The spleens from ED12 embryos (n=37) were extracted, pooled and smashed, and the lymphocyte fraction was isolated by density gradient centrifugation on Ficoll. The B cells were stained with Bu-1-AF647 antibody and Anti-Cy5/Anti-Alexa Fluor 647 MicroBeads for MACS and stained with Fixable Viability Dye eFluor™ 780 for flow cytometry. **A.** Percentage of Bu-1⁺ cells in the ED12 splenic sample before and after MACS. **B.** Percentage of PC7⁻ cells in the splenic sample before and after MACS. The graphs correspond to the same as in sample A. These figures were obtained from FlowJo™ v10.8 Software (BD Life Sciences) ¹⁰¹.

the purity parameter, this method seemed suitable for isolating splenic B cells in ED12. However, the percentage of alive splenic cells (PC7⁻) decreased from 12.00 % to 0.62 % after MACS (**Figure 13 B**). Therefore, even though MACS significantly increased the percentage of Bu-1⁺ cells in the splenic sample, it was very harmful to the cells.

The MACS methodology was also evaluated in ED12 bursal B cells (**Figure 14**). The percentage of Bu-1⁺ cells after MACS increased from 0.65 % to 15.40 % (**Figure 14 A**), and the percentage of live cells decreased from 3.29 % to 0.09 % (**Figure 14 B**). These results indicate that MACS was unsuitable to enrich the B cell content in the bursa, and was damaging the cells. In line with the MACS results, another method was assessed to isolate B cells.

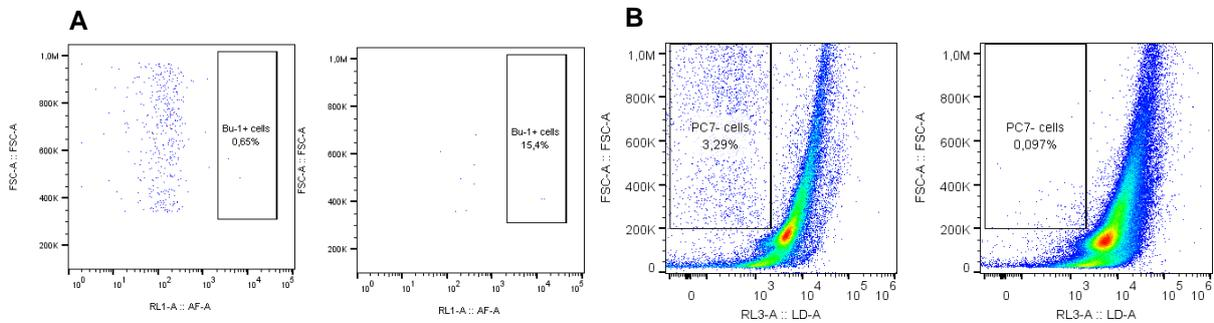


Figure 14. MACS flow cytometrical data of Bu-1⁺ cells (A) and PC7⁻ cells (B) from ED12 bursal B cells. The bursae from ED12 embryos (n=35) were extracted, pooled and smashed, and the lymphocyte fraction was isolated by density gradient centrifugation on Ficoll. The B cells were stained with Bu-1-AF647 antibody and Anti-Cy5/Anti-Alexa Fluor 647 MicroBeads for MACS, and after stained with Fixable Viability Dye eFluor™ 780 for flow cytometry. **A.** Percentage of Bu-1⁺ cells in the ED12 bursal sample before and after MACS **B.** Percentage of PC7⁻ cells in the bursal sample before and after MACS. These figures were obtained from FlowJo™ v10.8 Software (BD Life Sciences) ¹⁰¹.

4.1.2. Fluorescence-activated cell sorting

The second technique evaluated to isolate B cells was fluorescence-activated cell sorting. FACS is characterised by more accurately separating different subpopulations of cells. Hence, a much higher purity of B cells was expected to be obtained comparative to MACS ⁹⁷. Nevertheless, FACS requires significantly more time to sort the cells due to its low throughput, and may result in lower absolute yields. One reason for this is that when gating to sort the B cells by FACS, one must exclude the dead cells and the multicellular aggregates, thus resulting in a diminished yet purer yield. In the MACS procedure, there is no imposition of these constraints, so the flow obtained is less pure but has a higher yield of cells ⁹⁷.

The antibody evaluated for FACS was the Bu-1-FITC, as the defined SOP suggested. Additionally, it showed promising results in the regular staining of B cells performed previously in this report (**Figure 10**) and other studies ^{7,10}. Even though this antibody was not strong/stable enough to perform MACS successfully, it was expected to yield reliable results in FACS, as this technique does not require a strong magnetic field. FACS resorting to the Bu-1-FITC antibody was performed for the ED14 splenic B cells, and a percentage of Bu-1⁺ from 8.66 % to 52.90 % after FACS was achieved (**Figure 15 A**). Comparable results were obtained for the ED14 bursal B cells, increasing from 14.70 % Bu-1⁺ cells to 43.40 % after FACS (**Figure 15 B**). These results suggest that the staining performed with the Bu-1-FITC antibody and the subsequent sort of cells through FACS worked, as an apparent increase in the B cell percentage was obtained for both organs. Therefore, all the subsequent FACS assays were

performed employing this antibody. However, analysis of the samples before they were subjected to FACS indicated that the percentage of live cells in both organs was very diminished (**Figure 15 left**). In the spleen, only 3.78 % of cells were alive before sorting (**Figure 15 A**), and in the bursa, there were just 2.01 % live cells (**Figure 15 B**).

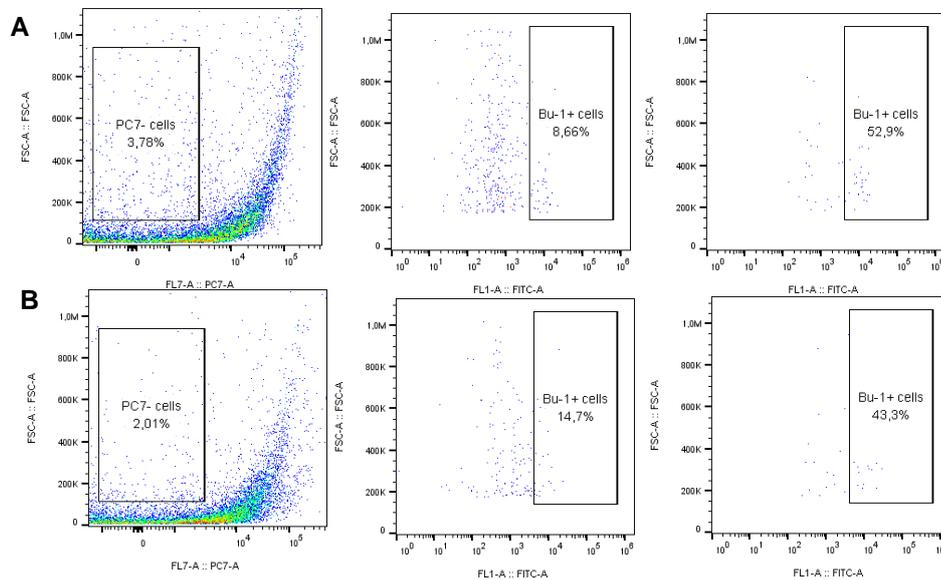


Figure 15. FACS flow cytometrical data of Bu-1⁺ cells from ED14 spleen (A) and bursa (B). The spleens (A) and bursae (B) from ED12 embryos (n=30) were extracted, pooled and smashed, and the lymphocyte fraction was isolated by density gradient centrifugation on Ficoll. The B cells were stained with Fixable Viability Dye eFluor™ 780 and Mouse Anti-Chicken Bu-1-FITC for flow cytometry. **A.** The left panel shows the percentage of live cells in the spleen sample before FACS, the middle panel represents the Bu-1⁺ cells in the spleen sample before FACS, and the right panel illustrates the percentage of Bu-1⁺ cells after performing FACS. **B.** The left panel shows the percentage of live cells in the bursa sample before FACS, the middle panel represents the Bu-1⁺ cells in the bursa sample before FACS, and the right panel illustrates the percentage of Bu-1⁺ cells after performing FACS. These figures were obtained from FlowJo™ v10.8 Software (BD Life Sciences) ¹⁰¹.

Hence, the methodology before FACS was optimised. For this, the most straightforward possibility was decreasing the time spent in the organ collection, as here the cells were in deteriorating conditions due to the content of the smashed organs being in the tube with the B cells, which could favour conditions for apoptosis ¹¹². To minimise the time spent, the total number of eggs was split into two groups and the extraction and smashing were performed at two separate times. So one batch of eggs was split in half, the first part were collected, processed, and sorted the organs. The subsequent half was utilised only once the sorting was finished for the first round. With such modification the time the cells and organs were exposed to deteriorating conditions was significantly reduced. This optimised procedure was performed in ED12 splenic B cells, and a percentage of 45.50 % live cells (**Figure 16 A**) was obtained, and for the ED12 bursal cells was obtained 5.94 % live cells (**Figure 16 B**). There was a substantial increase in the percentage of live cells in the spleen sample, however, the increase was not so high for

the bursal B cells. This can be explained by the fact that the bursal B cells on ED12 are extremely sensitive, and only a few cells are present, thus with the organ smashing most of them die ¹³.

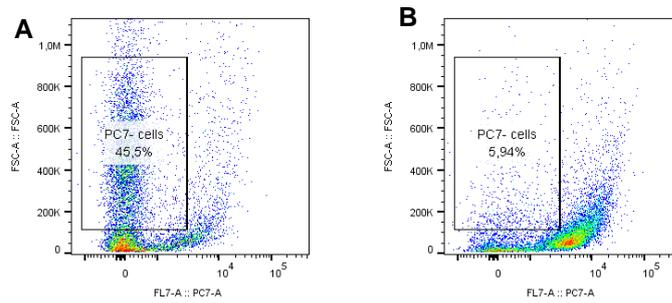


Figure 16. FACS flow cytometrical data of live cells from ED12 spleen (A) and bursa (B). The spleen (A) and bursa (B) from ED12 embryos (n=30) were extracted, pooled and smashed, and the lymphocyte fraction was isolated by density gradient centrifugation on Ficoll. The B cells were stained with Fixable Viability Dye eFluor™ 780 and Mouse Anti-Chicken Bu-1-FITC for FACS. **A.** Percentage of PC7⁺ cells (live cells) in the spleen sample after FACS was performed. **B.** Percentage of PC7⁺ cells (live cells) in the bursa sample after FACS. These figures were obtained from FlowJo™ v10.8 Software (BD Life Sciences) ¹⁰¹.

To test if this method optimisation was at least improving the yield of the remaining time points, it was employed instead in ED14. For the splenic B cells, 49.90 % of live cells (**Figure 17 A**) were obtained, and for the bursa 20.90 % (**Figure 17 B**). The bursal results in the ED14 time point are better than those obtained with the previous unoptimized methodology (**data not shown**). Hence, the optimised methodology was employed in the subsequent FACS assays.

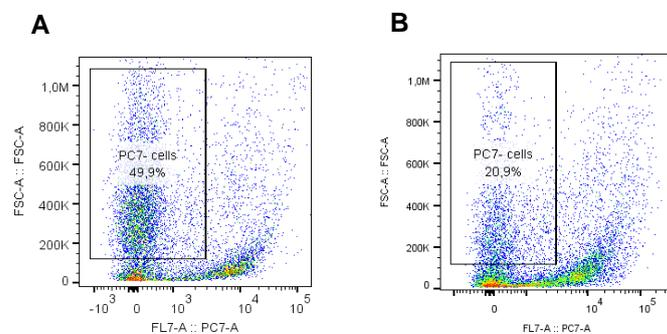


Figure 17. FACS flow cytometrical data of live cells from ED14 splenic (A) and bursal (B) B cells. The spleen (A) and bursa (B) from ED14 embryos (n=9) were extracted, pooled and smashed, and the lymphocyte fraction was isolated by density gradient centrifugation on Ficoll. The B cells were stained with Fixable Viability Dye eFluor™ 780 and Mouse Anti-Chicken Bu-1-FITC for FACS. **A.** Percentage of PC7⁺ cells (live cells) in the spleen sample after FACS was performed. **B.** Percentage of PC7⁺ cells (live cells) in the bursa sample after FACS. These figures were obtained from FlowJo™ v10.8 Software (BD Life Sciences) ¹⁰¹.

4.1.2.1 FACS successfully isolated B cells in the spleen and bursa

In splenic cells before FACS, the percentage of Bu-1⁺ cells was 9.51 %, and after FACS, increased to 88.10 % (**Figure 18 A**). This result was expected for the spleen, as such high purity was already achieved with MACS. For the bursal cells, the percentage of Bu-1⁺ prior to FACS was 0.92 %, and after the cell sorting, it increased to 74.00 % (**Figure 18 B**). This increase in B cell purity is much higher when compared to the reached with MACS, in which the maximum was 15.40 % of Bu-1⁺ cells (**Figure 14 A**). Additional to this, in both spleen and bursa, the percentage of live cells was higher than the achieved after MACS (**Figure 18 C & D**). In the splenic cells before FACS, the percentage of live cells was 14.50 %, and after FACS it increased to 55.60 % (**Figure 18 C**). This increase in the percentage of live cells after performing cell sorting can be explained if most dead cells were not B cells, thus after sorting our cells of interest the debris were removed, and the percentage of live cells increased. For the bursa, the value of live cells decreased from 25.80 % to 18.90 % after FACS (**Figure 18 D**). Regardless, this is a better result than the ones obtained with MACS, in which there were practically no alive B cells in the bursal sample after the cell sorting (**Figure 14 C & D**). Henceforth, in line with the results obtained for the spleen and bursa, FACS was the sorting method selected to isolate the B cell. The option of considering an approach which included MACS followed by FACS to obtain a higher purity of B cells was not evaluated and was disregarded, because only with MACS the cells were almost all dead (**Figure 14 C & D**), hence if after this technique one performed FACS the percentage of alive cells would be nearly 0 %^{97,111}.

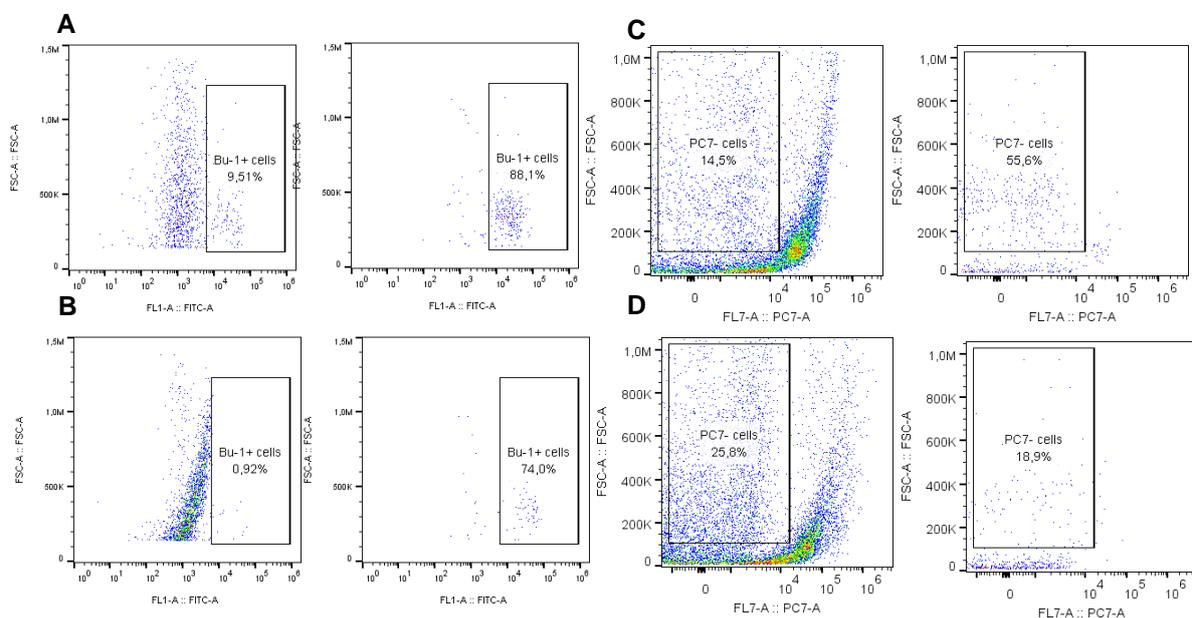


Figure 18. FACS flow cytometrical data of Bu-1⁺ cells (A & B) and PC7⁻ cells (C & D) from an ED13 splenic (A,C) and bursal sample (B,D). The organs from ED13 embryos (n=15) were extracted, pooled and smashed, and the lymphocyte fraction was isolated by density gradient centrifugation on Ficoll. The B cells were stained with Bu-1-FITC and with Fixable Viability Dye eFluor™ 780 for flow cytometry. **A.** Percentage of Bu-1⁺ cells in the ED13 spleen sample before and after FACS. **B.** Percentage of Bu-1⁺ cells in the ED13 bursa sample before and after FACS. **C.** Percentage of PC7⁻ cells in the spleen sample before and after FACS. **D.** Percentage of PC7⁻ cells in the bursa sample before and after FACS. These figures were obtained from FlowJo™ v10.8 Software (BD Life Sciences)¹⁰¹.

4.2. The migration of B lymphocytes into the bursa might occur at later time points

The development of B cells in the embryonic chicken involves different organs and processes. Broadly, the spleen is colonised by hematopoietic stem cells (HSC) at ED6-7 from the intraembryonic mesenchyme of the chicken embryo. From this time in the spleen, some HSCs undergo the first step of the V(D)J recombination processes and can become committed to the B cell lineage. Around ED8-14, the B cell precursors initiate their migration via blood circulation towards the bursa. In this location, the lymphocytes finalise the V(D)J recombination events and undergo the process of gene conversion, becoming fully mature and diversified B cells. From around ED18, the functional lymphocytes start to emigrate from the bursa to secondary lymphoid organs to exert their function ¹³. As reported, the detection of B cells can be performed from incredibly early stages, since ED9 where pre-bursal B cell precursors begin to express the Bu-1 antigen ¹⁰⁸. The B cells of the spleen, bursa and blood in ED12, ED14 and ED16 were stained with Bu-1-FITC antibody and detected in the sorter.

4.2.1. Bu-1⁺ cell percentage in the ED12 bursa was higher than in the ED12 spleen

The results obtained for ED12 are represented in **Figure 19 A**, ED14 in **Figure 19 B** and ED16 in **Figure 19 C**. Starting with ED12, the percentage of Bu-1⁺ cells obtained in the spleen was 7.58 %, in the bursa 8.62 % and in the blood 0.75 % (**Figure 19 A**). On ED14, there was a higher percentage of Bu-1⁺ cells in every location, the spleen 10.10 %, the bursa 14.60 % and the blood 1.53 % Bu-1⁺ cells (**Figure 19 B**). Lastly, in ED16 there was a decrease in the percentage of B cells in the spleen, with a value of 1.83 %, for the bursa an increase was visible, with 33.80 %, and the blood had also a decrease, with 0.53 % of Bu-1⁺ cells (**Figure 19 C**).

So far, it is alleged that from ED8 to ED14 the B cell precursors should start to emigrate from the spleen to the bursa ⁶¹. Henceforth, at ED12 the percentage of Bu-1⁺ in the spleen should be the highest when compared to ED14 and ED16 spleen. For the bursa, on ED12 as cells are still entering, the percentage of Bu-1⁺ cells should increase until, at least, ED14. Concerning the blood, the percentage of B cell precursors should be the highest in ED12 and decrease until ED16, as cells should finish their migration on ED14, so no substantial number of B cells should be identified in the blood ¹³. When analysing the results for the three locations on ED12, the bursa had the highest value of Bu-1⁺ cells compared to the spleen and blood (**Figure 19 A**). In this stage, it was expected that the spleen had a higher fraction of Bu-1⁺ cells, as the B cell precursors have almost just colonised this organ and some B cells are probably still undergoing the V(D)J processes, while only the remaining part of the cells are migrating. Also indicated by M. Lapidou *et al.*, the migration of the B cell precursors should be more preeminent from the ED12 time point, thus the spleen should have more Bu-1⁺ cells than the bursa in this time point ⁷. For the blood, a small percentage of B cells was also expected when compared to the spleen and bursa, as in this location cells are only migrating, and thus are transiently present ¹³.

4.2.2. Bu-1⁺ cell percentage in the spleen and bursa increased in ED14

Subsequent, when comparing the ED12 (**Figure 19 A**) results with ED14 (**Figure 19 B**), some inconsistencies with the observed in previous studies are also visible. Inside the spleen, the number of B cells was expected to decrease, as at ED12 the B cell precursors should only be exiting this organ. Hence at ED14, the percentage of B cells should be lower than 7.58 % at ED12 (**Figure 19 A**), however in this work a higher value of 10.10 % was achieved (**Figure 19 B**)¹³. This is not concordant with the reported in previous studies, however, these observations were identical in all the assays performed between ED12 and ED14 in this project. If the B cell migration inside the spleen and emigration towards the bursa occurred later, this could explain such results. Or even if the migration to the bursa started on ED8, these results indicate that it is more preponderant after ED14, as the B cell percentage in the spleen still increased from ED12 to ED14. As the B cells move into the spleen from the blood, the relative number of lymphocytes trafficking in these stages may provide clues about the migration period. The percentage of B cells in the blood was examined in a study performed by M. Laparidou *et al.*, where it was seen that from ED8 to ED10 the number of cells trafficking was very diminished, so it was suggested that the migration of the B cells via the blood occurred at least after ED10⁷. Additionally, in that study it was seen that the ratio of blood B cells expressing the CXCR4 receptor is the highest in ED14, which is a receptor employed by the cells to migrate towards the CXCL12 in the bursa⁷. These reports in combination with the results obtained in this project, suggest that the migration to the bursa may occur more prominently in stages later than ED12, such as in ED14 to ED16. Now comparing the ED12 (**Figure 19 A**) with the ED14 blood (**Figure 19 B**), there is an increase in the percentage of Bu-1⁺ cells, which again is concordant with the hypothesis of later cell migration proposed in this project. Nevertheless, for the blood, M. Laparidou *et al.* obtained a higher value of Bu-1⁺ cells in ED12 compared to ED14, which goes against the results obtained in this work⁷.

4.2.3. Bu-1⁺ cell percentage increased in the ED16 bursa and decreased in the ED16 spleen

When discussing the results obtained for ED16, it is visible that for the spleen and blood there was a reduction in the B cell percentage, from 10.1 % to 1.83 %, and from 1.53 % to 0.53 %, respectively. For the bursa an increase from 14.60 % to 33.8 % was seen (**Figure 19 C**). These results coincide with previous studies, as by this stage, all B cells were expected to have emigrated from the spleen, so the lymphocyte percentage should be the lowest in this organ and in circulation. The B cells still present in the spleen are referent to the ones that failed to migrate to the bursa, possibly by not expressing the necessary molecules to do so^{7,8}. For the bursa, as expected for ED16, there was a higher percentage of Bu-1⁺ cells compared to ED12 and ED14.

Interestingly, when comparing the percentage of Bu-1⁺ cells between ED14 and ED16, an intense migration of B cells can be seen, as the values decreased around 10 times in the spleen and increased by half in the bursa. These results were not observed when comparing ED12 with ED14, which was the interval anticipated for B cells to migrate. Collectively, the results for B cell migration from the spleen to the bursa to give rise to the hypothesis that cell migration occurs mostly at a later time point, from ED14 to ED16. However, further analysis on ED13 and ED15 should be performed to correctly define the interval in which the migration of Bu-1⁺ is mostly occurring.

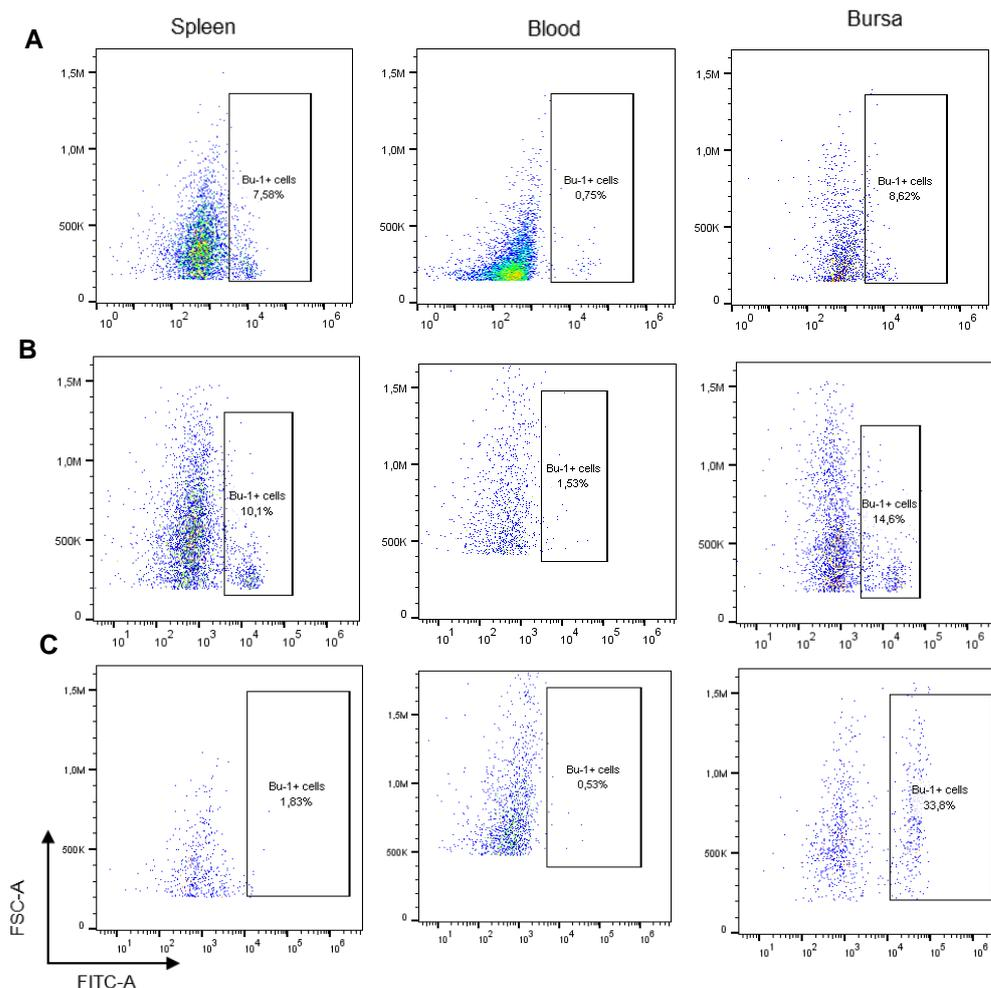


Figure 19. Flow cytometrical data of Bu-1⁺ cells from the spleen (left), blood (middle) and bursa (right) on ED12 (A), ED14 (B) and ED16 (C). The spleens and bursae (ED12: n=15, ED14: n=11, ED16: n= 30) were extracted from the embryos, pooled, smashed, and blood was collected. The lymphocyte fraction was isolated by density gradient centrifugation on Ficoll. The B cells were stained with Fixable Viability Dye eFluor™ 780 and Mouse Anti-Chicken Bu-1-FITC for FACS. These figures were obtained from FlowJo™ v10.8 Software (BD Life Sciences) ¹⁰¹. **A.** Percentage of Bu-1⁺ cells in ED12 spleen, blood and bursa, respectively. **B.** Percentage of Bu-1⁺ cells in ED14 spleen, blood and bursa, respectively. **C.** Percentage of Bu-1⁺ cells in ED16 spleen, blood and bursa, respectively.

The data for the migration of the B cells throughout the spleen, blood and bursa from ED12 to ED16, with all the replicate experiments considered was summarised (**Figure 20**). Regarding the spleen, the percentage of B cells increased until ED14, then occurred the migration of the cells until ED16, where the lowest lymphocyte fraction is achieved (**Figure 20 A**). For the bursa, the most considerable increase in the Bu-1⁺ percentage was from ED14 to ED16, which again indicates that was from ED14 that most B cells entered this organ. Indeed, from ED12 to ED14 an increase is also notable, but is not as considerable as in ED16 (**Figure 20 A**). For the blood, the percentage of Bu-1⁺ cells increased again until ED14 and was lower in ED16 (**Figure 20 B**). The results for the blood are against what was seen previously, but it correlates with the hypothesis proposed in this project of a later B cell migration ^{7,13}.

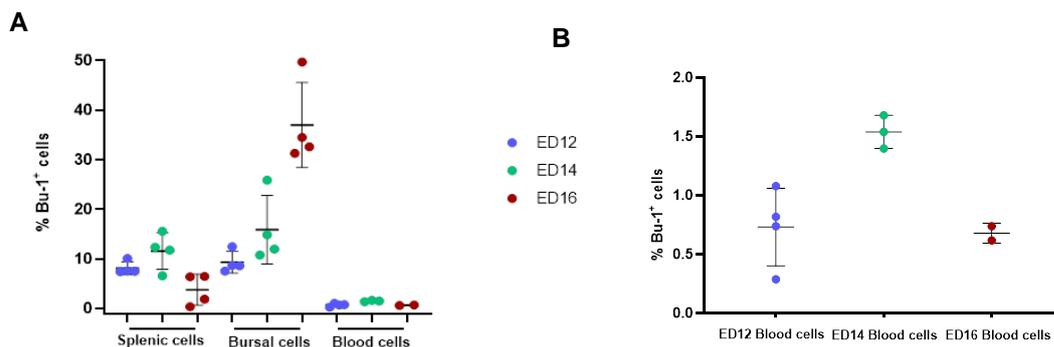


Figure 20. Summary of the migration of B cells in their developmental stages. A. Percentage of Bu-1⁺ cells in the spleen, bursa and blood for the time points ED12 (blue), ED14 (green) and ED16 (red). **B.** Amplification of the data from the blood represented in A. Each dot corresponds to one experiment. For each location and time point, at least three replicates were obtained. The data was plotted in a scatter plot with the mean, and the error bars correspond to the standard deviation (SD). This figure was designed with GraphPad Prism ¹⁵³.

4.3. Gene expression analysis of B cells in the early stages of development

The mechanisms and signals involved in the migration steps of B cells during embryonic development are not fully elucidated. To expand the knowledge in this matter, B cells were isolated at different time points and locations during embryonic development, to perform RNA-sequencing. With the differentially expressed genes, it was possible to infer which mechanisms are employed by B cells for migration into the different organs during development. The RNA samples with a high integrity number and concentration were selected to send for cDNA synthesis and further sequencing (**Table 7**). For some of the locations and time points, replicates could be obtained, yet most of the samples do not have three replicates (**Table 7**). Besides this, for the ED12 bursal samples, no data was obtained as far as the completion of this project. Nevertheless, this data made it possible to have an overview of the genes differentially expressed by the B cells in the early stages of development.

The cDNA library integrity was high, as seen by the electropherogram with a broad peak in the expected range (200 bp – 2000 bp) and an average fragment size of about 472 bp (**Table 8 A**). Regarding the quantification, the concentrations obtained were 3.8 nM and 4.73 nM with the Qubit[®] assay and

NEBNext assay[®], respectively (**Table 8 A**). A further library quality evaluation was performed after sequencing, and a Q30 score of 86.7 % indicated good quality (Q30 \geq 85 %). The total sequencing output was 40.4 Gb (**Table 8 B**).

Table 7. Data sent for Next Generation Sequencing. The embryonic day, date, origin of the B cells, RNA concentration measured in the bioanalyzer in pg/ μ L and the RNA integrity number are displayed for the 27 samples selected for sequencing. For each time point and location three replicates were obtained.

Embryonic day	Date	B cell origin	RNA conc. Bioanalyzer (pg/ μ L)	RIN
ED12	13.06.22	Spleen	189	8.8
	20.06.22		94	8.9
	20.06.22	Blood	160	9.8
ED14	03.06.22	Spleen	820	10.0
	15.06.22		2,427	10.0
	03.06.22	Bursa	63	8.9
	03.06.22	Blood	79	9.4
	15.06.22		60	8.4
ED16	25.05.22	Spleen	89	8.3
	25.05.22		104	8.7
	17.06.22		162	9.3
	25.05.22	Bursa	2,389	10.0
	25.05.22		3,163	10.0
	17.06.22		2,075	10.0
	25.05.22		Blood	97

Table 8. Quantity and quality parameters of the library pool. A. Quantification via Qubit[®] dsDNA HS Assay Kit and the qPCR-based NEBNext[®] Library Quant Kit. The sample ID, library size in base pairs, the calculated concentration from Qubit[®] and the measured concentration from NEBNext[®] in nanomolar (nM) are shown. **B. Quality parameters of the library pool by the SAV software.** The ID of the run and sample, the yield in Gigabytes (Gb) and the percentage of Q30 bases.

A	IMGM cDNA library sample ID	Library size Bioanalyzer [bp]	Calculated conc. Qubit [®] [nM]	Measured conc. NEBNext [®] [nM]
		22075-0001	472	3.80
B	NovaSeq [®] run	Sample	Yield [Gb]	Q30 bases [%]
	220707_A00726_0539_BHGGF2DRX2_22075	22075-0001	40.40	86.70

4.3.1. Similarity of the replicates was approved by Pearson correlation

The first step of the analysis was to evaluate the similarity of the gene expression levels between replicates. For this, the replicates were compared using the squared Pearson correlation test performed in ArrayStar^{®96} and the r^2 values obtained are represented in **Figure 21 A, B & C**. The Cross- r^2 statistical test compares pairwise combinations of selected replicates and calculates an r^2 value, and the higher the r^2 value the more identical the two replicates are ¹¹³. The r^2 values obtained for each sample are shown in **Figure 21**. First, analysing the r^2 values calculated between each spleen replicate, it is visible that the ED12 splenic B cell replicates, sample 1 (S1) and S3, have a high value of r^2 between the two, indicating that they are similar. The same occurs for in S4 and S7 of ED14 spleen (**Figure 21 A**). However, in ED16 the S13 is more similar to the ED12 and ED14 sample clusters compared to the remaining ED16 replicates, hence this replicate was excluded. Regarding the bursal samples, it was seen that ED16 and ED14 bursal B cell replicates clustered amongst themselves and not with each other, hence no replicate was excluded (**Figure 21 B**). For the blood, the replicates of ED14 are similar to the one of ED12, and both are distinct from the ED16 (**Figure 21 C**). No ED14 sample was excluded for the blood, as both ED14 replicates (S6 and S8) are similar to S2 of ED12. This can be explained if these two time points do not differ much in gene expression.

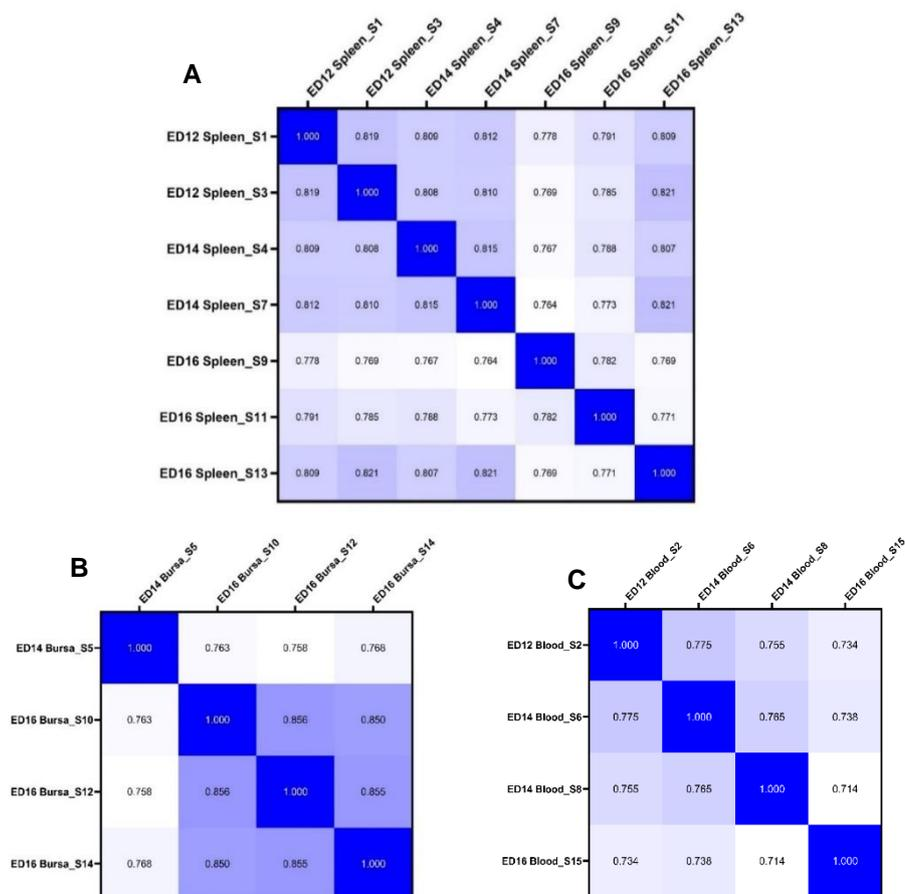


Figure 21. Heat map representation of the Pearson correlation test for the replicates of each sample in each time point, for spleen (A), bursa (B) and blood (C). Each square contains one r^2 value, and the darker the blue, the higher the value, hence the more similar the replicates are. The r^2 values presented were calculated in ArrayStar^{®96} and the heat maps were obtained with GraphPad Prism ¹⁵³.

4.3.2. Analysis of the differentially expressed genes between samples

The methodology to isolate the B cells utilised the Bu-1-FITC antibody, which binds to the Bu-1 receptor in the B cells. However, an important detail that must be considered is that this antibody is not only specific for B cells but is also expressed on subsets of macrophages and monocytes^{114,115}. In addition to this, as the efficacy of the sorter was not 100%, there may be some other cells besides B cells, such as cells from the tissue or different cell types. Besides, as the antibody is binding to a cell receptor, one could hypothesize that the cell is activating a signalling cascade to respond to this binding. The Bu-1 receptor is a cell death receptor, once it is activated it can lead to the overexpression of genes that can trigger apoptosis¹¹⁶. Henceforth, it is necessary to account for these premises while analysing the sequencing data obtained, as some genes appearing as highly expressed can be originated from other cell types isolated, or from the activated receptor signalling. Regarding the gene expression analysis, to visualise and analyse the DEGs from **Table 6** comparisons a hierarchical clustering was made to obtain heat maps. After completing these, a further protein-protein interaction network (PPI) analysis was performed resorting to the STRING®¹⁰⁶ website. This tool also permitted the evaluation of which pathways were the most represented in the DEGs. As shown in **Table 6**, the first three comparisons made were at the same B cell location and different time points, while the other three were at the same time point but different B cell locations.

ED12, ED14 and ED16 splenic B cells

In **Figure 24 A** is the heat map for the DEGs in the ED12, ED14 and ED16 splenic B cell comparisons. This list of DEGs was utilised to obtain a protein interaction network in STRING®¹⁰⁶ (**Figure 22**). In the PPI network, one isolated cluster of 11 proteins is visible in red, corresponding to the proteins involved in Cytokine-cytokine interactions. Additionally, resorting to the pathway and network cluster analysis of STRING®¹⁰⁶, it was possible to detect that a large number of proteins was also involved in MAPK pathway (blue), in axon guidance (green) and the Wnt pathway (yellow). Besides this, the most up and down-regulated genes between each samples were investigated. For example, when comparing the DEGs between ED12 and ED14, the most up-regulated gene in ED12 was EPHB1, and in ED14 was CXCL13. These may be relevant for cell migration due to their highly different expression in each sample. The most up-regulated genes among the three samples were EPHB1, CXCL13, CCL19, NTN1, CCL1 and NRG1 (**Figure 24 A**). As visible in **Figure 22**, CXCL13, CCL19 and CCL1 are involved in the Cytokine-cytokine receptor interactions, and are highly expressed by ED12 and ED14 compared to ED16 (**Figure 24**), thus revealing a possible importance in the emigration of the B cells from the spleen. Regarding NTN1, this gene is the most up-regulated in ED16 when compared to ED12 (**Figure 24 A**), and it is involved in axon guidance mechanisms (**Figure 22**). So, this gene is probably not related to the emigration of the B cells, as, at this point, the cells should have already migrated. NRG1 is highly expressed in the ED16 spleen compared to ED14 and is related to the proliferation and differentiation of tissues, thus is probably not associated with B cell migration¹¹⁷.

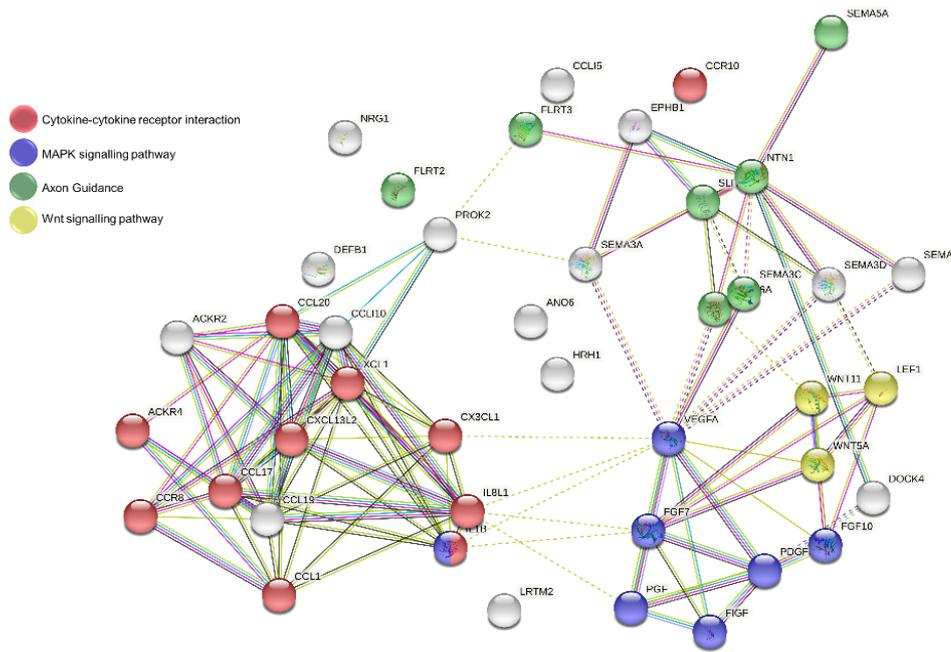


Figure 22. Protein-Protein Interaction Network of the DEGs in ED12, ED14 and ED16 spleen. The list of DEGs obtained from ArrayStar[®] 96 was subjected to a PPI analysis with the STRING[®] 106 tool. The cytokine-cytokine receptor interactions (red), MAPK signalling pathway (blue), axon guidance (green) and the Wnt signalling pathway (yellow) were the most prevalent pathways. The edges represent the protein-protein associations, the known interactions (light blue and purple), the predicted interactions (green, orange, blue) and others (yellow, black, violet). A kmeans clustering was performed with the creation of 3 clusters shown by the dotted line between the proteins.

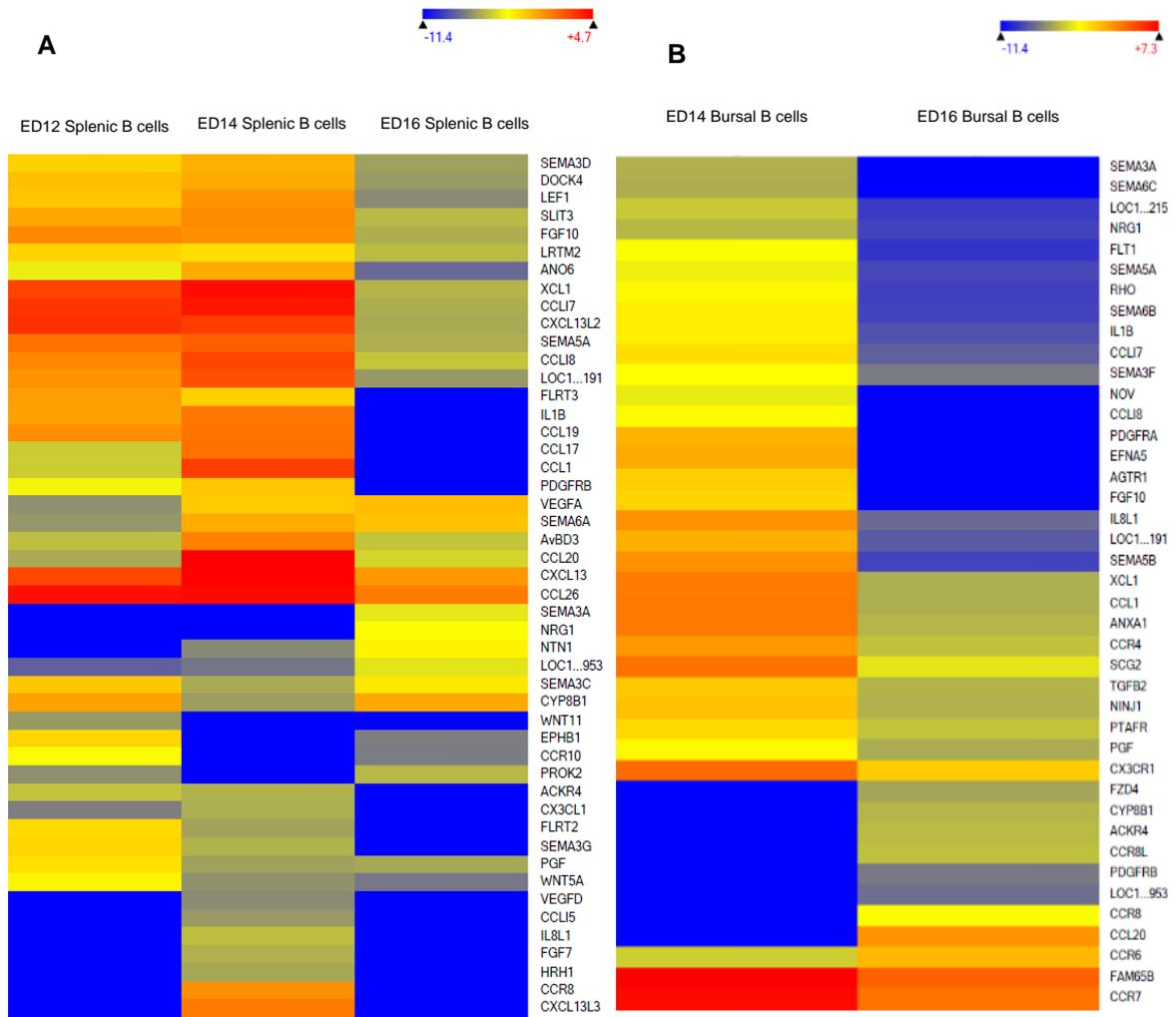


Figure 24. Heat map of the DEGs between ED12, ED14 and ED16 splenic B cells (A) and ED14 and ED16 bursal B cells (B). Hierarchical clustering was performed with the list of DEGs and the corresponding samples. In blue are the low expressed genes, in yellow the medium expressed and in red the highly expressed. This figure was obtained with ArrayStar[®] 96.

ED12, ED14 and ED16 Blood B cells

Next, evaluating the PPI obtained with the DEGs between the blood samples in the three time points (**Figure 25**), one can perceive that the most expressed pathways are again the cytokine receptor interactions (red), MAPK signalling (blue), axon guidance (green) and Wnt signalling (yellow). From evaluating the DEGs between the three samples (**Figure 26 A**), the highest expressed in each comparison are APOA1, AGTR1, XCL1, CCL5 and RHO. Regarding XCL1 and CCL5, these are represented mainly in ED14 and ED16 blood samples, and according to **Figure 25**, they are related to cytokine signalling. The elevated expression in these time points may indicate that B cells are migrating intensely, as cytokines are known to regulate cell migration and are highly expressed in these time points ¹¹⁸. The APOA is most prevalent in ED12 and is involved in macrophage-repellent chemotaxis ¹¹⁹. AGTR1 was expressed in ED14 and ED16 and is suggested to have a role in the proliferation and movement of cancer cells ¹²⁰. RHO is a GTPases involved in coordinating cell responses required for migration and is expressed in ED12 and ED14 blood samples ¹²¹.

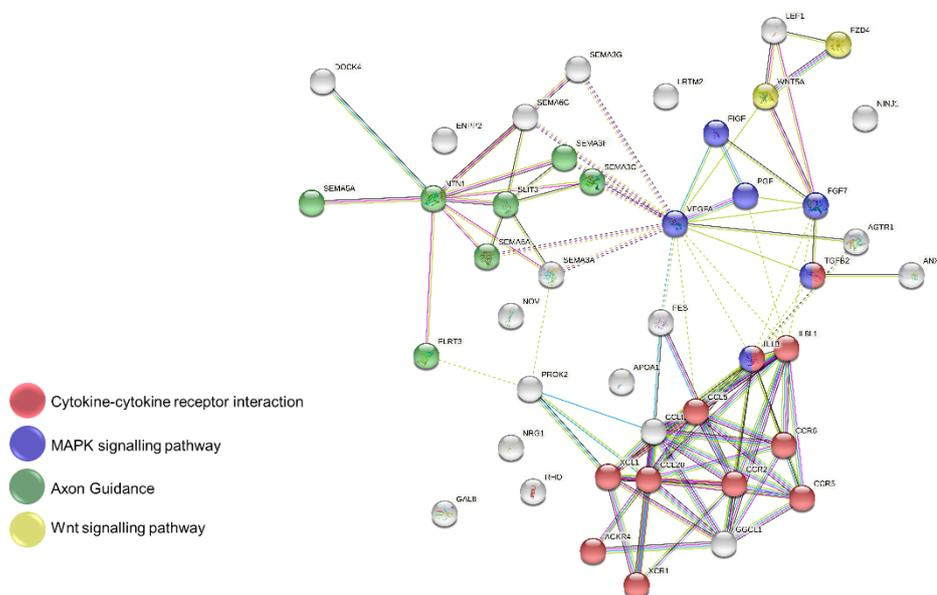


Figure 25. Protein-Protein Interaction Network of the DEGs in ED12, ED14 and ED16 blood. The list of DEGs obtained from ArrayStar[®] ⁹⁶ was subjected to a PPI analysis with the STRING[®] ¹⁰⁶ tool. The cytokine-cytokine receptor interactions (red), MAPK signalling pathway (blue), axon guidance (green) and the Wnt signalling pathway (yellow) were the most prevalent pathways. The edges represent the protein-protein associations, the known interactions (light blue and purple), the predicted interactions (green, orange, blue) and others (yellow, black, violet). A kmeans clustering was performed with the creation of 3 clusters shown by the dotted line between the proteins.

ED12 splenic and blood B cells

The final comparisons were at the same time point but between different locations. For ED12, only spleen and blood samples were obtained. From the list of DEGs, a PPI network was obtained (**Figure 27**), and the cytokine receptor signalling (red), the MAPK pathway (blue), the axon guidance (green), the focal adhesion (yellow) and the Toll-like receptor pathway (purple) were the most expressed

pathways (**Figure 27**). The up-regulated genes in the spleen and blood were CCL26 and CCL4 (**Figure 26 B**), and both are related to cytokine receptor signalling. While CCL26 is associate to the recruitment of diverse cell types, CCL4 participates in the negative regulation of B cell migration ^{118,122}.

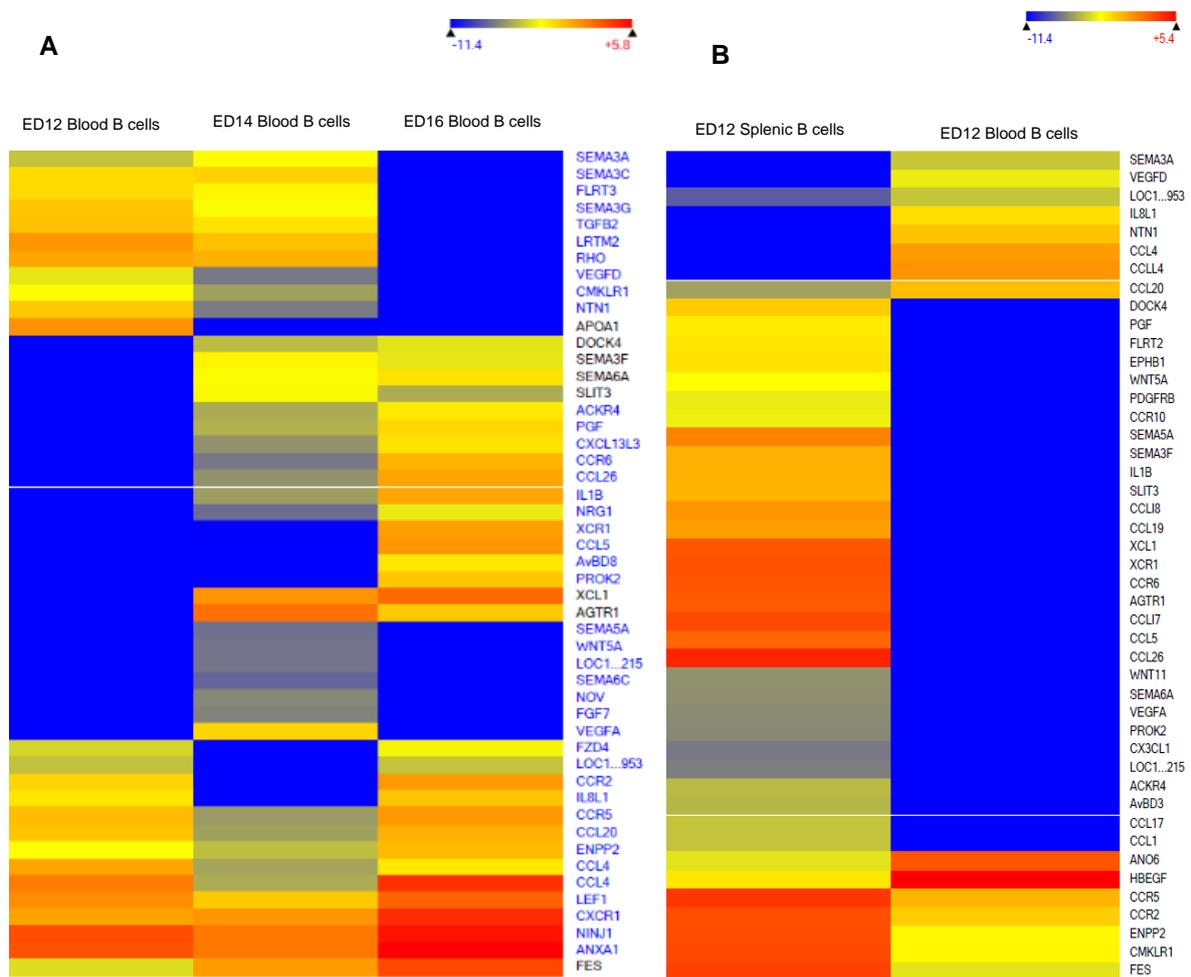


Figure 26. Heat map of the DEGs between ED12, ED14 and ED16 blood B cells (A) and ED12 splenic and blood B cells (B). Hierarchical clustering was performed with the list of DEGs and the correspondent samples. In blue are the low expressed genes, in yellow the medium expressed and in red the highly expressed. This figure was obtained with ArrayStar[®] ⁹⁶.

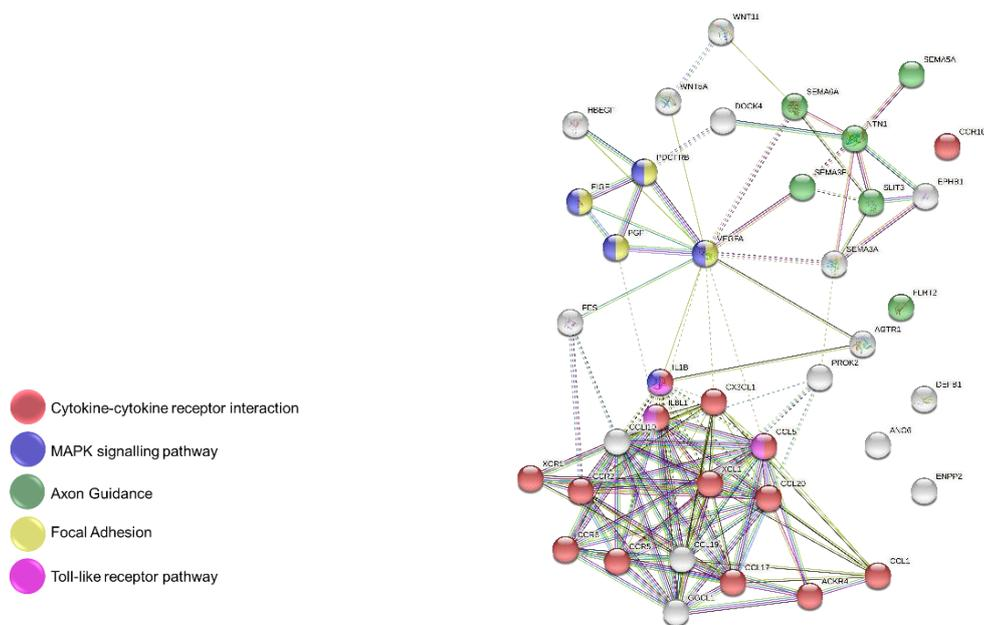


Figure 27. Protein-Protein Interaction Network of the DEGs in ED12 spleen and blood. The list of DEGs obtained from ArrayStar[®] 96 was subjected to a PPI analysis with the STRING[®] 106 tool. The cytokine-cytokine receptor interactions (red), MAPK signalling pathway (blue), axon guidance (green), the focal adhesion (yellow) and the Toll-like receptor pathway (purple) were the most prevalent pathways. The edges represent the protein-protein associations, the known interactions (light blue and purple), the predicted interactions (green, orange, blue) and others (yellow, black, violet). A kmeans clustering was performed with the creation of 3 clusters shown by the dotted line between the proteins.

ED14 splenic, bursal and blood B cells

Concerning ED14, **Figure 28** shows the PPI network of the DEGs between the spleen, bursa and blood. The most prevalent pathways are the cytokine receptor interaction (red), MAPK (blue), axon guidance (green) and focal adhesion (yellow). The genes most upregulated in each comparison are CCL20, NOV, CCL5, CCL4, CXCL13 and ANO6 (**Figure 30 A**). From these, the CCL20, CCL5, CCL4 and CXCL13 are related to cell migration via chemotaxis. Considering that this time point is crucial for cell migration, it was expected that most of the highly expressed genes would be related to chemotaxis mechanisms. The bursal environment has elevated levels of the CXCL13 ligand (**Figure 30 A**), which suggests that this mechanism may be fundamental to attract B cells. Regarding NOV and ANO6, both are proposed to promote the migration and proliferation of cancer cell lines. Hence they may have a similar role in the B cell development, as they are highly expressed in this crucial stage for migration ^{123,124}.

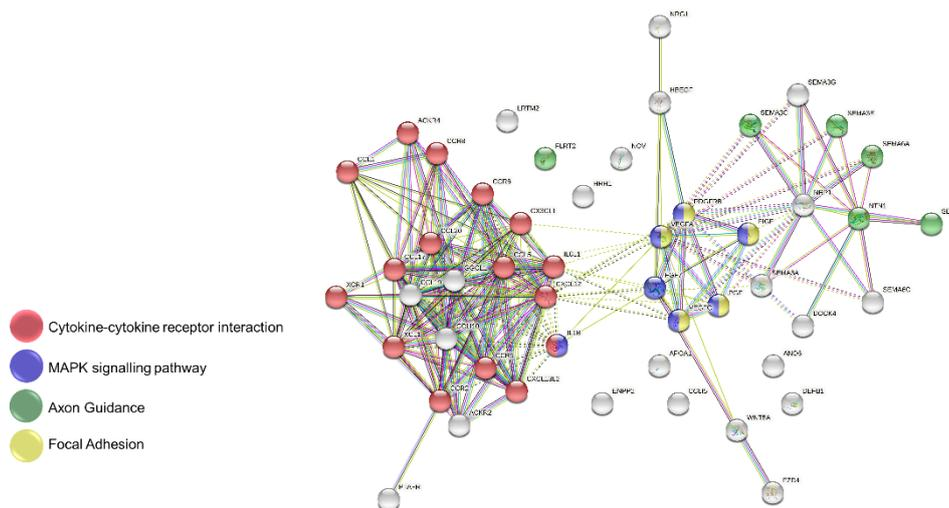


Figure 28. Protein-Protein Interaction Network of the DEGs in ED14 spleen, bursa and blood. The list of DEGs obtained from ArrayStar[®] 96 was subjected to a PPI analysis with the STRING[®] 106 tool. The cytokine-cytokine receptor interactions (red), MAPK pathway (blue), axon guidance (green) and focal adhesion (yellow) were the most prevalent pathways. The edges represent the protein-protein associations, the known interactions (light blue and purple), the predicted interactions (green, orange, blue) and others (yellow, black, violet). A kmeans clustering was performed with the creation of 3 clusters shown by the dotted line between the proteins.

ED16 splenic, bursal and blood B cells

Lastly, for the ED16 time point, **Figure 29** shows the PPI interaction, where the most represented pathways are the cytokine receptor interactions (red), MAPK pathway (blue), axon guidance (green), focal adhesion (yellow) and Intestinal immune network for IgA production (purple). When evaluating the most expressed genes in each comparison (**Figure 30 B**), the AGTR1, CXCL13L3, APOA1, CCL17 and CCL4 genes show up. Some are related to cell migration via cytokine receptor interactions, as CXCL13, CCL17 and CCL4. Regarding AGTR1 and APOA1, as mentioned earlier, they are involved in macrophage-repellent chemotaxis and in the proliferation and migration of cells in cancers, respectively 119,120.

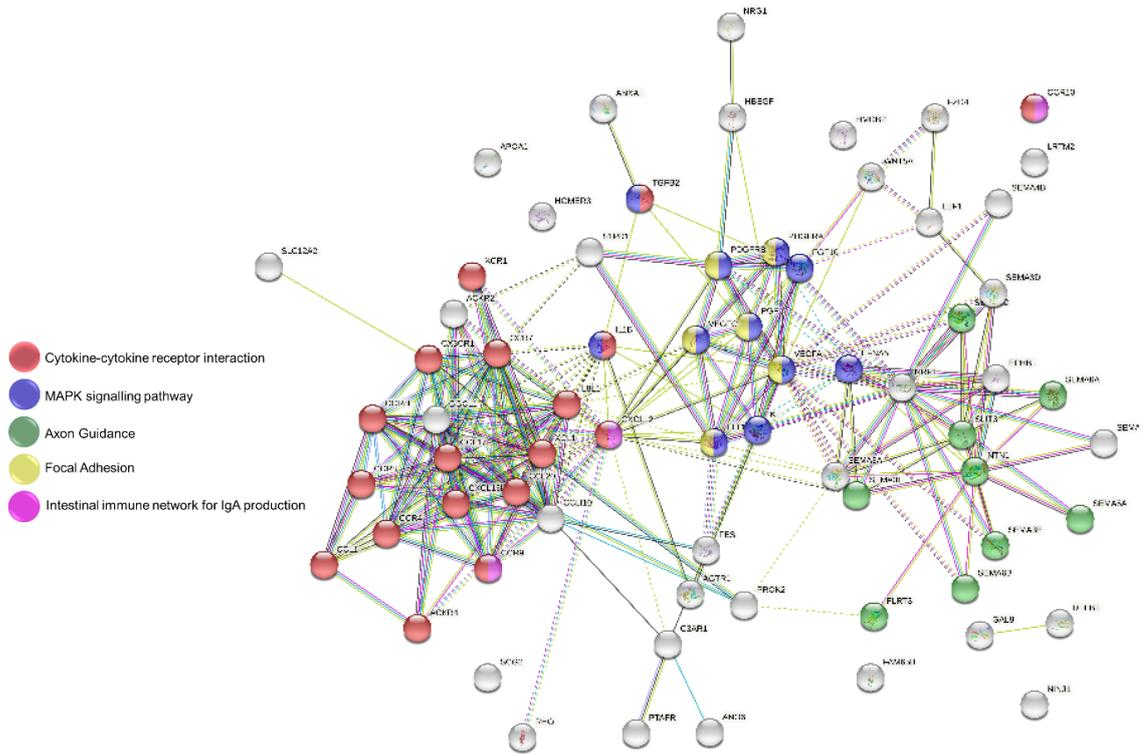


Figure 29. Protein-Protein Interaction Network of the DEGs in ED16 splenic, bursal and blood B cells. The list of DEGs obtained from ArrayStar[®] 96 was subjected to a PPI analysis with the STRING[®] 106 tool . The cytokine-cytokine receptor interactions (red), MAPK signalling pathway (blue), axon guidance (green), focal adhesion (yellow) and the intestinal immune network for IgA production (purple) were the most prevalent pathways. The edges represent the protein-protein associations, the known interactions (light blue and purple), the predicted interactions (green, orange, blue) and others (yellow, black, violet). A kmeans clustering was performed with the creation of 3 clusters shown by the dotted line between the proteins.

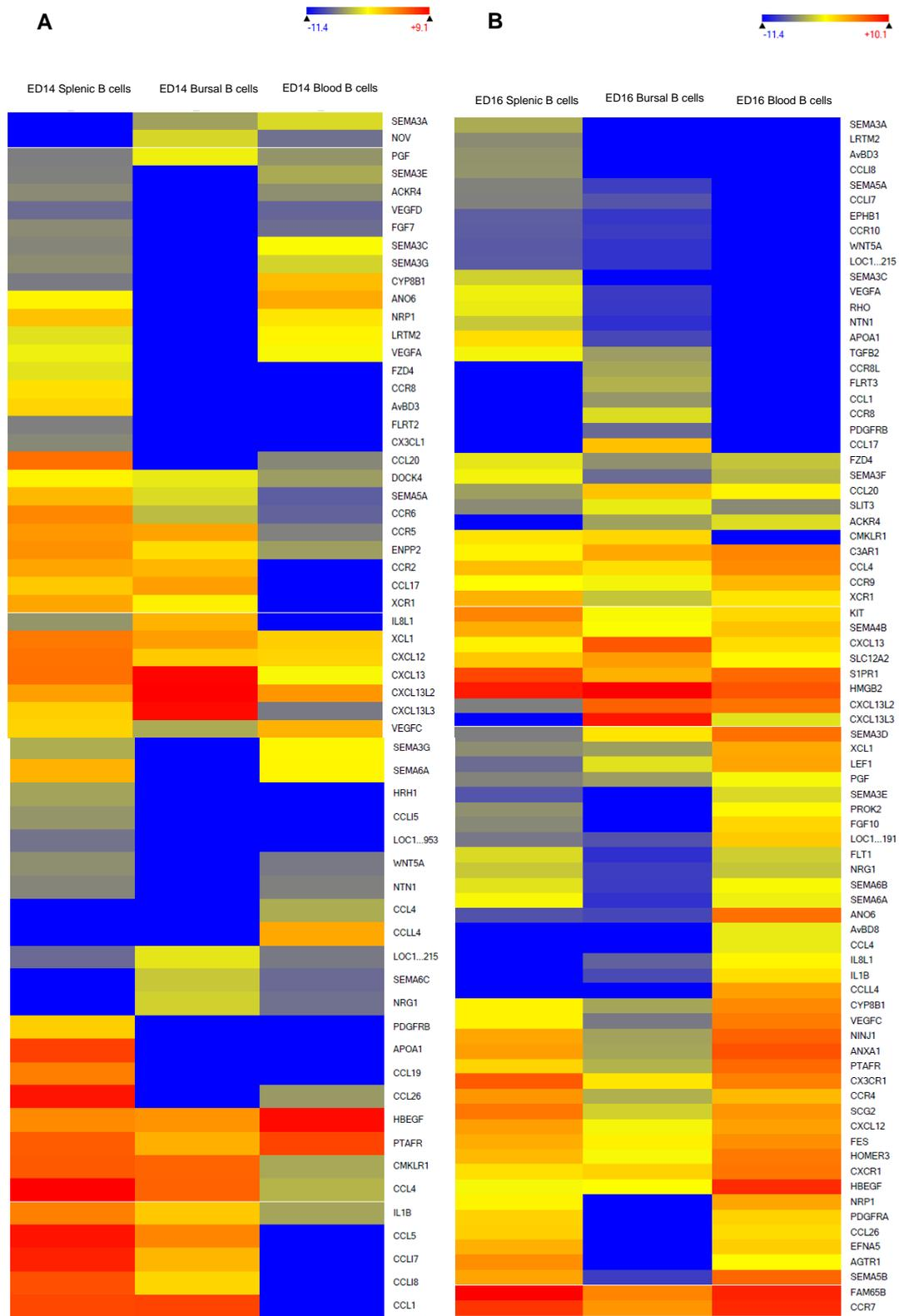


Figure 30. Heat map of the DEGs between ED14 splenic, bursal and blood B cells (A) and ED16 splenic, bursal and blood B cells (B) . Hierarchical clustering was performed with the list of DEGs and the correspondent samples. In blue are the low expressed genes, in yellow the medium expressed and in red the highly expressed. This figure was obtained with ArrayStar[®] 96.

4.3.3. Pathway Analysis

For a broader analysis of the data, the most prevalent pathways in each comparison were assessed resorting to the STRING[®] 106 tool. The DEGs were mainly implicated in the cytokine receptor signalling, MAPK signalling, axon guidance, focal adhesion, Wnt signalling and Toll-Like receptor pathway. The genes involved in focal adhesion, as most of these genes were included in the MAPK pathway analysis, and in the Wnt signalling pathway and Toll-Like receptor pathway are not discussed in this project, as these do not appear so often in the PPI networks.

4.3.3.1. Cytokine-cytokine receptor interaction

To widely evaluate which cytokines and receptors are the most used in the various locations and time points of embryonic development, the genes involved to this pathway were selected and plotted in a heat map against all the samples (**Figure 31**). Instead of only selecting the DEGs, for the case of this pathway, it was preferred to analyse all the genes involved in the cytokine signalling. This selection permits a complete analysis and avoids missing important information. One example of this is the CXCR4 gene, it would not be analysed if just the DEGs were selected, as CXCR4 is highly expressed

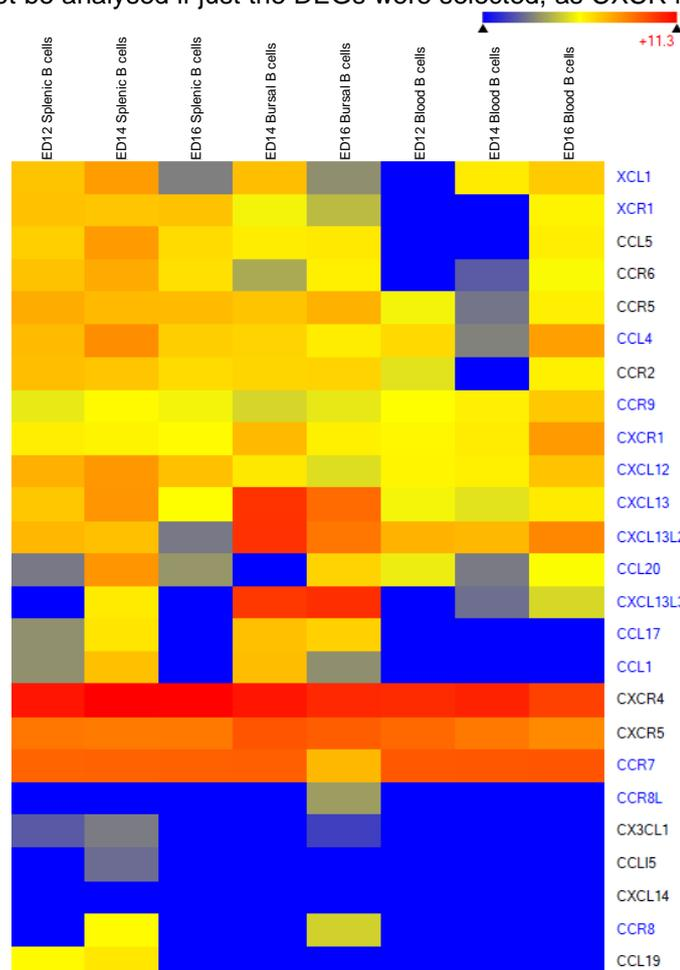


Figure 31. Heat map of the genes involved in cytokine-cytokine interaction. The genes involved in the cytokine pathway were selected and plotted in a heat map to compare the expression between the samples. In blue are the low expressed genes, in yellow the medium expressed and in red the highly expressed. This figure was obtained with ArrayStar[®] 96.

in all the samples (**Figure 31**); yet this molecule has been reported to be involved in B cell migration ^{7,8}. It is also essential to consider the genes expressed by the B cells in this list, as some most likely appear due to macrophages, monocytes or tissue cells expression. From the list presented in **Figure 31**, the B cells have been reported to express CXCR4, CXCR5, CCR2, CCR5, CCR6, CCR7, CCR9, CCL4 and CCL17, hence the focus of this analysis regards these genes and their ligands or receptors.

CXCR4/CXCL12

The first gene to be analysed codifies for the CXCR4 receptor expressed by B cells, which interacts with the chemokine CXCL12 (SDF-1) ¹¹⁸. This pair has been reported to be involved in B cell migration in humans, mice, and more recently chickens ⁸. In the chicken bursa there are high levels of CXCL12, which attracts the CXCR4^{pos} B cells from the spleen and blood ^{7,8}. For migration to occur via this chemokine signalling, the BCR signalling was necessary, however, BCR^{neg} cells were reported to migrate into the bursa ⁷. Hence with this, the signalling involving CXCR4 and CXCL12 was suggested as involved, but not necessary or not the only trigger for B cell migration into the bursa ⁷. Nevertheless, it is still interesting to study the expression of these genes throughout the three-time points and locations, as, so far, this has never been performed before. As visible in the heat map in **Figure 31**, the expression of the CXCR4 gene is remarkably high (red) in all the samples, being the least expressed in the ED16 blood. It is also interesting to notice that this is the most expressed gene throughout the experiments, similarly to CXCR5 and CCR7. It was previously reported by M. Laparidou *et al.* that the percentage of B cells expressing this receptor was around 40% in ED12, then increased to 70% in ED14, and in ED16 was about 65 % ⁷. These percentages seem concordant to the ones obtained in this project, as from ED12 until ED16 there is a high CXCR4 expression in all locations. This suggests that CXCR4 is being highly utilised in the migration of B cells, even though it was seen as not necessary for this process to occur, or not the only molecule employed. When evaluating the expression of the ligand CXCL12, this data is probably referent to the macrophages and monocytes, that express it ¹²⁵. **Figure 31** shows the highest levels of CXCL12 in the spleen, which would not be expected, as this molecule is known to attract the B cells mostly towards the bursal environment ⁸. However this result may occur due to the cells that produce most CXCL12 in the bursa, the stromal cells, were not selected. Instead, the B cells or macrophages were sorted, and as they also produce CXCL12 but in much lower amounts, may have led to an increase in the relative amount of CXCL12 in the spleen compared to the bursa. Nevertheless, in normal conditions, the relative amount of CXCL12 in the spleen is negligible compared to that expressed by stromal bursal cells ⁸.

CXCR5/CXCL13

The following candidates suggested by N. Nagy *et al.* to be necessary for the migration of B cells towards the bursa were the receptors CXCR5 and the CCR6, which have as ligands the CXCL13 and CCL20, respectively. Both chemokines were reported to be involved in B cell migration in humans and mice, so they may have a crucial role in the chicken lymphocyte migration ^{7,118}.

In humans, the CXCR5 is expressed in all B cells in the peripheral blood, lymph node, and some T cells, while the ligand is present in the follicles. Another critical aspect reported was that in CXCR5^{neg} and CXCL13^{neg} mice, the migration of B cells to the lymph nodes and Peyer's patches is severely hampered,

and these animals lack some lymph nodes^{126–128}. Henceforth, one could also hypothesise that this signal may be necessary for B cells to migrate towards the CXCL13^{pos} bursa in the chicken. The heat map in **Figure 31** shows that the CXCR5 gene has a similar level of expression as CXCR4, it is expressed throughout all the stages and locations, being the most intense in the ED14 and ED16 bursal B cells. This expression corroborates with the expected, as if the B cells employed this receptor for migration towards the bursa, they should express it more in the period of movement towards the organ. Thus, the B cells that arrive at the bursa would probably be at the peak of expressing the CXCR5 receptor, to move in the direction of the CXCL13. Additionally, B cells probably need high receptor expression in these later stages to guarantee that they stay in the bursal environment, and do not emigrate too early. Regarding the ligand CXCL13, it is the most expressed on ED14 and ED16 bursal samples. However, CXCL13 is possibly represented by either macrophages and monocytes, or by the bursal tissue itself, as B cells have never been described to express it. Nevertheless, the high expression of the ligand in such time points is another indicative that this mechanism may be needed for attracting B cells towards the bursa. Overall, findings suggest that the CXCR5/CXCL13 signalling may be necessary for the B cell migration towards the bursa. Nevertheless, further chemotaxis assays would be needed to evaluate this proposal fully.

CCR6/CCL20

The receptor CCR6 and its ligand CCL20 were suggested as a candidate mechanism to mediate the migration of the B cells towards the bursa by N. Nagy *et al.*⁸. The expression of the CCR6 is remarkably high in antigen-specific memory B cells (B_{mem}) when compared to naïve B cells in mice. In CCR6 deficient mice, the primary humoral response and the generation of B_{mem} cells still occur, yet the secondary response to antigens is hampered, and B cell distribution in the spleen is disrupted. Thus, these results suggest that CCR6 has an essential role in the secondary B cell response and is necessary for the migration of B_{mem} cells¹²⁹. The importance of CCR6 in the early stages of B cell development in mice has also been assessed, as pre-B cells were reported to express low levels of CCR6. This receptor was thought to be relevant in balancing the formation of the germinal centres, as loss of CCR6 increased the appearance of dark zones in the GC¹³⁰. Henceforth, in mice, the CCR6 and CCL20 are not crucial for migrating the B cells from the spleen to the secondary lymphoid organs. Thus, this suggests that if CCR6 has a role in the embryonic B cell migration in chicken, it is also probably unnecessary.

When analysing the heat map in **Figure 31**, it is visible that the CCR6 gene is slightly expressed throughout all samples, except ED12 bursa and ED12, ED14 blood. Regarding CCL20, it was expressed in the ED14 and ED16 spleen, in the ED16 bursa and in the ED12, ED16 blood. This reduced expression of the CCR6 in the initial stages of development is concordant with the reported in mice¹³⁰. The B cells express the receptor more in the ED16 bursa, which can be due to the migration of the lymphocytes inside the bursa. Nevertheless, as CCR6 is also represented by B cells in the early stages of the spleen, it may also be involved in the emigration from this organ. Interestingly, the expression of the CCR6 after ED14 increases in the bursa and decreases in the spleen, which is concordant to the later cell migration hypothesis suggested in the project, where most cells travelled after ED14. To conclude, it is proposed

that this receptor participates in the migration of cells to the CCL20^{pos} bursa, yet probably is not sufficient, as deletions of CCR6 in mice showed a standard establishment of the immune responses ¹³⁰.

CCR7/CCL21/CCL19

Similar to CXCR5, the CCR7 receptor and their ligands CCL21/CCL19 regulate the migration of cells in the immune system, and in the homing of T cells to the spleen in chickens. Additionally, CCR7^{neg} mice showed a reduced and irregular distribution of T and B cells in the lymph nodes and spleen. As in mice, B cell migration towards secondary organs was not affected, in chickens the signalling via this receptor is probably also insufficient, and its disruption does not affect B cell migration into the bursa ¹²⁶. In mice, the receptor is also important in the B cell motility inside the follicle, as cells that highly express CCR7 migrate more towards the CCL21 T-zone. In conclusion, the CCR7/CCL19 or CCL21 are hypothesized to be more related to the migration inside the bursa than to the migration from the spleen towards this organ ¹³¹.

Regarding the expression of the CCR7 gene in **Figure 31**, it is present throughout all the time points and locations yet is less prominent in the ED16 bursal B cells. This is contrary to the expected, as CCR7 was proposed to be involved in the migration of B cells inside the bursa, thus should be the most expressed in the ED16 bursal sample. However, with these results, one could hypothesise that B cells in chickens may also resort to CCR6 to migrate towards the bursa, and at ED16, the lymphocytes would be already assorted inside the follicles, thus would downregulate CCR7. In line with this, it was identified that for B cells to leave the bursa, they must downregulate the expression of this receptor ¹¹⁸. Hence, these statements could explain the low expression of CCR7 observed in this work.

CCR2/CCL2

The following gene to be evaluated if it has a crucial role in the migration of B cells is the CCR2. The CCR2 is highly expressed in immature B cells, and down-regulated in mature mammal cells. The importance of this receptor in the homing of naïve B cells was assessed, and it was found that in CCR2^{neg} mice, the population of B cells in the spleen was similar to the wild-type. On the other hand, in these mice, B cells had a much higher migration towards the CXCL12 chemokine, and the lymph nodes had a higher number of B cells ¹³². Regarding CCL2, it can be produced by macrophages and B cells, thus in the latter this CCR2/CCL2 mechanism works in an autoregulation form. The CCR2 receptor and CCL2 ligand are suggested to be involved in the negative autoregulation of the migration of B cells in the early development, as in its absence, the B cells respond more intensely to the chemokine stimulation and migrate more. More precisely, it was suggested that CCR2 activates a signalling pathway that reduces the CXCR4 signalling cascade ¹³². For instance, mechanisms that inhibit cell migration may be relevant to prevent the premature migration of B cells to the bursa.

Regarding the data obtained, as visible in **Figure 31**, the CCR2 gene was expressed throughout all stages of development except in the ED14 blood. Regarding the CCL2, it was not present in these developmental stages. This result was expected as CCR2 inhibits B cell migration once stimulated by its ligand. As the time points analysed in this project correspond to a period where B cells migrate extensively, it was expected that inhibitory molecules such as CCL2 were not expressed. The B cells

express CCR2, as was seen in early stage B cells in mice, yet most likely, it only becomes active at the time when the B cell migration must cease.

CCR5/CCL5/CCL4/CCL3

The CCR5 is expressed in B cells since the initial stages of ontogeny in humans and is involved in the negative regulation of the CXCL12/CXCR4 axis. It was found that CCL4 did not elicit chemotaxis in B cells and that when stimulating the cells with this ligand, the chemotaxis was decreased towards the CXCL12^{pos} bone marrow. The same occurred with the remaining ligands CCL3 and CCL5¹²². It was perceived that the interaction with the CCR5 receptor, and not the ligands itself, was inhibiting the migration towards CXCL12. Once again these negative regulation mechanisms may be relevant for B cells to move towards other chemokines temporarily or permanently to different microenvironments, such as to enter into circulation¹²². Henceforth, CCR5 and its ligands are probably not essential for the B cell migration towards the bursa, as they are involved in the inhibition of movement.

Regarding the expression of the CCR5 gene, it is expressed throughout all the stages of the spleen and bursa, and is less present in the blood (**Figure 31**). The time point in which CCR5 is most expressed is in the ED16 bursa. The expression of CCR5 in these early stages is concordant with the described in humans, which occurs already in pro-B cells¹²². Concerning the ligands for which there is data (CCL4 and CCL5), both are present throughout all stages except the blood. The CCL5 is the most expressed in the spleen and the lowest in the blood, and the CCL4 is more present in the ED14 spleen and ED16 blood and less in the ED14 blood. The ligands should exist in the early stages of the spleen and the later bursa, as in here the migration is less prominent, and the CXCL12/CXCR4 mechanism is not highly employed. However, CCL4 and CCL5 are expressed from ED12 to ED16 in the spleen and bursa, which goes against the projected high migration of B cells in these stages. As the CXCL12/CXCR4 axis is involved in the migration, the expression of their inhibitors in these time periods probably is crucial to avoid B cells leaving the spleen or bursa too early time periods.¹²².

CCR9/CCL25

The receptor CCR9 responds to the ligand CCL25, a thymus-expressed chemokine. This chemokine signalling is relevant for T cell migration in mice. For B cells in mice, it was found that the pre-pro-B cells migrate towards the CCL25, yet the mature B cells do not¹³³. In the CCR9 deficient mice, the number of mature B cells in the spleen and lymph nodes was normal, yet there was a 3-fold decrease in the number of pre-pro-B cells¹³³. In chickens, it was suggested that CCR9 was directing the migration of cells to GALS, yet as seen in CCR9^{neg} mice, this mechanism may be involved in cell migration but is probably insufficient¹³⁴.

Regarding the expression of the CCR9 gene (**Figure 31**), it is present in all stages yet is not highly expressed and does not vary between samples. Such results align with previous studies, as B cells in early stages express the CCR9 gene and migrate towards CCL25. However, as this signal is not essential for their movement, they do not vary or increase CCR9 expression¹³³. Thus, other signalling mechanisms must also be participating in homing the B cells.

4.3.3.2. The CXCR5/CXCL13 mechanism may be necessary and sufficient for B cell migration to the bursa

From the seven cytokine receptor signalling mechanisms analysed (**Table 9**), the CXCR5/CXCL13 emerged as possibly both a necessary and sufficient for B cell migration. Studies performed with mice harbouring a CXCR5 or CXCL13 deletion observed that most B cells failed to migrate towards the lymph nodes and Peyer's patches, and the transgenic mice manifested severely impaired lymph nodes^{126-128,135}. These results suggest that the CXCR5/CXCL13 signalling may have an important role in the migration to the bursa, and perhaps be sufficient. Regarding the remaining mechanisms discussed, the CXCR4/CXCL12, CCR6/CCL20, CCR7/CCL21/CCL19 and CCR9/CCL25 were suggest being involved in the migration of B cells, as their genes were highly expressed in the samples. However, studies in humans and mice revealed that these mechanisms were insufficient for cell migration, as deletions of the receptors did not stop B cells from migrating towards the lymph nodes and did not significantly alter their development. Besides this, two mechanisms with a negative regulation in B cell migration were uncovered, the CCR2/CCL2 and the CCR5/CCL5/CCL4/CCL3.

Table 9. Summary of the mechanisms investigated that are involved in the cytokine receptor interaction. The receptor, ligand, importance and outcome as possible mechanisms for cell migration are shown.

Receptor	Ligand	Importance	Outcome
CXCR4	CXCL12	CXCR4 ^{pos} B cells migrate towards CXCL12 in the bursa. Yet CXCR4 ^{neg} chicken B cells can still migrate inside the bursa.	Involved but probably not necessary
CXCR5	CXCL13	CXCR5 ^{pos} B cells migrate towards CXCL13. In mice CXCR5 ^{neg} most B cells failed to migrate towards lymph nodes. And mice deficient in CXCL13 or its receptor CXCR5 manifested severely impaired lymph nodes.	May be necessary and sufficient
CCR6	CCL20	CCR6 ^{pos} B cells migrate towards CCL20. Deletion of CCR6 in mice only hampered the secondary immune response.	May be involved but probably not necessary
CCR7	CCL21 CCL19	CCR7 ^{pos} B cells migrate towards CCL21 and CCL19. CCR7 ^{neg} mice have reduced B cells in the lymph nodes and spleen.	May be involved but probably not necessary
CCR2	CCL2	CCR2 and CCL2 are probably involved in the negative regulation of B cell migration, as they inhibit cell migration via the CXCL12/CXCR4 axis.	Involved in negative regulation
CCR5	CCL5 CCL4 CCL3	CCR5 signals are probably involved in the negative regulation of B migration, as they inhibit cell migration via the CXCL12/CXCR4 axis.	Involved in negative regulation
CCR9	CCL25	CCR9 ^{pos} B cells migrate towards CCL21. A CCR9 deficient mice has B cells in the spleen and lymph nodes.	May be involved but probably not necessary

4.3.3.2. MAPK signalling Pathway

The MAPK pathway has been reported to have a crucial role in cell migration ¹³⁶. Thus the genes that were differentially expressed and involved in this pathway were assessed, and a heat map was made to compare their expression throughout the samples (**Figure 32**). The molecules from the MAPK pathway that would be the most relevant in the migration of the B cells from the spleen to the bursa are the ones overexpressed in the ED12-ED14 spleen and bursa, as this is the time point where the majority of B cells migrate ¹³. The molecules that satisfy this condition are FTL1, FGF10, PDGFRA, EFNA5, VEGFC, KIT, PGF, TGFB2 and IL-1 β . Additionally, most of these molecules are not expressed in the

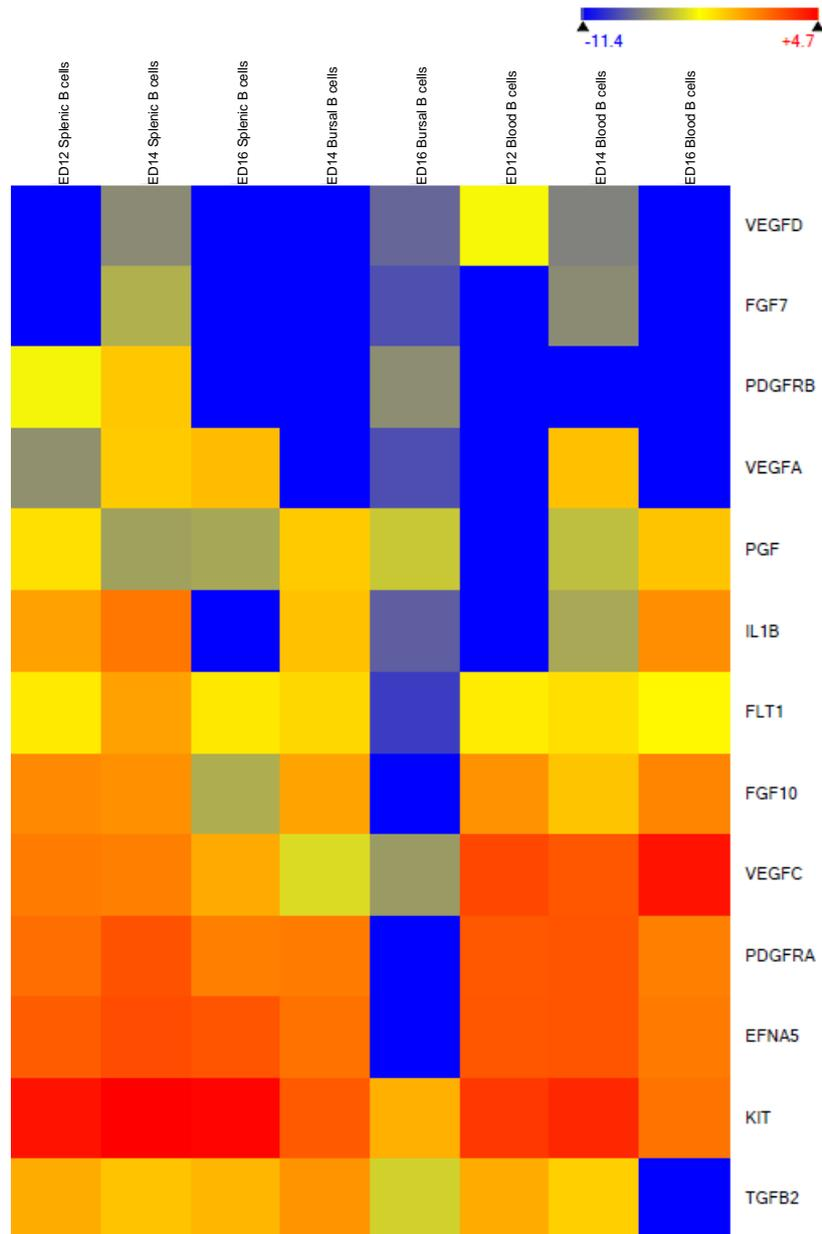


Figure 32. Heat map representation of the differentially expressed between all samples involved in MAPK pathway. The genes that were differentially expressed between each sample and involved in the MAPK pathway were selected and plotted in a heat map to compare the expression between the samples. In blue are the low expressed genes, in yellow the medium expressed and in red the highly expressed. This figure was obtained with ArrayStar[®] 96.

ED16 bursa, which could also reveal that they are needed only for the migration until the bursa. Henceforth, it is interesting to analyse these molecules as they pose new signals for B cell migration.

FTL1, FGF10, PDGFRA, VEGFC, PGF, TGFB2 and IL-1 β

The MAPK includes three kinases relevant to cell migration, namely Jun N-terminus kinase (JNK), p38 and extracellular signal-regulated kinases (ERK), and each one regulates cell migration by different mechanisms. JNK phosphorylates paxillin and microtubule-associated proteins, p38 phosphorylates a MAPK-activated protein kinase relevant for the direction of migration, and ERK phosphorylates the myosin light chain kinase, calpain or FAK ¹³⁶. JNK becomes active in response to extracellular stimuli like tumour necrosis factor (TNF), epidermal growth factor (EGF), platelet-derived growth factor (PDGF), and transforming growth factor β (TGF- β). From the genes in the heat map (**Figure 32**), PDGFRA, TGFB2, PGF, and VEGFC are part of the stimuli that activate JNK, which may correlate with an increased cell migration as many targets of this kinase are proteins involved in cell migration ^{136,137}. The p38 kinase is stimulated by factors such as vascular endothelial growth factor (VEGF), fibroblast growth factor (FGF), PDGF, TNF and interleukins (IL). Besides VEGFC, PGF and PDGFRA already mentioned earlier for the JNK activation, for the p38 kinase, FGF10 and IL-1 β are also relevant. This kinase has been reported to stimulate the migration of diverse cell types, such as endothelial cells, fibroblasts, muscle cells and others. Hence it may have a crucial role in the migration of the B cells in this context, as many activators of this kinase are being highly expressed ^{9,136,137}.

KIT and EFNA5

Regarding KIT and EFNA5, these did not appear as activators of the JNK or p38 kinases. The first one codifies for a receptor tyrosine kinase which was suggested to be involved in the intracellular signalling of the migration of neural stem cells ¹³⁸. This receptor's activation leads to the ERK cascade's activation, which engages in cell migration ¹³⁹. The EFNA5 gene codifies the ephrin-A5 ligand, which binds to an Eph receptor tyrosine kinase. These molecules participate in processes of cell positioning and movement. Additionally, the binding of ephrin-A5 binds to its cognate Eph receptor resulting in MAPK pathway activation, which is related to cell mobility ¹⁴⁰.

4.3.3.3. Axon guidance

The differentially expressed genes involved in axon guidance were analysed (**Figure 33**). This group of genes was investigated as novel migration signals have been discovered by studying molecules involved in other cells' migration processes, such as axon guidance or neural cells ⁸. The genes analysed more deeply were the SEMA5A, SEMA3F, SLIT3 and SEMA6, as they are highly expressed in the ED14-16 Bursal B cells, thus may pose attractant molecules for the B cells.

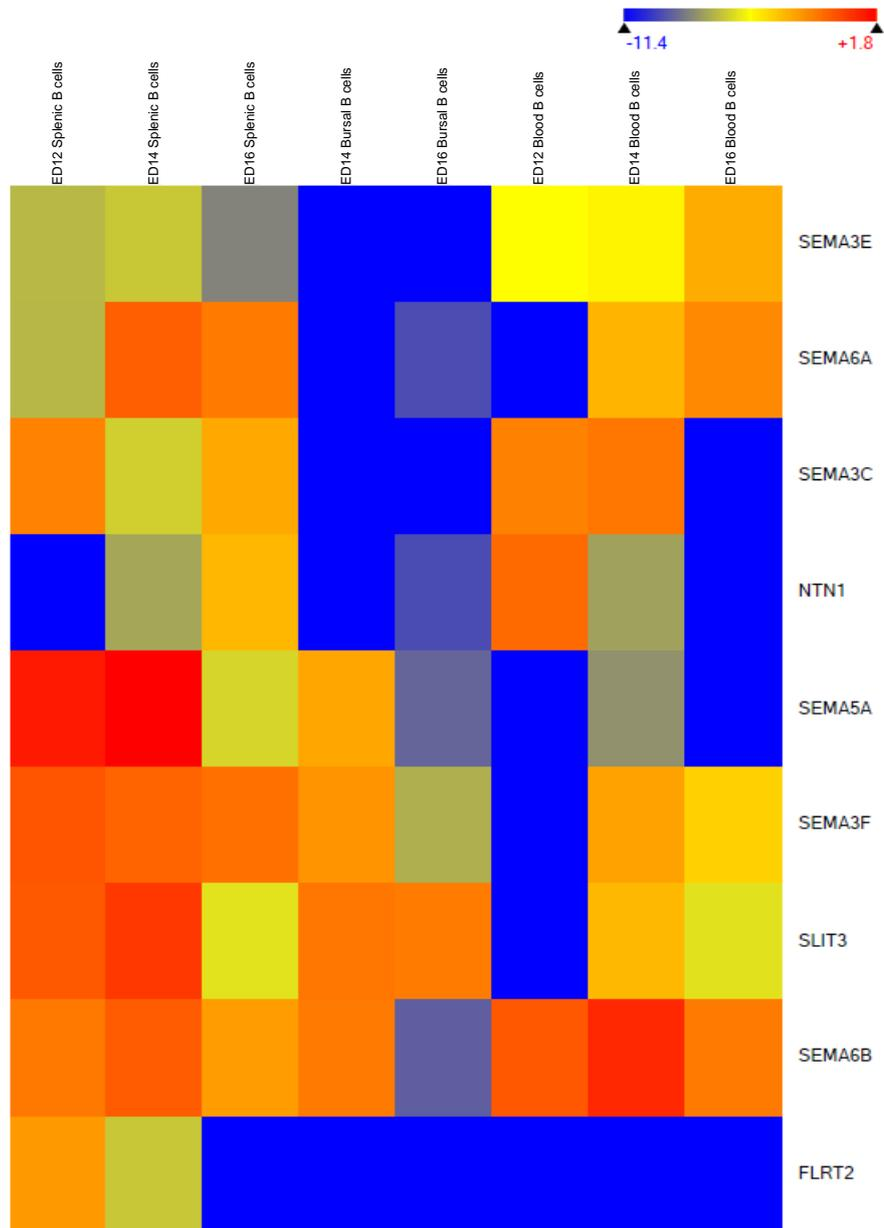


Figure 33. Heat map representation of the differentially expressed genes between the samples involved in Axon guidance. The genes that were differentially expressed between each sample and involved in Axon guidance were selected and plotted in a heat map to compare the expression between the samples. In blue are the low expressed genes, in yellow the medium expressed and in red the highly expressed. This figure was obtained with ArrayStar[®] 96.

SEMA5A, SEMA3F and SEMA6B

The genes SEMA5A, SEMA3F and SEMA6B codify for semaphorins; this family of proteins participates in the regulation of neuronal migration, immune responses, cardiac/skeletal development, tumour growth and angiogenesis ¹⁴¹. Recent reports identified one semaphorin that could modify the CD40-CD40L signalling in B cells, which resulted in aggregation and survival of the cells ¹⁴². Such observations reveal the potential of this family in regulating B lymphocytes. Regarding SEMA5A, when binding to its receptor, Plexin-B3, it was reported to elicit endothelial cell proliferation and reduce apoptosis¹⁴³. Hence, maybe this semaphorin could contribute to the migration signalling of B cells, as it is highly expressed

in the ED14 bursa and has a role in eliciting cell proliferation. The SEMA3F was suggested to have a chemorepulsive function in the nervous system and thymocyte migration. The thymocytes strongly express the receptor NRP2, a chemorepulsive mechanism, along with the SEMA3F. Additionally, this semaphorin inhibited the migration of the thymocytes towards the chemokine CXCL12¹⁴⁴. Hence, SEMA3F probably has an inhibitory role in the migration of lymphocytes. However, no reports regarding the SEMA3F action have been made for B cells.

Regarding SEMA3F expression, as it is highly present in ED14 bursa and less in ED16 bursa, it indicates an attractive role instead of a chemorepulsive one reported for thymocyte migration. Nevertheless, further studies are needed to understand better how this molecule regulates B cell migration. For SEMA6B, functional experiments indicated that this semaphorin was related to cell viability, migration and invasiveness in many cancer cell lines, via regulation of the Notch signalling pathway¹⁴⁵. Additionally, the inhibition of SEMA6B severely interfered with the migration of gastric cancer cells *in vitro*¹⁴⁶. Besides these functions, this semaphorin is also involved in neural development, for example, neural crest cell migration and axon guidance¹⁴⁷. These results infer that SEMA6B has a positive role in signalling cells to migrate. Hence one could hypothesize that as it is being highly expressed in the stages of B cell migration, it could also have a role in regulating the migration of these cells.

SLIT3

Regarding SLIT3, a large matrix protein secreted by endothelial cells, it belongs to the slit family and interacts with the Roundabout1 (Robo1) receptor¹⁴⁸. The Robo and Slit family regulates cell interactions during migration in embryonic development¹⁴⁹. Slit signalling has been reported to inhibit the chemoattractant-induced migration of various cell types, such as leucocytes. Nevertheless, a more recent study showed that when stimulated with Slit3, monocytes had an increased spontaneous and chemoattractant-induced migration. This molecule did not function as a chemoattractant but promoted the migration via chemoattractants, such as CXCL12¹⁵⁰. Another molecule from the slit family, Slit2, was reported to impair the migration of T cells towards the CXCL12 chemoattractant, when bound to the Robo1 receptor. Thus, the slit family can have both an attractive and repulsive effect on cells. Nevertheless, the Slit3/Robo1 most likely has a positive role in regulating the migration of B cells, as the SLIT3 gene has a reduction of expression in the spleen and increases highly in the bursa. Thus suggesting that it may be relevant for cell migration, via increasing chemoattractant mechanisms like CXCL12/CXCR4¹⁵¹.

5. Conclusions and Future Perspectives

B cells are a crucial part of the immune system. However, the signals that regulate their development, such as the migration from the spleen to the bursa, are still unclear ^{7,8,10,70}. The discovery of novel mechanisms involved in lymphocyte trafficking in the early developmental stages has been hindered, as it is particularly challenging to isolate the cells in these preliminary time points ¹³.

In this study, a FACS-based methodology FACS was established to isolate B cells at key time points and locations of their development, such as ED12, ED14 and ED16, from the spleen, bursa and blood ⁸. This protocol permitted isolating the very few existing B cells with a high purity percentage. Once B cells were isolated, an RNA-sequencing analysis was performed, and the DEGs that could have a role in lymphocyte migration were identified. The mechanisms involving CXCR4/CXCL12, CCR6/CCL20, CCR7/CCL21/CCL19 and CCR9/CCL25 were proposed here to probably be involved the B cell migration, yet are most likely not sufficient ^{7,126,129,133}. However, the signalling comprising the B cell receptor CXCR5, and the ligand CXCL13 present in the bursa, was suggested to maybe be both necessary and sufficient for cells to migrate ^{126,127}. Additionally, multiple pathways regulating the trafficking of B cells were underlined, such as the cytokine receptor interaction, MAPK signalling and axon guidance. To fully evaluate and confirm if the mechanisms proposed in this work are involved, and if the CXCR5/CXCL13 axis is sufficient for B cell migration, future chemotaxis assays and adoptive cell transfers assays would need to be performed. For instance, by either knocking out the chemokine receptors in the B cell line or treating the cells with a receptor antagonist and assessing if the migration into the ligand and the bursa is maintained ⁷. The RNA-sequencing data obtained in this work will facilitate new studies to perform a more exceptional and profound analysis of the chicken's B cell development. Accordingly, this project has contributed with a defined protocol to isolate B cells and, besides, allowed to expand the knowledge regarding the immune system development in chickens.

6. References

1. Food and Agriculture Organization. Poultry development review. In: ; 2013.
2. Herrero M, Havlík P, Valin H, et al. Biomass use, production, feed efficiencies, and greenhouse gas emissions from global livestock systems. *Proc Natl Acad Sci U S A*. 2013;110(52):20888-20893. doi:10.1073/pnas.1308149110
3. Bergeron S, Pouliot E, Doyon M. Commercial Poultry Production Stocking Density Influence on Bird Health and Performance Indicators. *Animals* 2020, Vol 10, Page 1253. 2020;10(8):1253. doi:10.3390/ANI10081253
4. Payne LN, Nair V. The long view: 40 years of avian leukosis research. *Avian Pathology*. 2012;41(1):11-19. doi:10.1080/03079457.2011.646237
5. Feng M, Zhang X. Immunity to avian leukosis virus: Where are we now and what should we do? *Front Immunol*. 2016;7(DEC). doi:10.3389/fimmu.2016.00624
6. Mastellera EL, Pharra GT, Funk' PE, Thompson CB. *Avian B Cell Development*. Vol 15.; 1997.
7. Laparidou M, Schlickerieder A, Thoma T, Lengyel K, Schusser B. Blocking of the CXCR4-CXCL12 Interaction Inhibits the Migration of Chicken B Cells Into the Bursa of Fabricius. *Front Immunol*. 2020;10:3057. doi:10.3389/FIMMU.2019.03057/BIBTEX
8. Nagy N, Busalt F, Halasy V, et al. In and Out of the Bursa—The Role of CXCR4 in Chicken B Cell Development. *Front Immunol*. 2020;11:1468. doi:10.3389/FIMMU.2020.01468/BIBTEX
9. Liu X dong, Zhang F, Shan H, Wang S bai, Chen PY. mRNA expression in different developmental stages of the chicken bursa of Fabricius. *Poult Sci*. 2016;95(8):1787-1794. doi:10.3382/PS/PEW102
10. Ko KH, Lee IK, Kim G, et al. Changes in bursal B cells in chicken during embryonic development and early life after hatching. *Scientific Reports* 2018 8:1. 2018;8(1):1-12. doi:10.1038/s41598-018-34897-4
11. Tizard I. *Avian Immune Responses: A Brief Review*. Vol 23.; 1979.
12. Ratcliffe MJH. Antibodies, immunoglobulin genes and the bursa of Fabricius in chicken B cell development. *Dev Comp Immunol*. 2006;30(1-2):101-118. doi:10.1016/J.DCI.2005.06.018
13. Kaspers B, Schat KA (Karel A, Göbel TW, Vervelde L. *Avian Immunology*. 3rd ed.; 2022.
14. Reynaud CA, Bertocci B, Dahan A, Weill JC. Formation of the chicken B-cell repertoire: Ontogenesis, regulation of Ig gene rearrangement, and diversification by gene conversion. *Adv Immunol*. 1994;57:353-378. doi:10.1016/s0065-2776(08)60676-8

15. Reynaud CA, Imhof BA, Anquez V, Weill JC. Emergence of committed B lymphoid progenitors in the developing chicken embryo. *EMBO J.* 1992;11(12):4349-4358. doi:10.1002/J.1460-2075.1992.TB05534.X
16. Smith SB, Macchi V, Parenti A, de Caro R. Hieronymus [corrected] Fabricius Ab Acquapendente (1533-1619). *Clin Anat.* 2004;17(7):540-543. doi:10.1002/CA.20022
17. Glick B, Chang TS, Jaap RG. The Bursa of Fabricius and Antibody Production. *Poult Sci.* 1956;35(1):224-225. doi:10.3382/ps.0350224
18. Toivanen P, Toivanen A. Bursal and postbursal stem cells in chicken. functional characteristics. *Eur J Immunol.* 1973;3(9):585-595. doi:10.1002/EJI.1830030912
19. Olah I, Toro I. *Bursal Development in Normal and Testosterone-Treated Chick Embryos 1.*; 1986. <http://ps.oxfordjournals.org/>
20. Hirai K, Shimakura S, Kawamoto E, et al. *The Immunodepressive Effect of Infectious Bursal Disease Virus in Chickens.* Vol 18.; 1974. <http://www.jstor.orgURL:http://www.jstor.org/stable/1589241>
21. Reynaud CA, Anquez V, Grimal H, Weill JC. A hyperconversion mechanism generates the chicken light chain preimmune repertoire. *Cell.* 1987;48(3):379-388. doi:10.1016/0092-8674(87)90189-9
22. Schaffner T, Mueller J, Hess MW, Cottier H, Sordat B, Ropke C. The bursa of fabricius: A central organ providing for contact between the lymphoid system and intestinal content. *Cell Immunol.* 1974;13(2):304-312. doi:10.1016/0008-8749(74)90247-0
23. Olah I, Glick B. The number and size of the follicular epithelium (FE) and follicles in the bursa of Fabricius. *Poult Sci.* 1978;57(5):1445-1450. doi:10.3382/ps.0571445
24. Nera KP, Kyläniemi MK, Lassila O. Bursa of Fabricius. *eLS.* Published online November 16, 2015:1-8. doi:10.1002/9780470015902.A0000506.PUB4
25. Pink JR, Vainio O, Rünbeek A -M. Clones of B lymphocytes in individual follicles of the bursa of Fabricius. *Eur J Immunol.* 1985;15(1):83-87. doi:10.1002/EJI.1830150116
26. Click B, Oláh J. A bursal secretory dendritic cell and its contributions to the microenvironment of the developing bursal follicle. *Res Immunol.* 1993;144(6-7):446-447. doi:10.1016/0923-2494(93)80127-K
27. Nagy N, Oláh I. Experimental evidence for the ectodermal origin of the epithelial anlage of the chicken bursa of Fabricius. *Development.* 2010;137(18):3019-3023. doi:10.1242/dev.055194
28. Davani D, Pancer Z, Ratcliffe MJH. Ligation of Surface Ig by Gut-Derived Antigen Positively Selects Chicken Bursal and Peripheral B Cells. *The Journal of Immunology.* 2014;192(7):3218-3227. doi:10.4049/jimmunol.1302395

29. Ekino S. Role of environmental antigens in B cell proliferation in the bursa of Fabricius at neonatal stage. *Eur J Immunol.* 1993;23(3):772-775. doi:10.1002/EJI.1830230331
30. John JL. *The Avian Spleen: A Neglected Organ.* Vol 69.; 1994. <http://www.journals.uchicago.edu/t-and-c>
31. Hegde SN, Rolls BA, Turvey A, Coates ME. *Influence of Gut Microflora on the Lymphoid Tissue of the Chicken (Gallus Domesticus) and Japanese Quail (Coturnix Coturnix Japonica).*; 1982. doi:10.1016/0300-9629(82)90034-2
32. Roco JA, Mesin L, Binder SC, et al. Class-Switch Recombination Occurs Infrequently in Germinal Centers Article Class-Switch Recombination Occurs Infrequently in Germinal Centers. *Immunity.* 2019;51:337-350. doi:10.1016/j.immuni.2019.07.001
33. Arakawa H, Furusawa S, Ekino S, Yamagishi H. Immunoglobulin gene hyperconversion ongoing in chicken splenic germinal centers. *EMBO J.* 1996;15(10):2540-2546. doi:10.1002/J.1460-2075.1996.TB00611.X
34. Jeurissen SHM. Structure and function of the chicken spleen. *Res Immunol.* 1991;142(4):352-355. doi:10.1016/0923-2494(91)90090-6
35. Nagy N, Bíró É, Takaács Á, Pólos M, Magyar A, Oláh I. Peripheral blood fibrocytes contribute to the formation of the avian spleen. *Developmental Dynamics.* 2005;232(1):55-66. doi:10.1002/DVDY.20212
36. Jeurissen SHM. The role of various compartments in the chicken spleen during an antigen-specific humoral response. *Immunology.* 1993;80(1):29. Accessed November 26, 2021. [/pmc/articles/PMC1422104/?report=abstract](https://pubmed.ncbi.nlm.nih.gov/1422104/)
37. Ekino A, Shimizu H, Yamagishi H, Arakawa KI, Kuma M, Yasuda S. Productive V-J Joins in the Bursa Diversification and the Selection of Effect of Environmental Antigens on the Ig. Published online 2002. doi:10.4049/jimmunol.169.2.818
38. Underdown BJ, Schiff JM. Immunoglobulin A: Strategic Defense Initiative at the Mucosal Surface. <http://dx.doi.org/10.1146/annurev.iy04040186002133>. 2003;4:389-417. doi:10.1146/ANNUREV.IY.04.040186.002133
39. Kincade PW, Cooper MD. Immunoglobulin A: Site and sequence of expression in developing chicks. *Science (1979).* 1973;179(4071):398-400. doi:10.1126/SCIENCE.179.4071.398
40. Carlander D, Stålborg J, Larsson A. Chicken Antibodies. *Ups J Med Sci.* 1999;104(3):179-189. doi:10.3109/03009739909178961
41. Benatar T, Tkalec L, Ratcliffe MJH. Stochastic rearrangement of immunoglobulin variable-region genes in chicken B-cell development. *Proc Natl Acad Sci U S A.* 1992;89(16):7615-7619. doi:10.1073/PNAS.89.16.7615

42. Schat KA, Kaspers B, Kaiser P. *Avian Immunology Second Edition.*; 2014.
43. Masteller EL, Thompson CB. B cell development in the chicken. *Poult Sci.* 1994;73(7):998-1011. doi:10.3382/ps.0730998
44. Bucchini D, Reynaud CA, Ripoché MA, Grimal H, Jami J, Weill JC. Rearrangement of a chicken immunoglobulin gene occurs in the lymphoid lineage of transgenic mice. *Nature* 1987 326:6111. 1987;326(6111):409-411. doi:10.1038/326409a0
45. McCormack WT, Tjoelker LW, Carlson LM, et al. Chicken IgL gene rearrangement involves deletion of a circular episome and addition of single nonrandom nucleotides to both coding segments. *Cell.* 1989;56(5):785-791. doi:10.1016/0092-8674(89)90683-1
46. Reynaud C -A, Anquez V, Weill J -C. The chicken D locus and its contribution to the immunoglobulin heavy chain repertoire. *Eur J Immunol.* 1991;21(11):2661-2670. doi:10.1002/EJL.1830211104
47. Reynaud CA, Dahan A, Anquez V, Weill JC. Somatic hyperconversion diversifies the single VH gene of the chicken with a high incidence in the D region. *Cell.* 1989;59(1):171-183. doi:10.1016/0092-8674(89)90879-9
48. Butler JE. Immunoglobulin diversity, B-cell end antibody repertoire development in large farm animals Introduction: antibodies in. *Rev sci tech Off int Epiz.* 1998;17(1):43-70.
49. Reynaud CA, Anquez V, Dahan A, Weill JC. A single rearrangement event generates most of the chicken immunoglobulin light chain diversity. *Cell.* 1985;40(2):283-291. doi:10.1016/0092-8674(85)90142-4
50. Thompson CB, Neiman PE. Somatic diversification of the chicken immunoglobulin light chain gene is limited to the rearranged variable gene segment. *Cell.* 1987;48(3):369-378. doi:10.1016/0092-8674(87)90188-7
51. Arakawa H, Buerstedde JM. Immunoglobulin gene conversion: Insights from bursal B cells and the DT40 cell line. *Developmental Dynamics.* 2004;229(3):458-464. doi:10.1002/DVDY.10495
52. Carlson LM, McCormack WT, Postema CE, Humphries EH, Thompson CB. Templated insertions in the rearranged chicken IgL V gene segment arise by intrachromosomal gene conversion. *Genes Dev.* 1990;4(4):536-547. doi:10.1101/GAD.4.4.536
53. McCormack WT, Thompson CB. Chicken IgL variable region gene conversions display pseudogene donor preference and 5' to 3' polarity. *Genes Dev.* 1990;4(4):548-558. doi:10.1101/GAD.4.4.548
54. Kim S, Humphries EH, Tjoelker L, Carlson, And L, Thompson' CB. Ongoing diversification of the rearranged immunoglobulin light-chain gene in a bursal lymphoma cell line. *Mol Cell Biol.* 1990;10(6):3224-3231. doi:10.1128/MCB.10.6.3224-3231.1990

55. Kurosawa K, Ohta K. Genetic diversification by somatic gene conversion. *Genes (Basel)*. 2011;2(1):48-58. doi:10.3390/GENES2010048
56. Arakawa H, Hauschild J, Buerstedde JM. Requirement of the activation-induced deaminase (AID) gene for immunoglobulin gene conversion. *Science*. 2002;295(5558):1301-1306. doi:10.1126/SCIENCE.1067308
57. Arakawa H, Saribasak H, Buerstedde JM. Activation-Induced Cytidine Deaminase Initiates Immunoglobulin Gene Conversion and Hypermutation by a Common Intermediate. *PLoS Biol*. 2004;2(7):e179. doi:10.1371/JOURNAL.PBIO.0020179
58. Stavnezer J, Guikema JEJ, Schrader CE. Mechanism and Regulation of Class Switch Recombination. <http://dx.doi.org/10.1146/annurev.immunol26021607090248>. 2008;26:261-292. doi:10.1146/ANNUREV.IMMUNOL.26.021607.090248
59. Peled JU, Fei LK, Iglesias-Ussel MD, et al. The Biochemistry of Somatic Hypermutation. <http://dx.doi.org/10.1146/annurev.immunol26021607090236>. 2008;26:481-511. doi:10.1146/ANNUREV.IMMUNOL.26.021607.090236
60. Lassila O, Eskola J, Toivanen P. Prebursal Stem Cells in the Intraembryonic Mesenchyme of the Chick Embryo at 7 Days of Incubation. *The Journal of Immunology*. 1979;123(5).
61. Houssaint E, Belo M, le Douarin NM. Investigations on cell lineage and tissue interactions in the developing bursa of Fabricius through interspecific chimeras. *Dev Biol*. 1976;53(2):250-264. doi:10.1016/0012-1606(76)90227-X
62. Weber WT, Foglia LM. Evidence for the presence of precursor B cells in normal and in hormonally bursectomized chick embryos. *Cell Immunol*. 1980;52(1):84-94. doi:10.1016/0008-8749(80)90402-5
63. Houssaint E, Lassila O, Vainio O. Bu-1 antigen expression as a marker for B cell precursors in chicken embryos. *Eur J Immunol*. 1989;19(2):239-243. doi:10.1002/EJI.1830190204
64. Mansikka A, Sandberg M, Lassila O, Toivanen P. Rearrangement of immunoglobulin light chain genes in the chicken occurs prior to colonization of the embryonic bursa of Fabricius. *Proceedings of the National Academy of Sciences*. 1990;87(23):9416-9420. doi:10.1073/PNAS.87.23.9416
65. Ratcliffe MJH, Lassila O, Pink JRL, Vainio O. Avian B cell precursors: Surface immunoglobulin expression is an early, possibly bursa-independent event. *Eur J Immunol*. 1986;16(2):129-133. doi:10.1002/EJI.1830160204
66. McCormack WT, Tjoelker LW, Barth CF, et al. Selection for B cells with productive IgL gene rearrangements occurs in the bursa of Fabricius during chicken embryonic development. *Genes Dev*. 1989;3(6):838-847. doi:10.1101/GAD.3.6.838

67. Houssaint E, Toraño A, Ivanyi J. Ontogenic restriction of colonization of the bursa of Fabricius. *Eur J Immunol.* 1983;13(7):590-595. doi:10.1002/EJI.1830130715
68. Masteller EL, Larsen RD, Carlson LM, et al. Chicken B cells undergo discrete developmental changes in surface carbohydrate structure that appear to play a role in directing lymphocyte migration during embryogenesis. *Development.* 1995;121(6):1657-1667. doi:10.1242/DEV.121.6.1657
69. Palojoki E, Jalkanen S, Toivanen P. Sialyl LewisX carbohydrate is expressed differentially during avian lymphoid cell development. *Eur J Immunol.* 1995;25(9):2544-2550. doi:10.1002/EJI.1830250921
70. Nuthalapati NK, Evans JD, Taylor RL, Branton SL, Nanduri B, Pharr GT. Transcriptomic analysis of early B-cell development in the chicken embryo. *Poult Sci.* 2019;98(11):5342-5354. doi:10.3382/PS/PEZ354
71. Lassila O. Emigration of B cells from chicken bursa of Fabricius. *Eur J Immunol.* 1989;19(5):955-958. doi:10.1002/eji.1830190527
72. Schusser B, Collarini EJ, Pedersen D, et al. Expression of heavy chain-only antibodies can support B-cell development in light chain knockout chickens. *Eur J Immunol.* 2016;46(9):2137-2148. doi:10.1002/EJI.201546171
73. Schusser B, Collarini EJ, Yi H, et al. Immunoglobulin knockout chickens via efficient homologous recombination in primordial germ cells. *Proc Natl Acad Sci U S A.* 2013;110(50):20170-20175. doi:10.1073/PNAS.1317106110
74. Pike KA, Baig E, Ratcliffe MJH. The avian B-cell receptor complex: Distinct roles of Ig α and Ig β in B-cell development. *Immunol Rev.* 2004;197:10-25. doi:10.1111/J.0105-2896.2004.0111.X
75. Schneider K, Kothlow S, Schneider P, et al. Chicken BAFF—a highly conserved cytokine that mediates B cell survival. *Int Immunol.* 2004;16(1):139-148. doi:10.1093/INTIMM/DXH015
76. Kothlow S, Morgenroth I, Graef Y, et al. Unique and conserved functions of B cell-activating factor of the TNF family (BAFF) in the chicken. *Int Immunol.* 2007;19(2):203-215. doi:10.1093/INTIMM/DXL137
77. Bockman DE, Cooper MD. Pinocytosis by epithelium associated with lymphoid follicles in the bursa of fabricius, appendix, and Peyer's patches. An electron microscopic study. *American Journal of Anatomy.* 1973;136(4):455-477. doi:10.1002/aja.1001360406
78. Paramithiotis E, Jacobsen KA, Ratcliffe MJH. Loss of surface immunoglobulin expression precedes B cell death by apoptosis in the bursa of Fabricius. *Journal of Experimental Medicine.* 1995;181(1):105-113. doi:10.1084/JEM.181.1.105

79. Sayegh CE, Drury G, Ratcliffe MJH. Efficient antibody diversification by gene conversion in vivo in the absence of selection for V(D)J-encoded determinants. *EMBO Journal*. 1999;18(22):6319-6328. doi:10.1093/EMBOJ/18.22.6319
80. Paramithiotis E, Ratcliffe MJH. Bursa-dependent subpopulations of peripheral B lymphocytes in chicken blood. *Eur J Immunol*. 1993;23(1):96-102. doi:10.1002/EJI.1830230116
81. Yasuda M, Kajiwara E, Ekino S, et al. Immunobiology of chicken germinal center: I. Changes in surface Ig class expression in the chicken splenic germinal center after antigenic stimulation. *Dev Comp Immunol*. 2003;27(2):159-166. doi:10.1016/S0145-305X(02)00066-6
82. Cabatingan MS, Schmidt MR, Sen R, Woodland RT. Naive B Lymphocytes Undergo Homeostatic Proliferation in Response to B Cell Deficit. *The Journal of Immunology*. 2002;169(12):6795-6805. doi:10.4049/JIMMUNOL.169.12.6795
83. Tregaskes CA, Glansbeek HL, Gill AC, Hunt LG, Burnside J, Young JR. Conservation of biological properties of the CD40 ligand, CD154 in a non-mammalian vertebrate. *Dev Comp Immunol*. 2005;29(4):361-374. doi:10.1016/J.DCI.2004.09.001
84. Rolink AG, Melchers F. BAFFled B cells survive and thrive: roles of BAFF in B-cell development. *Curr Opin Immunol*. 2002;14(2):266-275. doi:10.1016/S0952-7915(02)00332-1
85. Lane P, Traunecker A, Hubele S, Inui S, Lanzavecchia A, Gray D. Activated human T cells express a ligand for the human B cell-associated antigen CD40 which participates in T cell-dependent activation of B lymphocytes. *Eur J Immunol*. 1992;22(10):2573-2578. doi:10.1002/EJI.1830221016/FORMAT/PDF
86. Herzog S, Reth M, Jumaa H. Regulation of B-cell proliferation and differentiation by pre-B-cell receptor signalling. *Nat Rev Immunol*. 2009;9(3):195-205. doi:10.1038/NRI2491
87. Yadav A, Olaru A, Saltis M, Setren A, Cerny J, Livák F. Identification of a ubiquitously active promoter of the murine activation-induced cytidine deaminase (AICDA) gene. *Mol Immunol*. 2006;43(6):529-541. doi:10.1016/J.MOLIMM.2005.05.007
88. Nera KP, Alinikula J, Terho P, et al. Ikaros has a crucial role in regulation of B cell receptor signaling. *Eur J Immunol*. 2006;36(3):516-525. doi:10.1002/EJI.200535418
89. López-Cotarelo P, Gómez-Moreira C, Criado-García O, Sánchez L, Rodríguez-Fernández JL. Beyond Chemoattraction: Multifunctionality of Chemokine Receptors in Leukocytes. *Trends Immunol*. 2017;38(12):927-941. doi:10.1016/J.IT.2017.08.004
90. Koskela K, Kohonen P, Nieminen P, Buerstedde JM, Lassila O. Insight into lymphoid development by gene expression profiling of avian B cells. *Immunogenetics*. 2003;55(6):412-422. doi:10.1007/S00251-003-0592-7/FIGURES/6

91. Sun Y, Cheng Z, Ma L, Pei G. β -Arrestin2 Is Critically Involved in CXCR4-mediated Chemotaxis, and This Is Mediated by Its Enhancement of p38 MAPK Activation. *Journal of Biological Chemistry*. 2002;277(51):49212-49219. doi:10.1074/JBC.M207294200
92. Staal FJT, Luis TC, Tiemessen MM. WNT signalling in the immune system: WNT is spreading its wings. *Nature Reviews Immunology* 2008 8:8. 2008;8(8):581-593. doi:10.1038/nri2360
93. Monson MS, van Goor AG, Ashwell CM, et al. Immunomodulatory effects of heat stress and lipopolysaccharide on the bursal transcriptome in two distinct chicken lines. *BMC Genomics*. 2018;19(1):1-15. doi:10.1186/S12864-018-5033-Y/TABLES/4
94. Goitsuka R, Morimura T, Miyatani S, Kitamura D. Serrate2/Notch1 in the Bursa of Fabricius Spatially Restricted Expression of in Expression in Chicken B Cells: Implication Notch Signaling Suppresses IgH Gene. *J Immunol References*. 2001;166:3277-3283. doi:10.4049/jimmunol.166.5.3277
95. Morimura T, Goitsuka R, Zhang Y, Saito I, Reth M, Kitamura D. Cell Cycle Arrest and Apoptosis Induced by Notch1 in B Cells *. *Journal of Biological Chemistry*. 2000;275(47):36523-36531. doi:10.1074/JBC.M006415200
96. Lasergene Genomics®. Version 17.3.3. DNASTAR. Madison, WI.
97. Sutermaister BA, Darling EM. Considerations for high-yield, high-throughput cell enrichment: fluorescence versus magnetic sorting. *Scientific Reports* 2019 9:1. 2019;9(1):1-9. doi:10.1038/s41598-018-36698-1
98. *Streptavidin MicroBeads*. Accessed January 7, 2022. www.miltenyibiotec.com/
99. BENCHTOP CYTOMETRY WITHOUT COMPROMISES CYTOFLEX FLOW CYTOMETER Every Event Matters.
100. Doublet Discrimination - Flow Cytometry Guide | Bio-Rad. Accessed August 20, 2022. <https://www.bio-rad-antibodies.com/flow-cytometry-doublet-discrimination.html>
101. FlowJo™ Software (for Windows) Version 10.8. Becton, Dickinson and Company; 2021. .
102. Bio USA T. SMART-Seq® v4 PLUS Kit User Manual SMART-Seq v4 PLUS Kit User Manual.
103. Technologies A. Agilent Technologies Agilent High Sensitivity DNA Kit Guide Agilent High Sensitivity DNA.
104. Illumina. NovaSeq 6000 Sequencing System. Accessed October 12, 2022. www.illumina.com.
105. National Center for Biotechnology Information (NCBI)[Internet]. Bethesda (MD): National Library of Medicine (US), National Center for Biotechnology Information; [1988] – [cited 2022 Jun-Sep]. Available from: <https://www.ncbi.nlm.nih.gov/>.

106. Szklarczyk D, Gable AL, Nastou KC, et al. The STRING database in 2021: customizable protein-protein networks, and functional characterization of user-uploaded gene/measurement sets. *Nucleic Acids Res.* 2021;49(D1):D605-D612. doi:10.1093/NAR/GKAA1074
107. Kanehisa M, Goto S. KEGG: Kyoto Encyclopedia of Genes and Genomes. *Nucleic Acids Res.* 2000;28(1):27-30. doi:10.1093/NAR/28.1.27
108. Houssaint E. Cell lineage segregation during bursa of Fabricius ontogeny. *The Journal of Immunology.* 1987;138(11).
109. Lee IK, Gu MJ, Ko KH, et al. Regulation of CD4+CD8-CD25+ and CD4+CD8+CD25+ T cells by gut microbiota in chicken. *Sci Rep.* 2018;8(1). doi:10.1038/S41598-018-26763-0
110. Bertzbach LD, Laparidou M, Härtle S, et al. Unraveling the role of B cells in the pathogenesis of an oncogenic avian herpesvirus. *Proc Natl Acad Sci U S A.* 2018;115(45):11603-11607. doi:10.1073/PNAS.1813964115/SUPPL_FILE/PNAS.1813964115.SAPP.PDF
111. Moore DK, Motaung B, du Plessis N, Shabangu AN, Loxton AG, Su-Irg C. Isolation of B-cells using Miltenyi MACS bead isolation kits. *PLoS One.* 2019;14(3). doi:10.1371/JOURNAL.PONE.0213832
112. Uysal O, Sevimli T, Sevimli M, Gunes S, Sariboyaci AE. Cell and Tissue Culture: The Base of Biotechnology. *Omics Technologies and Bio-engineering: Towards Improving Quality of Life.* 2018;1:391-429. doi:10.1016/B978-0-12-804659-3.00017-8
113. Koch CM, Chiu SF, Akbarpour M, et al. TRANSLATIONAL REVIEW A Beginner's Guide to Analysis of RNA Sequencing Data. Published online 2018. doi:10.1165/rcmb.2017-0430TR
114. Houssaint E, Diez E, Pinktt JRL. Ontogeny and tissue distribution of the chicken Bu-la antigen. *Immunology.* 1987;62:463-470.
115. Mouse Anti-Chicken Bu-1 . Accessed August 27, 2022. www.southernbiotech.com
116. Pifer J, Robison D, Funk PE. The Avian Chb6 Alloantigen Triggers Apoptosis in a Mammalian Cell Line. *The Journal of Immunology.* 2002;169(3):1372-1378. doi:10.4049/JIMMUNOL.169.3.1372
117. Lemmens K, Doggen K, de Keulenaer GW. Role of Neuregulin-1/ErbB Signaling in Cardiovascular Physiology and Disease. *Circulation.* 2007;116(8):954-960. doi:10.1161/CIRCULATIONAHA.107.690487
118. Yoshie O. Chemokines and chemokine receptors. *Nihon Rinsho.* 2012;70 Suppl 8:212-217. doi:10.1016/B978-0-7020-6896-6.00010-7
119. Iqbal AJ, Barrett TJ, Taylor L, et al. Acute exposure to apolipoprotein A1 inhibits macrophage chemotaxis in vitro and monocyte recruitment in vivo. *Elife.* 2016;5(AUGUST). doi:10.7554/ELIFE.15190

120. Oh E, Kim JY, Cho Y, et al. Overexpression of angiotensin II type 1 receptor in breast cancer cells induces epithelial–mesenchymal transition and promotes tumor growth and angiogenesis. *Biochimica et Biophysica Acta (BBA) - Molecular Cell Research*. 2016;1863(6):1071-1081. doi:10.1016/J.BBAMCR.2016.03.010
121. Ridley AJ. Rho GTPases and cell migration. *J Cell Sci*. 2001;114(Pt 15):2713-2722. doi:10.1242/JCS.114.15.2713
122. Honczarenko M, Le Y, Glodek AM, et al. CCR5-binding chemokines modulate CXCL12 (SDF-1)-induced responses of progenitor B cells in human bone marrow through heterologous desensitization of the CXCR4 chemokine receptor. *Blood*. 2002;100(7):2321-2329. doi:10.1182/BLOOD-2002-01-0248
123. Liang T, Shen L, Ji Y, Jia L, Dou Y, Guo L. NOV/CCN3 Promotes Cell Migration and Invasion in Intrahepatic Cholangiocarcinoma via miR-92a-3p. *Genes (Basel)*. 2021;12(11). doi:10.3390/GENES12111659
124. Xuan ZB, Wang YJ, Xie J. ANO6 promotes cell proliferation and invasion in glioma through regulating the ERK signaling pathway. *Onco Targets Ther*. 2019;12:6721-6731. doi:10.2147/OTT.S211725
125. Sánchez-Martín L, Estecha A, Samaniego R, Sánchez-Ramón S, Vega MÁ, Sánchez-Mateos P. The chemokine CXCL12 regulates monocyte-macrophage differentiation and RUNX3 expression. *Blood*. 2011;117(1):88-97. doi:10.1182/BLOOD-2009-12-258186
126. Müller G, Lipp M. Shaping up adaptive immunity: The impact of CCR7 and CXCR5 on lymphocyte trafficking. *Microcirculation*. 2003;10(3-4):325-334. doi:10.1038/SJ.MN.7800197
127. Ansel KM, Ngo VN, Hyman PL, et al. A chemokine-driven positive feedback loop organizes lymphoid follicles. *Nature*. 2000;406(6793):309-314. doi:10.1038/35018581
128. Förster R, Mattis AE, Kremmer E, Wolf E, Brem G, Lipp M. A putative chemokine receptor, BLR1, directs B cell migration to defined lymphoid organs and specific anatomic compartments of the spleen. *Cell*. 1996;87(6):1037-1047. doi:10.1016/S0092-8674(00)81798-5
129. Noelle Samuel RO, Hess H, Lord GM, et al. CCR6-Dependent Positioning of Memory B Cells Is Essential for Their Ability To Mount a Recall Response to Antigen. Published online 2022. doi:10.4049/jimmunol.1401553
130. Reimer D, Lee AY, Bannan J, et al. Early CCR6 expression on B cells modulates germinal centre kinetics and efficient antibody responses. Published online 2016. doi:10.1038/icb.2016.68
131. Pedro Pereira J, Kelly LM, Cyster JG. Finding the right niche: B-cell migration in the early phases of T-dependent antibody responses. *Int Immunol*. 22(6):413-419. doi:10.1093/intimm/dxq047

132. Flaishon L, Becker-Herman S, Hart G, Levo Y, Kuziel WA, Shachar I. Expression of the chemokine receptor CCR2 on immature B cells negatively regulates their cytoskeletal rearrangement and migration. *Blood*. 2004;104(4):933-941. doi:10.1182/BLOOD-2003-11-4013
133. Wurbel MA, Malissen M, Guy-Grand D, et al. Mice lacking the CCR9 CC-chemokine receptor show a mild impairment of early T- and B-cell development and a reduction in T-cell receptor $\gamma\delta^+$ gut intraepithelial lymphocytes. *Blood*. 2001;98(9):2626-2632. doi:10.1182/BLOOD.V98.9.2626
134. Annamalai T, Selvaraj RK. Interleukin 4 increases CCR9 expression and homing of lymphocytes to gut-associated lymphoid tissue in chickens. *Vet Immunol Immunopathol*. 2012;145(1-2):257-263. doi:10.1016/J.VETIMM.2011.11.016
135. Han X. Constitutively Active Chemokine CXC Receptors. *Adv Pharmacol*. 2014;70:265-301. doi:10.1016/B978-0-12-417197-8.00009-2
136. Huang C, Jacobson K, Schaller MD. MAP kinases and cell migration. *J Cell Sci*. 2004;117(Pt 20):4619-4628. doi:10.1242/JCS.01481
137. Yu J, Moon A, Kim HRC. Both platelet-derived growth factor receptor (PDGFR)- α and PDGFR- β promote murine fibroblast cell migration. *Biochem Biophys Res Commun*. 2001;282(3):697-700. doi:10.1006/BBRC.2001.4622
138. Lam LPY, Chow RYK, Berger SA. A transforming mutation enhances the activity of the c-Kit soluble tyrosine kinase domain. *Biochemical Journal*. 1999;338(Pt 1):131. doi:10.1042/0264-6021:3380131
139. Babaei MA, Kamalidehghan B, Saleem M, Huri HZ, Ahmadipour F. Receptor tyrosine kinase (c-Kit) inhibitors: a potential therapeutic target in cancer cells. *Drug Des Devel Ther*. 2016;10:2443. doi:10.2147/DDDT.S89114
140. Davy A, Robbins SM. Ephrin-A5 modulates cell adhesion and morphology in an integrin-dependent manner. *EMBO J*. 2000;19(20):5396. doi:10.1093/EMBOJ/19.20.5396
141. Ko PH, Lenka G, Chen YA, et al. Semaphorin 5A suppresses the proliferation and migration of lung adenocarcinoma cells. *Int J Oncol*. 2020;56(1):165. doi:10.3892/IJO.2019.4932
142. Hall KT, Bousmell L, Schultze JL, et al. Human CD100, a novel leukocyte semaphorin that promotes B-cell aggregation and differentiation. *Proc Natl Acad Sci U S A*. 1996;93(21):11780-11785. doi:10.1073/PNAS.93.21.11780
143. Saxena S, Hayashi Y, Wu L, et al. Pathological and functional significance of Semaphorin-5A in pancreatic cancer progression and metastasis. *Oncotarget*. 2018;9(5):5931-5943. doi:10.18632/ONCOTARGET.23644

144. Mendes-da-Cruz DA, Brignier AC, Asnafi V, et al. Semaphorin 3F and Neuropilin-2 Control the Migration of Human T-Cell Precursors. *PLoS One*. 2014;9(7):103405. doi:10.1371/JOURNAL.PONE.0103405
145. Lv XJ, Chen X, Wang Y, Yu S, Pang L, Huang C. Aberrant expression of semaphorin 6B affects cell phenotypes in thyroid carcinoma by activating the Notch signalling pathway. *Endokrynol Pol*. 2021;72(1):29-36. doi:10.5603/EP.A2020.0072
146. Ge C, Li Q, Wang L, Xu X. The role of axon guidance factor semaphorin 6B in the invasion and metastasis of gastric cancer. *Journal of International Medical Research*. 2013;41(2):284-292. doi:10.1177/0300060513476436
147. Andermatt I, Wilson NH, Bergmann T, et al. Semaphorin 6B acts as a receptor in post-crossing commissural axon guidance. *Development (Cambridge)*. 2014;141(19):3709-3720. doi:10.1242/DEV.112185/-/DC1
148. Dun X peng, Carr L, Woodley PK, et al. Macrophage-Derived Slit3 Controls Cell Migration and Axon Pathfinding in the Peripheral Nerve Bridge. *Cell Rep*. 2019;26(6):1458. doi:10.1016/J.CELREP.2018.12.081
149. Schubert T, Denk AE, Ruedel A, et al. Fragments of SLIT3 inhibit cellular migration. *Int J Mol Med*. 2012;30(5):1133-1137. doi:10.3892/IJMM.2012.1098/HTML
150. Geutskens SB, Hordijk PL, Hennik PB van. The Chemorepellent Slit3 Promotes Monocyte Migration. *The Journal of Immunology*. 2010;185(12):7691-7698. doi:10.4049/JIMMUNOL.0903898
151. Jiang Z, Liang G, Xiao Y, et al. Targeting the SLIT/ROBO pathway in tumor progression: molecular mechanisms and therapeutic perspectives. *Ther Adv Med Oncol*. 2019;11. doi:10.1177/1758835919855238
152. Madej JP, Chrzaogonekstek K, Piasecki T, Wieliczko A. New insight into the structure, development, functions and popular disorders of Bursa Fabricii. *Journal of Veterinary Medicine Series C: Anatomia Histologia Embryologia*. 2013;42(5):321-331. doi:10.1111/ahe.12026
153. GraphPad Prism version 9.3.0 for Windows, GraphPad Software, La Jolla California USA, www.graphpad.com.

7. Annexes